New Simocetidae (Cetacea, Odontoceti) from the Pysht Formation in Washington State, U.S.A. (#80454)

First submission

Guidance from your Editor

Please submit by 27 Jan 2023 for the benefit of the authors (and your token reward) .



Structure and Criteria

Please read the 'Structure and Criteria' page for general guidance.



Custom checks

Make sure you include the custom checks shown below, in your review.



Author notes

Have you read the author notes on the guidance page?



Raw data check

Review the raw data.



Image check

Check that figures and images have not been inappropriately manipulated.

Privacy reminder: If uploading an annotated PDF, remove identifiable information to remain anonymous.

Files

Download and review all files from the <u>materials page</u>.

20 Figure file(s)

6 Table file(s)

1 Raw data file(s)



New species checks

Have you checked our <u>new species policies</u>?

Do you agree that it is a new species?

Is it correctly described e.g. meets ICZN standard?

Structure and Criteria



Structure your review

The review form is divided into 5 sections. Please consider these when composing your review:

- 1. BASIC REPORTING
- 2. EXPERIMENTAL DESIGN
- 3. VALIDITY OF THE FINDINGS
- 4. General comments
- 5. Confidential notes to the editor
- You can also annotate this PDF and upload it as part of your review

When ready submit online.

Editorial Criteria

Use these criteria points to structure your review. The full detailed editorial criteria is on your guidance page.

BASIC REPORTING

- Clear, unambiguous, professional English language used throughout.
- Intro & background to show context.
 Literature well referenced & relevant.
- Structure conforms to <u>PeerJ standards</u>, discipline norm, or improved for clarity.
- Figures are relevant, high quality, well labelled & described.
- Raw data supplied (see <u>PeerJ policy</u>).

EXPERIMENTAL DESIGN

- Original primary research within Scope of the journal.
- Research question well defined, relevant & meaningful. It is stated how the research fills an identified knowledge gap.
- Rigorous investigation performed to a high technical & ethical standard.
- Methods described with sufficient detail & information to replicate.

VALIDITY OF THE FINDINGS

- Impact and novelty not assessed.

 Meaningful replication encouraged where rationale & benefit to literature is clearly stated.
- All underlying data have been provided; they are robust, statistically sound, & controlled.



Conclusions are well stated, linked to original research question & limited to supporting results.



Standout reviewing tips



The best reviewers use these techniques

Τ	p

Support criticisms with evidence from the text or from other sources

Give specific suggestions on how to improve the manuscript

Comment on language and grammar issues

Organize by importance of the issues, and number your points

Please provide constructive criticism, and avoid personal opinions

Comment on strengths (as well as weaknesses) of the manuscript

Example

Smith et al (J of Methodology, 2005, V3, pp 123) have shown that the analysis you use in Lines 241-250 is not the most appropriate for this situation. Please explain why you used this method.

Your introduction needs more detail. I suggest that you improve the description at lines 57-86 to provide more justification for your study (specifically, you should expand upon the knowledge gap being filled).

The English language should be improved to ensure that an international audience can clearly understand your text. Some examples where the language could be improved include lines 23, 77, 121, 128 – the current phrasing makes comprehension difficult. I suggest you have a colleague who is proficient in English and familiar with the subject matter review your manuscript, or contact a professional editing service.

- 1. Your most important issue
- 2. The next most important item
- 3. ...
- 4. The least important points

I thank you for providing the raw data, however your supplemental files need more descriptive metadata identifiers to be useful to future readers. Although your results are compelling, the data analysis should be improved in the following ways: AA, BB, CC

I commend the authors for their extensive data set, compiled over many years of detailed fieldwork. In addition, the manuscript is clearly written in professional, unambiguous language. If there is a weakness, it is in the statistical analysis (as I have noted above) which should be improved upon before Acceptance.



New Simocetidae (Cetacea, Odontoceti) from the Pysht Formation in Washington State, U.S.A.

Jorge Velez-Juarbe Corresp. 1

¹ Department of Mammalogy, Natural History Museum of Los Angeles County, Los Angeles, California, USA

Corresponding Author: Jorge Velez-Juarbe Email address: jvelezjuar@nhm.org

Odontocetes first appeared by the early Oligocene and their early evolutionary history can provide clues as to how some of their unique adaptations, such as echolocation, evolved. Here, three new specimens from the middle Oligocene Pysht Formation are described further increasing our understanding of richness and diversity of early odontocetes, particularly for the North Pacific region. Phylogenetic analysis shows that the new specimens are part of a more inclusive, redefined Simocetidae, which now includes Simocetus rayi, Olympicetus sp. 1, Olympicetus avitus, O. thalassodon sp. nov.,, and a large unnamed taxon, all part of an endemic, North Pacific clade. Of these, Olympicetus thalassodon sp. nov. represents one of the best known simocetids, offering new information on the cranial and dental morphology of early odontocetes. Additionally, the inclusion of CCNHM 1000, here considered to represent a neonate of Olympicetus sp., as part of the Simocetidae, suggests that this group represents a clade of non-echolocating odontocetes, further implying that some morphological features that have been correlated with the capacity to echolocate appeared before the acquisition of ultrasonic hearing. Thedentition of simocetids is interpreted as being plesiomorphic, with a tooth count more akin to that of basilosaurids and early toothed mysticetes, while other features of the skull and hyoid suggests various forms of prey acquisition, including raptorial or combined feeding and in *Olympicetus* spp., and suction feeding in *Simocetus*. Finally, body size estimates show that small to moderately large taxa are present in Simocetidae, with a largest taxon represented by LACM 124104 with an estimated body length of 3 meters, which places it as the largest known simocetid, and amongst the largest Oligocene odontocetes. The new specimens described here add to a growing list of Oligocene marine tetrapods from the North Pacific, further promoting faunistic comparisons across other contemporaneous and younger assemblages, that will allow for an improved understanding of the evolution of marine faunas in the region.



New Simocetidae (Cetacea, Odontoceti) from the Pysht Formation in Washington State, U.S.A.

3

1

2

Jorge Vélez-Juarbe

5 6 7

Department of Mammalogy, Natural History Museum of Los Angeles County, Los Angeles, CA 90007, U.S.A.

9 10

8

11 Corresponding Author:

- 12 Jorge Vélez-Juarbe
- 13 Email address: jvelezjuar@nhm.org

14 15

Abstract

- Odontocetes first appeared by the early Oligocene and their early evolutionary history can
- 17 provide clues as to how some of their unique adaptations, such as echolocation, evolved. Here,
- 18 three new specimens from the middle Oligocene Pysht Formation are described further
- 19 increasing our understanding of richness and diversity of early odontocetes, particularly for the
- 20 North Pacific region. Phylogenetic analysis shows that the new specimens are part of a more
- 21 inclusive, redefined Simocetidae, which now includes Simocetus rayi, Olympicetus sp. 1,
- 22 Olympicetus avitus, O. thalassodon sp. nov., and a large unnamed taxon, all part of an endemic,
- 23 North Pacific clade. Of these, Olympicetus thalassodon sp. nov. represents one of the best known
- 24 simocetids, offering new information on the cranial and dental morphology of early odontocetes.
- 25 Additionally, the inclusion of CCNHM 1000, here considered to represent a neonate of
- 26 Olympicetus sp., as part of the Simocetidae, suggests that this group represents a clade of non-
- 27 echolocating odontocetes, further implying that some morphological features that have been
- 28 correlated with the capacity to echolocate appeared before the acquisition of ultrasonic hearing.
- 29 The dentition of simocetids is interpreted as being plesiomorphic, with a tooth count more akin to
- 30 that of basilosaurids and early toothed mysticetes, while other features of the skull and hyoid
- 31 suggests various forms of prey acquisition, including raptorial or combined feeding and in
- 32 Olympicetus spp., and suction feeding in Simocetus. Finally, body size estimates show that small
- 33 to moderately large taxa are present in Simocetidae, with a largest taxon represented by LACM
- 34 124104 with an estimated body length of 3 meters, which places it as the largest known
- 35 simocetid, and amongst the largest Oligocene odontocetes. The new specimens described here
- 36 add to a growing list of Oligocene marine tetrapods from the North Pacific, further promoting
- 37 faunistic comparisons across other contemporaneous and younger assemblages, that will allow
- 38 for an improved understanding of the evolution of marine faunas in the region.

39



40

59

60

61

62 63

64

65 66

67

68

69

70

Introduction

41 The Eastern North Pacific Region is recognized as one of the best sources for early marine mammals belonging to various groups, particularly desmostylians, pinnipeds, and early 42 mysticetes mysticetes (Emlong, 1966; Russell, 1968; Domning et al., 1986; Berta, 1991; Ray et 43 al., 1994; Barnes et al., 1995; Beatty, 2006; Beatty and Cockburn, 2015; Marx et al., 2015, 44 2016b; Peredo and Uhen, 2016; Peredo and Pvenson, 2018; Peredo et al., 2018; Poust and 45 46 Boessenecker, 2018; Shipps et al., 2019; Solis-Añorve et al., 2019; Hernández-Cisneros, 2018, 2022; Hernández-Cisneros and Nava-Sánchez, 2022). However, while odontocetes have also 47 48 been found in these units, and have been remarked in the literature in non-taxonomic context (e.g. Whitmore and Sanders, 1977; Goedert et al., 1995; Barnes, 1998; Barnes et al., 2001; Kiel 49 et al., 2013; Hernández Cisneros et al., 2017), only a handful are described (Fordyce, 2002; 50 Boersma and Pyenson, 2016; Vélez-Juarbe, 2017). These include Simocetus rayi Fordyce, 2002, 51 from the early Oligocene Alsea Formation, in Oregon, U.S.A., the platanistoid Arktocara 52 yakataga Boersma and Pyenson, 2016, from the middle Oli ene Poul Creek Fm., in Alaska, 53 54 U.S.A., and the more recently described, *Olympicetus avitus* Vélez-Juarbe, 2017, from the middle Oligocene Oligocene Pysht Fm., in Washington State. The presence of stem (i.e. 55 Simocetus, Olympicetus) and crown (Arktocara) odontocetes in similar-aged rocks point to a 56 complex early history for odontocetes, hence the description of new material will advance our 57 58 current understanding of odontocete evolution.

In this work three additional specimens of stem odontocetes collected from the mid-Oligocene Pysht Formation of Washington are described. The morphology of these new specimens show similariries with *Simocetus* and *Olympicetus*, and provide further insight into the diversity of early odontocetes in the North Pacific. The Pysht Fm. has a rich fossil record of marine tetrapods, including plotopterids (Olson, 1980; Dyke et al., 2011; Mayr and Goedert, 2016), desmostylians (Domning et al., 1986), aetiocetids (Barnes et al., 1995; Shipps et al., 2019), stem mysticetes (Peredo and Uhen, 2016), and many others still remaining to be described (Whitmore and Sanders, 1977; Hunt and Barnes, 1994; Barnes et al., 2001; Marx et al., 2016b). The fossils described in this work demonstrate that stem odontocetes were much more diverse in the North Pacific Region and hint at the presence of clade of stem odontocetes that were geographically confined to this region that parallels aetiocetid mysticetes (Hernández Cisneros and Vélez-Juarbe, 2021).

- 71 **Abbreviations—c.**, character state as described and numbered by Sanders and Geisler (2015)
- and subsequent works, e.g. (c.15[0]) refers to state 0 of character 15; LACM, Vertebrate
- 73 Paleontology Collection, Natural History Museum of Los Angeles County, Los Angeles, CA,
- 74 U.S.A.; KMNH VP, Kitakyushu Museum of Natural History, Kitakyushu City, Japan; USNM,
- 75 Department of Paleobiology, National Museum of Natural History, Smithsonian Institution,
- 76 Washington, D.C., U.S.A.
- 77 Materials & Methods
- 78 Phylogenetic analysis



- 79 The phylogenetic analysis was performed using the morphological matrix of Albright et al.
- 80 (2018) as modified recently by Boessenecker et al. (2020), with the addition of two new
- 81 characters. The first one (c.335) refers to the presence of a transverse cleft on the apex of the
- 82 zygomatic process of the squamosal (first noted by Racicot et al., 2019), while the other new
- character (c.336) relates to the morphology of the thyrohyoid/thyrohyal, for a total of 336
- 84 characters (see Supplemental File 1). Besides LACM 124104, LACM 124105 and LACM
- 85 158720, one additional odontocete from the Pysht Fm. was added, CCNHM 1000, based on the
- 86 description from Racicot et al. (2019:S1). All otherwise undescribed specimens in earlier
- 87 versions of this matrix were removed from this analysis as their character/states cannot be
- 88 independently corroborated, resulting in a total of three outgroup and 106 ingroup taxa. The
- 89 matrix was analyzed using PAUP* (v. 4.0a169; Swofford, 2003), all characters were treated as
- 90 unordered and with equal weights. A heuristic search of 10000 replicates was performed using
- 91 the tree bisection-reconnection (TBR) algorithm and using a backbone constraint based on the
- of the tree discensification (TDR) argorithm and using a backbone constraint based on the
- 92 phylogenetic tree from McGowen et al. (2020); bootstrap values were obtained by performing
- 93 10000 replicates.

9495 **Taxonomy**

- 96 The electronic version of this article in portable document format will represent a published work
- 97 according to the International Commission on Zoological Nomenclature (ICZN), and hence the
- 98 new names contained in the electronic version are effectively published under that Code from the
- 99 electronic edition alone. This published work and the nomenclatural acts it contains have been
- registered in ZooBank, the online registration system for the ICZN. The ZooBank LSIDs (Life
- 101 Science Identifiers) can be resolved and the associated information viewed through any standard
- web browser by appending the LSID to the prefix http://zoobank.org/. The LSID for this
- publication is LSIDurn:lsid:zoobank.org:pub:D190F6B6-FB67-4F2B-AC24-145DF06D3FD3
- The online version of this work is archived and available from the following digital repositories:
- 105 PeerJ, PubMed Central, and CLOCKSS.

106107

Systematic Paleontology

- 108 CETACEA Brisson, 1762
- 109 ODONTOCETI Flower, 1867
- 110 SIMOCETIDAE Fordyce, 2002
- 111 **Type**—*Simocetus rayi* Fordyce, 2002.
- 112 Included Species—Simocetus rayi; Olympicetus avitus Velez-Juarbe, 2017; Olympicetus
- thalassodon sp. nov.; Olympicetus sp. 1; Simocetidae gen. et sp. A.
- 114 Range—early-late Oligocene (Rupelian—early Chattian) of the eastern North Pacific.
- 115 **Emended Diagnosis**—Stem odontocetes displaying a mosaic of plesiomorphic and derived
- characters that sets them apart from other basal odontocetes, particularly the Xenorophidae,
- 117 Patriocetidae and Agorophidae. Characterized by the following combination of characters:
- 118 rostrum fairly wide (c.7[1]; shared with Ashleycetus planicapitis Sanders and Geisler, 2015,



119 Agorophius pygmaeus [Müller, 1849], and Ankylorhiza tiedemani [Allen, 1887]); palatine/maxilla suture anteriorly bowed (21[0]; shared with *Patriocetus kazakhstanicus* 120 Dubrovo and Sanders. 2000): seven to eight teeth completely enclosed by the maxilla (c.25[1]): 121 lacrimal restricted to below the supraorbital process of frontal (c.52[0]; shared with A. 122 123 planicapitis, P. kazakhstanicus and An. tiedemani); relatively small ventral (orbital) exposure of the lacrimal (c.56[0]; shared with A. planicapitis, Archaeodelphis patrius Allen, 1921, and P. 124 kazakhstanicus); postorbital process of frontal relatively long and oriented posterolaterally and 125 ventrally (c.62[0]; shared with A. planicapitis, Mirocetus riabinini and P. kazakhstanicus); lack 126 of a rostral basin (c.66[0]), differing from most xenorophids which have a well-defined basin; 127 presence of a long posterolateral sulcus extending from the premaxillary foramen (c.73[2]: 128 shared with A. planicapitis); maxilla only partially covering supraorbital processes (c.77[1]; 129 shared with A. planicapitis and Ar. patrius); posteriormost edge of nasals in line with the anterior 130 half of the supraorbital processes (c.123[1]); frontals slightly lower than nasals (c.125[0]; shared 131 132 with Cotylocara macei Geisler et al., 2014); supraoccipital at about the same level as the nasals (c.129[1]), differing from xenorophids where the supraoccipital is higher; intertemporal region 133 with an ovoid cross section (c.137[1]; shared with A. planicapitis, Echovenator sandersi 134 Churchill et al., 2016, and C. macei); floor of squamosal fossa thickens posteriorly (c.149[1]); 135 136 distal end of postglenoid process is anteroposteriorly wide (c.152[2]); anterior end of supraoccipital is semicircular (c.153[1]; shared with *P. kazakhstanicus*); occipital shield with 137 distinct sagittal crest (c.156[1]; shared with Albertocetus meffordorum Uhen, 2008, P. 138 kazakhstanicus, Ag. pygmaeus, and An. tiedemani); a nearly transverse pterygoid-palatine suture 139 (c.163[1]; shared with Ar. patrius); long and subconical hamular process of the ptervgoid 140 141 (c.173[1]); hamular processes unkeeled (c.174[0]); hamular processes extending to a point in line with the middle of the zygomatic processes (c.175[3]); cranial hiatus constricted by medial 142 projection of the parietal (c.184[2]); absent to poorly defined rectus capitus anticus muscle fossa 143 (c.193[0]), differing from the well-defined fossa of xenorophids; posteroventral end of 144 145 basioccipital crest forming a posteriorly oriented flange (c.194[2]); anterior process of periotic short (c.204[2]; shared with C. macei); anterior process of periotic with well-defined fossa for 146 contact with tympanic (c.210[3]); lateral tuberosity of periotic forming a bulbous prominence 147 lateral to mallear fossa (c.212[1]); tegment tympani at the base of the anterior process 148 149 unexcavated (c.232[0]), differing from the excavated surface in xenorophids; articular surface of the posterior process of periotic is smooth (c.242[0]) and concave (c.243[0]); posterolateral 150 151 sulcus of premaxilla deeply entrenched (c.310[1]).

152

- 153 SIMOCETIDAE GEN. ET SP. A
- 154 (Figs. 1-5; Tables 1-2)
- 155 Material—LACM 124104, posterior part of skull skull, missing most parts anterior to the
- 156 frontal/parietal suture and the left squamosal; including one molariform tooth and partial atlas,
- axis and third cervical vertebrae. Collected by J. L. Goedert and G. H. Goedert March 21, 1984.



- Locality and Horizon—LACM Loc. 5123, Murdock Creek, Clallam Co., Washington, U.S.A.
- 159 (48° 09' 25"N, 123° 52' 10"W; = locality JLG-76). At this locality specimens are found as
- 160 concretions along a beach terrace about 40 m north of the mouth of Murdock Creek. Besides
- 161 LACM 124104, additional specimens known from this locality include the desmostylian
- 162 Behemotops proteus (LACM 124106; Ray et al., 1994), additional material of the simocetid
- 163 Olympicetus spp. (LACM 124105 and LACM 158720; described below), aff. Olympicetus sp.
- (Racicot et al., 2019), and the aetiocetid *Borealodon osedax* (Shipps et al., 2019).
- 165 Formation and Age—Pysht Formation, between 30.5–26.5 Ma (Oligocene: late Rupelian-early
- 166 Chattian; Prothero et al., 2001; Vélez-Juarbe, 2017).
- 167 Range—Oligocene of Washington, U.S.A.

168169

Description

- 170 The partial skull, LACM 124104, is missing most parts anterior to the fronto-parietal suture, the
- left squamosal, and some parts of the palatines and earbones (Figs. 1-4). The preserved portion
- of the skull has a pachyostotic appearance, in comparison with the other described simocetids.
- 173 The estimated bizygomatic width, 322 mm (c.333[2]), suggests a body length of around 3 m
- 174 (based on equation "i" from Pyenson and Sponberg, 2011), which is larger than any of the other
- 175 described simocetids.
- 176 **Vomer**—Most of the palatal surface of the vomer is missing as is much of the rostrum.
- 177 Posteriorly, it seems to have been exposed along an elongated, diamond-shaped, window
- between the palatines and pterygoids as in other simocetids (Fig. 2C-D; Fordyce, 2002; Vélez-
- 179 Juarbe, 2017; see below). From this point, the vomerine keel extends posterodorsally, separating
- the choanae along the midline and extending to about 20 mm from the posterior edge of the bone
- 181 (Fig. 2C-D). The horizontal plate extends posteriorly to a point in line with the anterior end of
- the basioccipital crests, thus covering the suture between the basisphenoid and basioccipital
- 183 (c.191[0]; Fig. 2C-D). The choanal surface of the horizontal plate forms a ventrally concave
- 184 choanal roof, with its lateral edges slightly flared and forming a nearly continuous surface with
- the internal lamina of the pterygoid.
- 186 **Palatine**—Only the posteriormost parts of the palatines are preserved, these are separated along
- the midline by the vomer, resembling the condition of other simocetids (Fig. 2C-D; Fordyce,
- 188 2002; see below). In anterior view, the palatines formed the ventral and lateral surface of the
- internal nares, while the vomer formed the medial and dorsal surfaces. Ventrolaterally, the
- 190 palatines form a vertical to semilunar contact with the pterygoids, best observed in ventral,
- ventrolateral and lateral views (c.163[1]; Figs. 2C-D, 3-4), resembling the contact in *Simocetus*
- 192 rayi and Olympicetus spp. (Fordyce, 2002; Vélez-Juarbe, 2017). An elongated groove along the
- ventrolateral end of the left palatine seems to have been part of the palatine foramen/canal.
- 194 **Frontal**—Only the posteriormost portion of the frontals are preserved, but are eroded (Fig. 1).
- Dorsally, the interfrontal suture seems to have been completely fused, and posteriorly formed a
- broad V-shaped contact with the parietals, which continues as a vertical contact along the
- 197 temporal surface (Fig. 3).



198 **Parietal**—As in other simocetids, the parietals are broadly exposed dorsally, and the interparietal is either absent or fused early in ontogeny (c.135[0], 136[1]; Fig. 1). The parietals do not extend 199 anterolaterally, resembling Simocetus ravi, and differing from Olympicetus where the parietals 200 extend into the base of the supraorbital processes. The parietal exposure in the intertemporal 201 202 region is anteroposteriorly short and broad in dorsal view, with an ovoid cross section (c.137[1]). Posterodorsally, the parietal-supraoccipital contact is broad and anteriorly convex, while along 203 the temporal surface, it forms a vertical contact with the frontals (c.134[0]:Fig. 1), and seems to 204 have formed part of the posterior edge of the optic infundibulum; abaft to this point the parietals 205 become laterally convex towards the contact with the squamosals (Figs. 3-4). Anteroventrally, on 206 the temporal surface, the parietal descent to contact the orbitosphenoid, a portion of the dorsal 207 lamina of the pterygoid, the alisphenoid, and the squamosal, with which it forms part of the 208 subtemporal crest (Fig. 4). Its contact with the squamosal on the temporal surface becomes an 209 210 interdigitated, dorsally arched suture posterior to this point. In ventral view the parietals contact 211 the squamosal medially, partially constricting the cranial hiatus (c.184[2]; Figs. 2C-D, 4). **Supraoccipital**—The anterior half of the supraoccipital is not preserved, bu based on its contact 212 with the parietal, it anterior edge formed a gentle semicircular arch that reached anteriorly to a 213 level in line with the anterior half of the squamosal fossa (c.140[0], 153[1]; Fig. 1), resembling 214 the condition observed in *Olympicetus* spp. The preserved portion of the supraoccipital forms a 215 gently concave surface that seems to have lacked the sagittal crest (c.156[?0], 311[0]; Figs. 1, 216 2A-B) observed in other simocetids. The nuchal crest a riented dorsolaterally (c.154[1], 217 c.155[0]), and seem to have been gently sinuous, descending posterolaterally to meet the 218 supramastoid crest (Figs. 1,2A-B, 3). 219 220 **Exoccipital**—The occipital condyles are semilunar in outline, with well-defined edges, and bounded dorsally by shallow, transversely oval supracondylar fossae (c.157[1]; Fig. 2A-B) as in 221 222 Simocetus rayi and Olympicetus avitus. The foramen magnum has an oval outline, being slightly wider than high. The paroccipital processes are transversely broad and oriented posteroventrally, 223 224 approximating the posterior edge of the condyles (c.198[1]; Fig. 2). The ventral edge of the paroccipital processes are anteroposteriorly broad, becoming thinner medially towards the broad 225 jugular notch (c.197[0]). The hypoglossal foramen is rounded (~4 mm in diameter), located 226 ventrolateral to the occipital condyles and well separated from the jugular notch (c.196[0]; Fig. 227 228 2). 229 **Basioccipital**—The basioccipital crests are short, transversely thin, oriented ventrolaterally, and diverging posteroventrally at an angle between 58-60° (c.192[0], 195[2]; Fig. 2). The crest 230 contacts the posterior lamina of the pterygoid along a posteroventrally oriented suture. The 231 ventral surface between the crest is flat, with no distinct tus capitus anticus fossa (c.193[0]). 232 233 Anteriorly the contact with the basisphenoid is obscured by the vomer (Fig. 2C-D). **Squamosal**—The squamous portion is flat to gently convex, contacting the parietals along a 234 dorsally arched suture that extends along a sinuous path to form the posteromedial edge of the 235 236 subtemporal crest (Figs. 1, 3). Only the right zygomatic process is preserved, although 237 incompletely, missing its anterolateral corner. The process is long, oriented anteriorly, robust and



238 somewhat cylindrical when viewed dorsally, constricting the squamosal fossa (c.143[0], 189[3]; 239 Figs. 1, 2C-D, 3-4). The squamosal fossa is relatively deep, with a moderately sigmoidal outline and gently sloping anteriorly (c.147[2], 148[1], 149[1]; Fig. 1). When viewed laterally, the dorsal 240 edge of the zygomatic process is flat to gently convex (c.144[0]), while its ventral edge was 241 242 concave (c.151[0]; Fig. 3-4). The supramastoid crest is more prominent proximally, continuing posteromedially to join the nuchal crest (c.150[0]). The sternomastoid muscle fossa on the 243 posterior edge of the zyogomatic process is a large, shallow oval depression, broadly visible in 244 posterior or lateral view (c.145[1]; Figs. 2A-B, 3). The squamosal exposure lateral to the 245 paroccipital processes is moderate in posterior view (c.146[1]; Fig. 2A-B). Ventrally, the 246 postglenoid process is incompletely preserved, but seems to have been broad as in other 247 simocetids. Posterior to the base of the postglenoid process, the external auditory meatus seems 248 to have been broad (c.190[?0]; the posttympanic process is not preserved). The glenoid fossa is 249 250 shallowly concave with nearly indistinct borders. Medial to the glenoid fossa is a shallow, oval 251 tympanosquamosal recess (c.179[2]; Fig. 2C-D). The falciform process is anteroposteriorly long (c.177[0]; Figs. 2C-D, 3-4). The periotic fossa is partially obscured by a fragment of periotic; the 252 anterior part of the fossa contains a small foramen spinosum close to the medial suture with the 253 parietal (c.187[1]; Fig. 2C-D), resembling the condition observed in *Olympicetus avitus*. 254 Anteromedially, the squamosal contacts the alisphenoid along anterolaterally oriented suture that 255 follows the anterodorsal edge of the groove for the mandibular branch of the trigeminal nerve 256 (c.181[1]); the groove wraps around the posterior end of the pterygoid sinus fossa, opening 257 anteriorly (c.182[1]; Figs. 2C-D, 4). 258 Pterygoid—The pterygoids are incompletely preserved, missing the hamular processes (Fig. 2C-259 260 D). As in other simocetids, the palatal surface seems to have been separated along the midline by a diamond-shaped palatal exposure of the vomer (Fig. 2C-D). Anteriorly, the contact between the 261 ptervgoids and palatine is nearly vertical in lateral view. The ptervgoid sinus fossa is 262 anteroposteriorly long (99 mm) and dorsoventrally deep (at least 63 mm on the left side), 263 264 transversely narrower anteriorly (25 mm) and becoming broader posteriorly (46 mm) (Fig. 2C-D, 4). The anterior edge of the pterygoid sinus fossa is at the level of the pterygo-palatine suture, 265 extending posteriorly to the anterior edge of the foramen ovale (c.164[2]; Fig. 2C-D). The dorsal 266 lamina contacts the orbitosphenoid anterodorsally, the frontal and the alisphenoid 267 268 posterodorsally, along an irregularly sinuous contact, and forms the roof of the pterygoid sinus (c.166[0]; Fig. 4). The lateral lamina seems to have descended ventromedially, but its full extent 269 is unknown (c.165[?0]; Figs. 2C-D, 3-4). The medial lamina is incompletely preserved, but 270 medially contacts the lateral flanges of the horizontal plate of the vomer to form the lateral wail 271 of the choana, while laterally they form the medial wall of the sinus fossa (Figs. 2C-D, 3-4). 272 **Alisphenoid**—Only a small portion of the alisphenoid can be observed on the temporal wall. 273 where its exposure is small, wedged in between the squamosal, frontal and lateral lamina of the 274 ptervgoid (c.142[1]: Figs. 3-4). Ventrally, its suture with the squamosal runs along the anterior 275 276 border of the sulcus for the mandibular branch of the trigeminal nerve; its more anteromedal 277 portions are covered by sediment.

- **Orbitosphenoid/Optic Infundibulum**—The orbitosphenoid is exposed on the temporal wall
- where it is in contact with the parietal dorsally and palatine and pterygoid ventrally. Medially,
- 280 the bones are eroded and the distinct features of the optic infundibulum cannot be properly
- 281 interpreted.
- 282 Mandible—The mandible is missing for the most part, with the exception of the left coronoid
- process (Fig. 1). The process has a subtriangular outline, as preserved being about as long as
- 284 high, with the dorsal edge slightly recurved medially. The general outline resembles the coronoid
- process of *Olympicetus avitus* (Velez-Juarbe, 2017:fig. 7A–B).
- 286 **Dentition**—Only a double-rooted molariform is preserved in association with the specimen (Fig.
- 287 5A-C). The mesial root is mostly missing, but seems to have been buccolingually broader than
- 288 the distal root, which is more cylindrical and slightly recurved buccally. The crown (length = 10
- 289 mm; height = 7 mm; width = 8 mm) is worn, and is longer than tall, and buccolingually broader
- on its anterior half, somewhat resembling tooth 'mo3' of *Olympicetus avitus* (see Vélez-Juarbe,
- 291 2017:fig.70,Bb), however, differing by lacking a well-defined buccal ridge with denticles. The
- 292 crown has three denticles, with the apical one being slightly larger than the two on the distal
- 293 carina, while there are no denticles on the blunter, mesial carina (Fig. 5A-C). There are no buccal
- 294 cingula, and only a nearly inconspicuous cingula is present on the distolingual corner of the base
- 295 of the crown.
- 296 Cervical Vertebrae—Only the first three cervical vertebrae are preserved and are unfused
- 297 (c.279[0], 280[?0]; Fig. 5D-I). The dorsal arch of the atlas is missing, as are the distal end of the
- transverse processes. The anterior articular facets have a semilunar outline, and are shallowly
- 299 concave, with relatively poorly defined ventrolateral and medial edges. The posterior facets for
- articulation with the axis have a suboval outline, with gently convex articular surfaces and sharp,
- 301 well-defined edges. The posterior facets gently merge ventromedially with the articular surface
- for the odontoid (Fig. 5E). The ventral arch has a more prominent hypapophysis than that
- 303 observed in *Olympicetus* spp. (Fig. 5E). The base of the transverse processes flare
- 304 posterolaterally.
- The axis is missing most of the apex and left half of the dorsal arch and the left transverse
- process (Fig. 5F-G). The pedicle is anteroposteriorly broad, and flat transversely, the
- postzygapophysis is oriented posterolateroventrally, forming a flat, smooth surface (Fig. 5G).
- The anterior articular surface is broad, with a suboval outline, and raised edges, the surface is
- 309 shallowly concave, merging ventromedially with the ventral surface of the odontoid (Fig. 5F).
- 310 The odontoid is short, broad and blunt, with a mid-dorsal ridge that extends along the dorsal
- 311 surface of the centrum, reaching the distal end (Fig. 5F). Posteriorly, the centrum has a cardiform
- outline and the epiphysis is fused, and its surface is concave, and has a mid-ventral cleft that
- 313 slightly bifurcates its posteroventral end. The ventral surface of the centrum has a mid-ventral
- 314 keel that becomes broader and more prominent towards the posterior end of the centrum. The
- 315 transverse process is anteroposteriorly flat, and oriented mainly laterally, there are no transverse
- 316 foramina (Fig. 5F-G).



PeerJ

- 317 The third cervical preserves only a portion of the right neural arch; the pedicle is anteroposteriorly flat and transversely broad, both, anterior and posterior, epiphyses are fused 318 (Fig.5H-I). The prezygapophysis consists of a rounded, flat surface that is oriented 319 anterodorsomedially, complementing its counterpart in the axis. The transverse foramen is large, 320 321 being slightly broader than tall (16 mm x 11 mm). The transverse process is mainly oriented laterally, its posterior surface forms a low keel that extends from the base to the apex, and its 322 anteroventral edge is flared (Fig. 5I). The centrum is rounded, anteroposteriorly short, with 323 shallowly concave proximal and distal articular surfaces. Low midline keels are present along the 324 ventral and dorsal surfaces of the centrum. A pair of small (~4 mm) nutrient foramina are present 325 326 on each side of the middorsal keel. Remarks—LACM 124104 represents the largest known simocetid, with an estimated 327 bizygomatic width of 322 mm, in comparison with that of Simocetus ravi (238 mm), which 328 329 (using equation "i" from from Pyenson and Sponberg, 2011) results in estimated body lengths of 330 about 3 m and 2.3 m, respectively, both which are larger than those estimated for *Olympicetus* 331 spp. (see below). This large simocetid shows a unique combination of characters, some which are shared with *Olympicetus* spp. such as the more retracted position of the supraoccipital 332 (c.140[0]), the dorsolateral orientation of the lambdoidal crest (c.154[1]), a shallow 333 334 tympanosquamosal recess (c.179[1,2]), an alisphenoid/squamosal suture that courses along the groove for the mandibular branch of the trigeminal nerve (c.181[1]). At the same time, some of 335 the preserved characters seem to be unique to this taxon amongst simocetids, such as a deep 336 squamosal fossa (c.147[2]) and the path of the groove for the mandibular branch of the 337 trigeminal nerve which wraps around the posterior end of the pterygoid sinus fossa (c.182[1]). 338 339 This specimen does preserve a remarkable amount of details of the size and morphology of the pterygoid sinus fossa, which together with other simocetids, suggest that they had a well 340 developed, large fossae, particularly when compared to those of other early odontocetes, such as 341
- 342 Archaeodelphis patrius, which seems to have a much shorter fossa (pers. obs. LACM 149261,
- cast of type). LACM 124104 resembles, and may be congeneric, with an odontocete skull from
- 344 the early Oligocene Lincoln Creek Formation of Washington State, briefly described by Barnes
- et al. (2001), in many characters of its morphology, including its large size (bizygomatic width =
- 346 265 mm) and the pachyostotic appearance of some of the cranial bones, and will be addressed in
- 347 more detail in a follow-up study.

348

- 349 *OLYMPICETUS* Velez-Juarbe, 2017
- 350 **Type**—*Olympicetus avitus* Velez-Juarbe, 2017.
- **Included Species**—Olympicetus avitus; Olympicetus thalassodon sp. nov., Olympicetus sp. 1.
- 352 Range—Oligocene (late Rupelian–early Chattian; 33.7–26.5 Ma;) of Washington, U.S.A.
- 353 Emended Diagnosis mall odontocetes, with bizygomatic width ranging from 145–220 mm
- 354 (c.333[0,1]), with symmetric skulls and heterodont dentition, resembling *Simocetus rayi*
- Fordyce, 2002. Differs from *Simocetus*, other simocetids, and other stem odontocetes by the
- 356 following combination of characters: having a concave posterior end of the palatal surface of the



- 357 rostrum (c.19[0]; shared with Xenorophidae); posterior buccal teeth closely spaced (c.26[0]; shared with Ashleycetus planicapitis, Patriocetus kazakhstanicus, Agorophius pygmaeus and 358 Ankylorhiza tiedemani), differing from the widely-spaced teeth of S. ravi; buccal teeth with ecto-359 and entocingula (c.32[1], 33[0]; shared with *Xenorophus sloani* Kellogg, 1923, *Echovenator* 360 361 sandersi, Cotylocara macei and P. kazakhstanicus), and unlike S. rayi where these features are absent; lacrimal and jugal separated (c.54[0]; shared with CCNHM 1000, Xenorophidae, P. 362 kazakhstanicus, Ag. pygmaeus and An. tiedemani); presence of a short maxillary infraorbital 363 plate (c.60[1]; shared with CCNHM 1000 and Archaeodelphis patrius); infratemporal crest of 364 the frontal forming a well-defined ridge along the posterior edge of the sulcus for the optic nerve 365 (c.63[0]; shared with Xenorophidae); posteriormost end of the nasal process of the premaxilla in 366 line with the anterior half of the supraorbital process of the frontal (c.75[2]), differing from the 367 longer process of S. ravi; absence of a posterior dorsal infraorbital foramen (= maxillary 368 foramen; c.76[0]), differing from S. rayi which has two foramina on each side located medial to 369 370 the orbit; posteriormost end of the ascending process of the maxilla in line with the posterior half of the supraorbital process of the frontal (c.78[2]; shared with Ashleycetus planicapitis and 371 Archaeodelphis patrius); lack of a premaxillary cleft (c.110[0]; present in S. ravi); anteriormost 372 point of the supraoccipital in line with the floor of the squamosal fossa (c.140[0]), differing from 373 374 the more anterior position in S. ravi; having a relatively shallow squamosal fossa (c.147[1]; shared with Ar. patrius and P. kazakhstanicus), thus differing from the deeper fossae of 375 Simocetus rayi and Simocetidae gen. et sp. A; involucrum of the tympanic bulla lacking a 376 transverse groove (c.272[1]; shared with *C. macei*); dorsal process of atlas larger than ventral 377 process (c.278[2]); presence of three mesial and four distal denticles on main molars (c.328[1], 378 379 329[2]); presence of a transverse cleft on the apex of the zygomatic process of the squamosal (c.335[1]); arched palate, and, saddle-like profile of the skull roof (when viewed laterally). 380
- 381
- 382 *OLYMPICETUS THALASSODON*, sp. nov.
- 383 (Figs. 6-13; Tables 1-5)
- 384 Holotype—LACM 158720, partial skull with articulated mandibles, including 18 teeth,
- tympanic bullae, cervical vertebrae 1–6, and hyoids; missing distal end of rostrum/mandible.
- 386 Collected by J. L. Goedert and G. H. Goedert, July 30, 1983.
- 387 Type Locality and Horizon—LACM Loc. 5123, Murdock Creek, Clallam Co., Washington,
- 388 U.S.A. (48° 09' 25"N, 123° 52' 10"W). See above for additional details.
- **Formation and Age**—Pysht Formation, between 30.5–26.5 Ma (Oligocene: late Rupelian-early
- 390 Chattian; Prothero et al., 2001; Velez-Juarbe, 2017).
- 391 Range—Oligocene of Washington, U.S.A.
- 392 **Differential Diagnosis**—Species of relatively small bodied odontocete with bizygomatic width
- of about 220 mm (c. 333[1]), differing from other simocetids by the following combination of
- 394 characters: posterior wall of the antorbital notch formed by the lacrimal (c.16[1]; shared with
- 395 Simocetus rayi and Xenorophidae); mandible with a relatively straight profile in lateral view
- 396 (c.39[0]), differing from the more strongly arched mandible of *S. rayi*; mandibular condyle



397 positioned at about the same level as the alveolar row (c.46[1]); dorsal edge or orbit relatively low (c.48[2]: shared with Olympicetus avitus. Ashlevcetus planicapitis and Xenorophus spp.): 398 dorsolateral edge of ventral infraorbital foramen formed by lacrimal (c.58[2]; shared with 399 Archaeodelphis patrius, Albertocetus meffordorum and Inermorostrum xenops Boessenecker et 400 401 al., 2017), differing from *Olympicetus* sp. 1 where it is formed by the maxilla, and *O. avitus* where it is formed by the maxilla and lacrimal; posterior edge of zygomatic process forming 402 nearly a right angle with the dorsal edge of the process (c.145[0]); lack of a well-defined dorsal 403 condyloid fossa (c.157[0]; otherwise present on other simocetids); posterior process of the 404 periotic exposed on the outside of the skull (c.250[0]); tympanic bulla proportionately narrow 405 and long (c.252[0]; shared with Echovenator sandersi and Cotvlocara macei), differing from the 406 shorter, wider bulla of *Olympicetus avitus* and *Olympicetus* sp. 1; moderately large bizygomatic 407 width (c.333[2]; shared with S. ravi), differing from the smaller size of O. avitus and 408 Olympicetus sp. 1, or the relatively larger Simocetidae gen. et sp. A; parietals not forming part of 409 410 the supraorbital processes, differing from O. avitus where they extend into the posteromedial part of the process, nasals contacting the maxillae along their posterolateral corners; longer 411 paroccipital and postglenoid processes; teeth with more conical cusps, contrasting with the more 412 lanceolate ones of O. avitus; and, thyrohyals tubular and not fused to basihyal (c.336[0]). 413 Etymology—Combination of thalasso- from the Greek word 'thalassa' meaning 'sea' and -odon 414 from the Greek word 'odon' meaning 'tooth', in reference to the marine habitat of the species 415 and its particular tooth morphology. 416

418 Description

417

419 Description is based on the holotype (LACM 158720), which consists of a nearly complete skull of an adult individual with articulated mandibles and preserving 18 teeth, cervical vertebrae and 420 hyoid elements (Figs. 6-13). Some of the preserved mandibular and maxillary teeth are in situ, 421 allowing for determination of associated, loose teeth. The estimated body length is ~2.15 m, 422 based on equation "i" for stem Odontoceti in Pyenson and Sponberg (2011). The terminology 423 used herein follows Mead and Fordyce (2009). 424 **Premaxilla**—The part of the premaxillae anterior to the premaxillary foramen is not preserved. 425 Each premaxillae preserv single, small (diam. = 3 mm) foramen located far anterior to the 426 427 antorbital notch (c.70[1], 71[0], 72[0]; Fig. 6) The ascending process adjacent to the external nares is divided by a long posterolateral sulcus (c.73[2]) and a short, incipient, posteromedial 428 sulcus (c.319[1]), both which extend from the premaxillary foramen, forming the lateral and 429 anteromedial limits of the premaxillary sac fossa (Fig. 6). The premaxillary sac fossae are flat to 430 shallowly concave, transversely narrow and anteroposteriorly long (c.69[0]; 320[0], 324[1]). 431 432 resembling the condition observed in O. avitus. The premaxilla forms the lateral edges of the external nares and mesorostral canal (c.74[0]). Posterior to the premaxillary sac fossae, the 433 ascending process extends posteriorly as a transversely thin flange, reaching a level just beyond 434 the preorbital process of the frontal (c.75[2]), leaving a narrow gap where the premaxilla contacts 435 436 the nasal. In contrast, in O. avitus the ascending process extends farther posteriorly, to a point



- closer to the middle of the supraorbital processes, separating the nasals from the maxillae (Velez-
- 438 Juarbe, 2017).
- 439 Maxilla—As preserved, the palatal surface is anteroposteriorly concave and transversely convex
- 440 to flat (c.17[0]). Anteriorly the vomer is exposed ventrally through an elongated window
- between the maxillae as in *Simocetus rayi*, similarly, a pair of major palatine foramina are
- located on each side at the proximal end of this opening (c.18[0]; Fig. 7C-D). Posteriorly, the
- maxillentacts the palatines along an anteriorly-bowed contact (c.20[0], 21[0]). The alveolar
- row diverge posteriorly (c.23[0]); it is incompletely preserved anteriorly, but based on the
- preserved dentition and visible alveoli, there were at least seven closely-spaced maxillary teeth,
- with the most posterior six representing double-rooted P1-4, M1-2, with the most anterior of the
- preserved alveoli representing an anteroventrally-oriented single rooted ?canine (c.24[4], 26[0];
- 448 Fig. 8). Posteriorly, the maxillary tooth row extends beyond the antorbital notch, forming a short
- infraorbital plate (c.60[1]; Fig. 9). The ventral infraorbital foramen has an oval outline (15mm
- 450 wide by 9mm high) and is bounded laterally and dorsally by the lacrimal and ventrally and
- 451 medially by the maxilla (c.58[2], 59[0]; Fig. 9).
- 452 Proximally, the rostrum is wide, relative to the width across the orbits (c.7[1]) and the lateral
- edges of the maxillae are bowed out, giving the antorbital notch a 'V'-shaped outline (c.12[1];
- 454 Fig. 6). The surface of the maxillae anterior and anteromedial to the orbits is flat to shallowly
- convex (c.66[0]) lacking the rostral basin observed in some xenorophids (e.g. Cotylocara macei;
- 456 Geisler et al., 2014). As in O. avitus, this surface has clusters of three to four anterior dorsal
- infraorbital foramina with diameters ranging between 4-6 mm with the posteriormost foramen
- located dorsomedial to the antorbital notches (c.65[3]). However, in contrast to *O. avitus* the
- 459 maxillae does not extend anterolaterally to form the posterior wall of the antorbital notch
- 460 (c.16[1]; Figs. 6, 8), thus more closely resembling the condition observed in *Simocetus rayi*.
- Posteromedial to the antorbital notches, the maxillae extends over the supraorbital processes,
- 462 covering a little more than the anterior half of the processes and laterally to within 12 mm of the
- edge of the orbit, while medially they contact the ascending process of the premaxillae and the
- nasals, forming a gently sloping dorsolaterally-facing surface (c. 49[0], 77[1], 78[], 79[0], 80[0],
- 465 130[0], 308[1]; Figs. 6, 8).
- **Vomer**—Dorsally the vomer forms the ventral and lateral surfaces of the mesorostral fossa,
- which seems to have been dorsally open, at least for the length of the rostrum that is preserved,
- and has a V- to U-shaped cross section, having a more acute ventral edge anteriorly (c. 5[0]; Fig.
- 469 6). Anteriorly, along the palatal surface of the rostrum, the vomer is exposed through a narrow
- 470 elongate window mostly between the maxillae and the premaxillae distally, resembling the
- 471 condition in *S. ravi* and possibly, *Olympicetus avitus* (Fig. 7C-D; Fordyce, 2002; Velez-Juarbe,
- 472 2017). The vomer is exposed again towards the posterior end of the palate along a diamond-
- shaped window between the palatines and the pterygoids, resembling S. ravi (Fig. 7C-D:
- 474 Fordyce, 2002), similarly, the vomer seems to have been exposed posteriorly in *O. avitus*.
- although the window may have been comparably smaller. The choanae are not prepared thus
- 476 making it impossible to determine the posterodorsal extension of the vomer (c. 191[?]).



477 **Palatine**—As in *Simocetus* and *Olympicetus avitus* the anterior edge of the horizontal plate of the palatine tend to about 10 mm anterior to the level of the antorbital notches, forming the 478 shallowly concave proximal surface of the palate (Fig. 7C-D). The posterior edge of the palatines 479 are separated in the midline by the vomer even more than in Simocetus (Fig. 7C-D; Fordyce, 480 481 2002). Posterolaterally there is an elevated palatal crest that originates at the contact with the pterygoid hamuli and extends anterodorsally on the orbital lamina, approximating, but not 482 reaching, the infundibulum for the sphenopalatine and infraorbital foramina, it instead become a 483 shallow groove that reaches the sphenopalatine foramen as in O. avitus (Figs. 7C-D, 8). The 484 orbital lamina of the palatine contacts the frontal dorsally to form the posteroventral edge of the 485 sphenopalatine foramen, and the maxilla anteriorly, and forms the ventral edge of the 486 infundibulum for the sphenopalatine and infraorbital foramina (Figs. 8-9). In posterolateral view, 487 the infundibulum has an oval outline, measuring 28 x 15 mm, while the rounded sphenopalatine 488 foramen has a diameter of about 8 mm. Ventrally and laterally, the palatines have a nearly 489 490 transverse contact with the pterygoids (c. 163[1]; Figs. 7C-D, 8), resembling the condition observed in O. avitus, Simocetus rayi and Archaeodelphis patrius. 491 Nasal—The nasals are poorly preserved and seem to have formed the highest point of the vertex 492 (c. 114[?0], 124[0], 125[0], 312[0]; Figs. 6, 8) as in *Olympicetus avitus* and *Simocetus*). 493 Anteriorly, the nasals reach to about 24 mm beyond the antorbital notches, while posteriorly they 494 are in line with the preorbital process of the frontals (c. 81[3], 123[1]; Fig. 6). The nasals are 495 anteroposteriorly elongated, facing dorsally, forming a low transversely convex arch, are 496 dorsoventrally thin (<3 mm) and are separated posteriorly by the narial process of the frontal (c. 497 116[0], 118[0], 120[1], 121[2], 122[1], 312[0], 321[0]). The nasals seem to contact the ascending 498 499 process of the premaxillae for most of their lengths with only their posterolateral corners contacting the maxilla, differing from *Olympicetus avitus* where the premaxilla extend beyond 500 the posterior edge of the nasals (Velez-Juarbe, 2017). 501 Frontal—Dorsally along the midline, the frontals are wedged between the maxillae and 502 posterior edge of the nasals forming a large semi-rectangular surface (c. 126[1]; Fig. 6). At to 503 this point, the frontals are shallowly depressed towards their contact with the parietals, forming a 504 saddle-like outline of the skull roof in lateral view, resembling the condition observed in O. 505 avitus (Fig. 8). The interfrontal suture is completely fused; dorsally the frontals form a broad, V-506 507 shaped contact with the parietals, while its contact along the temporal surface is nearly vertical. The supraorbital processes gently slope ventrolaterally from the midline (c. 47[0]), and only their 508 anterior half is covered by the ascending process of the maxillae (Fig. 6, 8). The preorbital 509 processes are rounded and only partially covered by the maxilla and are thus exposed dorsally; 510 anteriorly they contact the maxilla and the lacrimals anteroventrally. The postorbital processes 511 are blunt, longer and oriented posterolaterally and ventrally to a level nearly in line with the 512 lacrimals when viewed laterally (c. 62[0]; Fig. 8). The orientation of the postorbital processes 513 give the orbit a slight anterolateral orientation in dorsal view, while in lateral view, the orbits are 514 highly arched and positioned high relative to the rostral maxillary edge as in O. avitus (c. 48[2]; 515 516 Figs. 6, 8). The posterior edge of the supraorbital process is defined by a relatively sharp



517

parietals. 518 Ventrally, in the orbital region, the frontals contact lacrimals anterolaterally to form the anterior 519 edge of the orbits (Figs. 8-9). More medially the frontals contact the maxillae and palatines, 520 521 forming the posterodorsal border of the infundibulum for the sphenopalatine and infraorbital foramina (Figs. 8-9). Medially, the optic foramen has an oval outline (~10 x 5 mm) and is 522 oriented anterolaterally: the posterior edge of the optic foramen and infundibulum is defined by a 523 low infratemporal crest (c. 63[0]; Fig. 9). As in Simocetus rayi and O. avitus a small (~3 mm 524 diameter) ethmoid foramen (sensu Fordyce, 2002) is located anterolateral to the optic foramen, 525 526 while a series of additional, smaller foramina (1-2 mm) are located more laterally. Lacrimal + Juga Only a small, cylindrical portion of the proximal end of the jugal is 527 preserved, it is set in a close-fitting socket formed by the lacrimal anterodosally, and the maxilla 528 529 anteriorly and ventrally (c. 54[0], 55[0]; Figs. 8-9). As preserved, the jugal is visible only in 530 lateral or ventral views, as dorsally it is covered by the lacrimal, and resembles the condition observed in cf. Olympicetus sp. of Racicot et al. (2019). The lacrimals are enlarged and shaped 531 like a thick rod that covers the anterior surface of the preorbital processes of the frontals (c. 532 51[1], 52[0], 53[1]; Figs. 6, 8-9). The lacrimals are broadly visible in dorsal view as they are not 533 covered by the maxilla as in *Olympicetus avitus*, thus resembling the condition observed in 534 Simocetus ravi: ventrally their exposure is anteroposteriorly short relative to the length of the 535 supraorbital process of the frontal (c. 56[0]), but are elongated mediolaterally, forming the 536 dorsolateral and dorsal edges of the ventral infraorbital foramen (c. 58[2]), differing from O. 537 avitus where it is formed by the maxilla and lacrimal. 538 539 Parietal—The parietals are broadly exposed in dorsal view, with no clear indication of the presence of an interparietal (c. 135[0], 136[1]; Fig. 6), although it is visible in some 540 ontogenetically young specimens that can be referred to Olympicetus (Racicot et al., 2019; see 541 discussion). Anteriorly in dorsal view, the parietals meet the frontals along a broad V-shaped 542 543 suture, with its anterolateral corners extending for a short distance along the base of the postorbital processes of the frontals, although not as far as in *Olympicetus avitus*. Posterior to the 544 frontal-parietal suture there is a low incipient crest that gives the intertemporal region an ovoid 545 cross section (c. 137[1]), similar to the condition in O. avitus and Simocetus rayi. As in O. avitus, 546 547 the parietals contact the supraoccipital along an anteriorly convex suture when viewed dorsally. The temporal surface of the parietal is flat to shallowly concave anteriorly, with a near vertical 548 suture with the frontal (c. 134[0]; Fig. 9) as it descends to form the posterior wall of the optic 549 infundibulum; the temporal surface of the parietal then becomes more inflated posteriorly and 550 posteroventrally where it contacts the squamosal and alisphenoid (Figs. 6, 8). The anteroventral 551 edge of the parietals form a semilunar notch that likely contacted part of the alisphenoid and the 552 dorsal lamina of the pterygoid, then continuing posteriorly to form part of the subtemporal crest. 553 **Supraoccipital**—The anterior edge of the supraoccipital form a semicircular arch when viewed 554 posteriorly and dorsally, extending as far anteriorly to nearly the anterior edge of the squamosal 555 556 fossa (c.140[0], 153[1]) as in Olympicetus avitus and Simocetus rayi (Figs. 6-7A-B). The

orbitotemporal crest that becomes blunter towards its contact with the orbital processes of the



557 posterior surface is incompletely preserved, but seems to have had a low sagittal crest (c.156[?1]. 311[?0]). The nuchal crest are oriented dorsolaterally (c.154[1]), curving posteriorly and 558 ventrally to meet the supramastoid crest of the squamosals (Figs. 6, 7A-B, 8). 559 Exoccipital—The occipital condyles have a semilunar outline and are transversely and 560 561 dorsoventrally convex, with sharp dorsal and lateral edges. Although the bone is poorly preserved, there is no indication for the presence of well-defined dorsal condyloid fossae 562 (c.157[0]), differing from *Olympicetus avitus* (Fig. 7A-B). The surface lateral to the condyles is 563 shallowly convex transversely and the paroccipital processes are broad, oriented posteroventrally 564 to a point nearly, but not reaching the posterior edge of the condyles (c.198[2]; Fig. 6). 565 **Basioccipital**—The basioccipital is partially covered by part of the atlas posteriorly and hyoids 566 posteroventrally (Fig. 7). The basioccipital crest are oriented ventrolaterally, diverging 567 posteriorly at about an angle of between 60-70°, and seem to have been transversely narrow 568 (c.192[0]); 195[2]), with their posteroventralmost end forming a small flange as in *Simocetus* 569 rayi (c.194[2]; Fig 7C-D). No well-developed ctus capitus anticus fossa is discernible on the 570 ventral surface (c.193[0]). 571 Squamosal—The zygomatic processes are partially eroded, more so on the left side, however, its 572 general morphology is conserved. The processes are oriented anteriorly (c.143[0]) and seems to 573 have been relatively long (c.189[?3]). In lateral view the dorsal edge of the zygomatic process is 574 greatly convex dorsally (c.144[0]), while ventrally they are strongly concave (c.151[0]) (Fig. 8). 575 The apex of the zygomatic process has a transverse cleft (best preserved on the right side: 576 c.335[1]; Fig. 8), which is present in the type of *Olympicetus avitus* as well as in CCNHM 1000, 577 and may as well be a unique feature of the genus (Racicot et al., 2019). Posteriorly the 578 579 sternomastoid fossa is nearly absent (c.145[0]), contrasting with the deeper fossa observed in O. avitus and Olympicetus sp. A (see below). In dorsal view, the zygomatic processes are 580 mediolaterally broad, forming a transversely narrow and relatively shallow squamosal fossa as in 581 O. avitus (c.147[1]; Fig. 6). The floor of the squamosal fossa is slightly sigmoidal, sloping gently 582 towards its anterior end (c.148[1], 149[0]), and is bounded laterally and posteriorly by a fairly 583 continuous supramastoid crest (c.150[0]), which extends medially to join the nuchal crest (Fig. 584 6). Medially, the squamous portion is flat, with an interdigitated suture with the parietals that 585 slope anteroventrally at about 45° towards the anterior edge of the squamosal fossa and 586 587 subtemporal crest and contacting the alisphenoid. Posteroventrally, the postglenoid process is long, more so than in Simocetus rayi and O. avitus, and anteroposteriorly broad, with near 588 parallel anterior and posterior borders that end in a squared-off ventral end (c.152[2]; Figs. 7C-589 D, 8). Abaft the postglenoid process, the external auditory meatus is deep and anteroposteriorly 590 broad (c.190[0]), bounded anteriorly by a low anterior meatal crest, that, as in O. avitus, seems to 591 592 have formed the posterior edge of a fossa for the reception of the sigmoid process of the squamosal. The posttympanic process does not extend as far ventrally as the postglenoid process: 593 its ventral surface is well sutured to the posterior process of the tympanic bulla (Figs. 7C-D, 8). 594 595 In ventral view, the glenoid fossa is poorly defined, although medially there is a very shallow, 596 nearly indistinguishable tympanosquamosal recess (c.179[?1,2]), as in O. avitus and S. rayi.



- Anteromedially the falciform process anteroposteriorly broad with a nearly square outline (about
- 598 15 mm by 15 mm; c.177[0]), contacting most of the anteriprocess of the periotic (fig. 10C). In
- posterior view, the squamosal has a relatively small exposure lateral to the exoccipitals (c.
- 600 146[1]; Fig. 7A-B).
- Pterygoid—In ventral view, the pterygoids form robust, cylindrical hamular processes that are
- not excavated by the pterygoid sinus (c.173[1], 174[0]) and are separated anteriorly along the
- 603 midline by a diamond-shaped exposure of the vomer, resembling the condition observed in
- 604 Simocetus rayi (Fig. 7; Fordyce, 2002:fig. 4). The hamuli are long, extending posteriorly as far as
- the level of the middle of the zygomatic processes (c.175[3]). Although not preserved, the lateral
- lamina likely formed the anterior and lateral surfaces of the pterygoid sinus fossa. The dorsal
- lamina extends dorsally, reaching the frontal, and, judging from the preserved sutures,
- posteriorly, to join the parietal and alisphenoid, forming the roof of the sinus fossa as in
- 609 Olympicetus avitus (c.166[0]; Fig. 8-9). As in Simocetus rayi, the ventralmost point of the
- 610 pterygoid sinus fossa is at the base of the hamuli just anterior to the eustachian notch, suggesting
- 611 that the nasal passages were underlaid by the sinus fossa (Fig. 7C-D). The medial lamina forms
- 612 the deep eustachian notch, and bulges laterally at this point; posteriorly, it extends to contact the
- 613 basioccipital crests. The pterygoid sinus fossa is dorsoventrally broad (~45 mm high), and
- 614 somewhat compressed mediolaterally (~23 mm wide), extending forwards to the level of the
- posterior edge of the supraorbital process of the frontal (c. 164[2]; Figs. 7C-D, 8-9).
- 616 **Alisphenoid**—Only small portions of the alisphenoids can be observed on both sides. In lateral
- only a small portion of the alisphenoid is exposed on the temporal fossa, where it forms the
- posteromedial part of the subtemporal crest (c.142[1], 166[0]) as in other Olympicetus (Velez-
- 619 Juarbe, 2017; see below).
- **Orbitosphenoid/Optic Infundibulum**—The orbitosphenoid is fused with surrounding bones,
- 621 unlike the ontogenetically younger specimen of *Olympicetus avitus*. Within the optic
- 622 infundibulum, the foramen rotundum and orbital fissure seem to have a similar diameter, both
- being transversely broader (~10 mm) than high (~6 mm) (Fig. 9), with the first located in a
- slightly more posteromedial position, resembling the condition in O. avitus (Fig. 9). However, no
- 625 distinct groove for the ophthalmic artery is preserved in *Olympicetus thalassodon*, differing from
- 626 Simocetus rayi, O. avitus and Olympicetus sp. A (Fordyce, 2002:fig.13; Figs. X-X). The foramen
- of rotundum is not prepared, but is inferred that, as in *O. avitus*, it opens ventrolateral to the orbital
- fissure, with the path for the maxillary nerve (V2) being bound ventrally by the pterygoid and
- 629 palatine (Fig. 9).
- 630 **Periotic**—Only a small portion is visible on the right side. The anterior process contacts the
- falciform process anteriorly for about half its length. Posterior to this contact, a portion of the
- anterior process is visible, as is the epitympanic hiatus, which is bounded posteriorly by a
- 633 prominent ventrolateral tuberosity (Fig. 10C).
- 634 **Tympanic Bulla**—Both bullae are still articulated with the cranium and mainly visible in ventral
- 635 view (Fig. 10). The tympanic bullae are transversely narrow and elongated (c.252[0]), differing
- from the proportionately broader bullae of *Olympicetus avitus* and *O.* sp. A (see below). In



637 ventral view, the lateral surface is more convex and the more straight medial side, anteriorly it is gently convex, with not indications of the presence of a spine (c.251[0]). The posterior surface of 638 the bullae is bilobed, being divided by a broad interprominential notch (c.267[1]) that is divided 639 by a transverse ridge (c.268[0]), differing from the bulla of *Olympicetus avitus*, but resembling 640 641 that of *Olympicetus* sp. A. Both posterior prominences are level with each other (c.270[0]), the ventromedial keel forms a smooth curve posteriorly (c.253[0]), while more anteriorly it is poorly 642 defined as this surface is nearly flat (c.274[2], 275[?0]). The outer posterior prominence forms a 643 continuous curve along its length, connecting with the conical process. 644 A vertical, broad lateral furrow can be observed in lateral view (c.257[0], 258[0]), while more 645 646 dorsally the sigmoid process curves posteriorly at the base, and is nearly vertical and perpendicular to the long axis of the bulla (c.259[0], 260[0]; Fig. 10B-C). Although not entirely 647 visible, the dorsal edge of the sigmoid process likely contacted the sigmoid fossa of the 648 squamosal (c.261[?0]). The posterior process is partially visible at its contact with the 649 650 posttympanic process and is visible in lateral view (c.250[0]; Figs. 7C-D, 8, 10A-B), and seems to have had more or less the same thickness throughout its length (c.266[0]). 651 Mandible—Left and right mandibular rami are nearly in articulation with the skull and are only 652 missing coronoid processes and their distal ends, including the symphyseal region (Figs. 7C-D. 653 8). As preserved, the mandibles are nearly straight, gently arching dorsally at about mid length 654 (c.39[0], 43[1]; Figs. 7C-D, 8), differing from the highly arched mandible of Simocetus ravi 655 (Fordyce, 2002). Proximally, the bone seems to be thin, likely forming an enlarged mandibular 656 fossa (c.44[1]). Posterodorsally on the right side, the lateral edge of the condyle can be observed, 657 suggesting that its dorsal surface sits at a level at, or below the alveolar row (c.46[1]; Fig. 8). 658 659 Anteriorly, the right ramus preserved five double-rooted teeth in-situ, which are interpreted as representing p3-4 and m1-3, while the left ramus preserves three, that are interpreted as m1-2 660 and p4 (Figs. 8-9, 11-12). Multiple mental foramina are longitudinally arranged along the rami 661 below the alveolar row, most are oval, ranging in size from 2 to 4 mm in height and up to 10 mm 662 663 long, with the more posterior ones connected by a fissure as in *Olimpicetus avitus* (Fig. 8; Velez-Juarbe, 2017:fig.7A). 664 **Dentition**—Taking a conservative approach to the tooth count, it is interpreted as non-polydont 665 as in Simocetus rayi (Fordyce, 2002), although incipient polydonty cannot be entirely ruled out, 666 667 as it seems to be present on other stem odontocetes from the eastern North Pacific (e.g. LACM 140702; Barnes et al., 2001). Between the teeth and alveoli, the preserved upper and lower 668 dentition is interpreted to represent C, P1-4, M1-2 and p3-4, m1-3 (Figs. 8-9, 11-12). The teeth 669 are proportionately large, heterodont, multicusped, transversely flattened and nearly as high as 670 long (c.31[1], 314[0]), resembling the condition observed in postcanine teeth of *Olympicetus* 671 avitus, Olympicetus sp. A and Simocetus ravi (Figs. 8-9, 11-12). As in Olympicetus avitus and 672 Simocetus ravi, the postcanine teeth of O. thalassodon have a more conca uccal surface. 673 while being more convex lingually, with the apex of the crowns slightly recurved lingually, the 674 675 base of the crowns are ornamented with vertical striae extending apically from ecto- and 676 entocingula, particularly on the posteriormost upper teeth (c.27[1], 32[1], 33[0]; Figs. 11-12).



677 The crowns consist of a main apical denticle, and smaller accessory denticles along the mesial and distal edges, both apical and accessory denticles are more triangular than the more lanceolate 678 ones observed in O. avitus (c.34[0]; 35[0]; Figs. 11-12; Velez-Juarbe, 2017). In double-rooted 679 teeth, the roots become fused proximally, with broad grooves on both, buccal and lingual sides 680 681 that extend to the base of the crowns, giving them an 8-shaped cross section as in Simocetus ravi (Fordyce, 2002). In P4 and M1 the anterior root is cylindrical, tapering distally, while the 682 posterior roots are buccolingually broader and oblong in cross section, while in M2 this 683 condition is reversed, with the anterior root being transversely broader; the roots of the lower 684 teeth seem to be subequal in size, both being cylindrical and tapering distally. 685 686 The anteriormost end of the right maxilla has a single alveolus (diameter = 6mm) that curves posterodorsally and is interpreted as that of a canine, which is separated by a short interalveolar 687 septum from two adjoining alveoli (each with a diameter ~7mm) for a double-rooted P1 (Figs. 8. 688 11B). The second (P2) and third (P3) upper premolars are missing on the left side and 689 690 incompletely preserved on the right, they are slightly higher than long, consisting of a main denticle with at least two accessory denticles on the mesial and distal edges, resembling teeth 691 'ap1' and ap2' of O. avitus (Velez-Juarbe, 2017:fig.7D-E, Q-R). Three closely associated teeth 692 that became disarticulated from the maxilla, but still joined by matrix, and three other loose 693 teeth, represent left and right P4, M1-2; these are more equilateral, being as long as wide, with 694 stronger lingual and labial cingula and ornamentation along the base of the crowns: P4 and M1 695 consist of a main apical denticle, with four distal and three mesial accessory denticles that 696 diminish in size towards the base (c.328[1], 329[2]; Figs. 11E-H, 12A-B, 12E-F), their overall 697 morphology resembles that of teeth 'mo1' and 'mo2' of Olympicetus avitus (Velez-Juarbe, 698 2017; fig. 7M-N, Z-Aa). The second molar (M2) is the smallest of the series and the crown is 699 longer than tall, it consists of a main apical denticle, four distal and two mesial accessory 700 denticles, the apices of all denticles are slightly slanted distally (Figs. 11D, 11I, 12C-D). As in 701 Simocetus rayi and Xenorophus sloanii, the mesial and distal keels on the upper posterior 702 703 postcanines trend towards the buccal side of the teeth so that in occlusal view, the apical and accessory denticles are arranged in an arch (Fordyce, 2002; Uhen, 2008). These characteristics 704 allow for the reassignment of some of the teeth of *Olympicetus avitus*, with teeth 'mol' and 705 'mo2' representing right and left M2, respectively, while 'ap1' and 'ap2' represent left upper 706 premolars (Velez-Juarbe, 2017:fig.7). An isolated single-rooted tooth is interpreted as a canine or 707 incisor (FIg. 12H-I). The crown is conical, with vertical striation along its lingual surface and a 708 buccal cingulum; anterior and posterior carinae seem to be present, with larger denticles along 709 the distal edge. Another isolated tooth adjacent to the posterior end of the left maxilla, seems to 710 represent a more anterior upper postcanine tooth (Fig. 12J). Overal resembles M2, but it's 711 712 mesial carina is partially damaged, so it is unclear if any accessory denticles were present, while the distal carina contains three denticles that diminish in size basally, however, the denticles are 713 714 not recurved distally, and is larger than M2, but smaller than M1. 715 The preserved lower dentition includes p3-4, m1-3, and p4, m1-2 on the right and left mandibles, 716 respectively (Figs. 8, 11A-C, 12C). As with the upper premolars, p3-4, m1-3 have a triangular



outline, with mesial and distal carinae aligned verticall trending lingually as the upper 717 molars. Furthermore, in p3-4 and m1-2 the mesial carinae has two accessory denticles that are 718 much smaller than the apical denticle, while along the distal carinae there are three to four 719 accessory denticles, with the apical ones being nearly as big as the apical denticle, and then 720 721 diminish in size towards the base of the crown (Fig. 8, 11A-C, 12C). There is nearly no ornamentation along the buccal side of the lower premolars and molars, with only a few 722 723 inconspicuous vertical striae, but no prominent cingulum, while lingually striae are more prevalent, and a cingulum is present (Figs. 11A-C, 12G). As in the upper toothrow, m3 is the 724 smallest in the series, seemingly lacking accessory denticles on the mesial carina, and having 725 726 three subequal ones along the distal carina. As with the preceding teeth, ornamentation is nearly absent on the buccal side (Fig. 11A). The lower postcanine dentition of Olympicetus thalassodon 727 then seems to be characterized by having less conspicuous ornamentation on the buccal side, and 728 729 more vertically aligned carinae, based on these characteristics, it is proposed that teeth 'pp1', 730 'pp2' and 'pp5', 'pp7' of Olympicetus avitus (see Velez-Juarbe, 2017:fig.7F-G, J, L, S-T, W, Y) represent lower anterior molars remolars from the left and right side respectively. 731 **Hvoid**—Most of the hvoid elements are preserved in LACM 158720, including the basihval. 732 stylohyals and thyrohyals (Fig. 13A-C). The basihyal has a rectangular, blocky outline, with both 733 ends expanded, forming broad, quadrangular rugose surfaces for the articulation of the paired 734 735 elements (stylo- and thyrohyals). The mid portion is subtriangular cross section, the dorsal surface is shallowly concave transversely, the partial, left thyrohyal obscures the posteroventral 736 surface of the bone. The partial left and the complete right thyrohyals and stylohyals are 737 preserved (Fig. 13A-C). The thyrohyals are not fused to the basihyal and are fairly straight, with 738 739 a transversely oval cross section at mid-length; overall they are shorter, but more robust than the stylohyals, and not flattened, wing-like as in derived mysticetes and odontocetes (c.336[0]; Fig. 740 13). The proximal articular surface has a rectangular outline, and the surface is rugose and 741 shallowly convex, distally, the shaft is twisted, so that the distal articular surface is nearly 742 743 perpendicular to the long axis of the proximal surface. The distal articular surface has a more oval outline that is rugose and shallowly convex. The stylohyals are long and slender, and, on the 744 right side, nearly in articulation with the paroccipital process (Fig. 13A-B). Along the long axis 745 they are bowed laterally, with the shaft having a more flattened, oval cross section along its 746 747 length, with both, proximal and distal ends expanded, being overall, nearly identical to the stylohyoid of *Olympicetus avitus* (Velez-Juarbe, 2017). The proximal end is transversely 748 expanded with a nearly flat, rugose articular surface, distally, the shaft becomes twisted, so that 749 the distal end is offset at about 45° from the proximal articular surface. The lack of fusion 750 between the thyrohyal and basihyal, and the cylindrical shape of the thyrohyal resembles the 751 752 condition observed in basilosaurids (e.g. Durodon atrox [Andrews, 1906], Cythiacetus peruvianus Martínez-Cáceres and de Muizon, 2011; Uhen, 2004; Martínez-Cáceres et al., 2017). 753 some stem mysticetes (e.g. Mammalodon colliveri Pritchard, 1939, Fucaia buelli Marx et al., 754 755 2015, Mystacodon selenensis Lambert et al., 2017; Fitzgerald, 2010; Muizon et al., 2019); while 756 in more derived odontocetes (e.g., Brygmophyseter shigensis (Hirota and Barnes, 1995), Kogia



- 757 breviceps (Blainville, 1838), Albireo whistleri Barnes, 1984, Kentriodon nakajimai Kimura and
- Hasegawa, 2019, *Tursiops truncatus* (Montagu, 1821); Fig. 13D-G) these bones are partially or
- 759 completely fused and the thyrohyals tend to be more flattened and plate- or wing-like
- 760 (Reidenberg and Laitman, 1994; Hirota and Barnes, 1995; Barnes, 2008; Johnston and Berta,
- 761 2011; Kimura and Hasegawa, 2019).
- 762 Cervical Vertebrae—The atlas, axis and C3-7 are partially preserved, and unfused (c.279[0],
- 763 280[0]; Fig. 14; Table 2). The dorsal arch of the atlas has a low, blunt middorsal ridge that
- extends nearly the whole length of the arch. The vertebral foramen is broken, although it seems
- to have occupied the same position as that of *Olympicetus avitus* (Velez-Juarbe, 2017). The
- anterior articular facets are obscured as the atlas is still attached to the skull, while the posterior
- facets have a reniform outline, and form a dorsoventrally elongate, smooth, flat surface that
- extends dorsal to the articulation for the odontoid (Fig. 14A). On the ventral arch, the
- 769 hypapophysis that would have articulated with the odontoid is short as in O. avitus and unlike the
- 1770 longer, more robust process of Simocetidae gen. et sp. A, and *Echovenator sandersi* (Churchill et
- al., 2016). The transverse processes are gently oriented posterolaterally, and are divided into a
- larger, more robust dorsal process and a smaller, knob-like ventral process that are divided by a
- broad, rounded notch (c.278[2]; Fig. 14A). The neural canal has an oval outline.
- 774 The axis is missing the dorsal arch, the odontoid is short and blunt. The anterior articular surface
- has a subtriangular outline forming a flat to shallowly concave surface that extends
- anteroventrally, being continuous with the ventral surface of the odontoid (Fig. 14B). The
- transverse processes are oriented posterolaterally, with a triangular outline when viewed
- anteriorly, their ventral surface is anteroposteriorly broad, forming a flat surface that faces
- ventrally and slightly posteriorly, with a sharp anterior edge (Fig. 14B-D). Dorsomedially, the
- 780 posterior surface of the transverse processes form a relatively deep, concave surface. Cervicals 3-
- 781 6 are missing their dorsal arches and transverse processes for the most part, while only a small
- 782 portion of C7 is preserved. The centra are anteroposteriorly flat and slightly wider than high, the
- 783 epiphyses are unfused (Fig. 14C-D). The transverse process of C3 is partially preserved and its
- 784 morphology is similar to that of the axis.
- 786 *OLYMPICETUS* sp. 1
- 787 (Figs. 15-19; Tables 1, 3, 6)
- 788 Material—LACM 124105, partial skull, including two partial teeth, left tympanic bulla and
- 789 right periotic; missing distal end of rostrum, zygomatic arches, parts of the neurocranium and
- 790 mandible. Collected by J. L. Goedert December 17, 1983.
- 791 Locality and Horizon—LACM Loc. 5123, Murdock Creek, Clallam Co., Washington, U.S.A.
- 792 (48° 09' 25"N, 123° 52' 10"W). See above for additional information from this locality.
- 793 Formation and Age—Pysht Formation, between 30.5–26.5 Ma (Oligocene: late Rupelian-early
- 794 Chattian: Prothero et al., 2001: Velez-Juarbe, 2017).
- 795 Range—Oligocene of Washington, U.S.A.

796

785

PeerJ

797

Description

- The description is based solely on LACM 124105 and will focus on morphological characters
- 799 that differentiates from Olympicetus avitus and O. thalassodon. As with the type of Olympicetus
- avitus, LACM 124105 seems to represent a subadult individual, showing some partially open
- sutures. Multiple areas of the skulls show evidence of erosion (e.g. rostrum, skull roof), likely as
- a result of wave action as specimens from this locality are usually recovered as concretions along
- 803 the beach.
- Premaxillae—Only part of the left ascending process of the premaxilla is preserved (Fig 15).
- The ascending process borders the external nares as it ascends towards the vertex (c.74[0]),
- 806 however, its incomplete preservation posterior to the nasals does not permit identification of its
- posteriormost extent. A relatively deep sulcus extends along its anterior border which is
- 808 consistent with the placement and morphology of the posterior extent of the posterolateral sulcus
- 809 in *Olympicetus avitus* (c.73[2); Fig. 15; Velez-Juarbe, 2017).
- 810 Maxilla—Only part of the rostral portion of the maxilla is preserved (Figs. 15-17). Ventrally, the
- palatal surface is incompletely preserved along the midline and along the alveolar rows,
- 812 however, the parts that are preserved indicate that it was transversely convex, with the alveolar
- 813 rows slightly more elevated. Posteriorly, the contact between the maxillae and palatines is bowed
- anteriorly (c.20[?0], 21[1]; Fig. 16) as in other *Olympicetus*. The alveolar row, although
- 815 incompletely preserved, diverged posteriorly, and had at least three pairs of closely-spaced,
- double-rooted postcanine teeth (c.23[0], 26[0]). Based on the preserved posterior border of the
- alveolar row, it seems that at least a short maxillary infraorbital plate was present (c.60[1]). In
- 818 posteroventral view, the ventral infraorbital foramen has an oval outline (~12 mm wide by 9 mm
- 819 high); its dorsolateral edge is formed by the maxilla, dorsomedially by the frontal, and ventrally
- and ventromedially by the maxilla (c.58[0], [59[0]).
- 821 In dorsal view, the rostrum seems to have been fairly wide (c.7[1]; Fig. 15). At the base of the
- 822 rostrum, the maxillary surface faces dorsolaterally, and is shallowly convex to flat as it ascends
- 823 over the supraorbital processes of the frontal, thus as in other species of *Olympicetus*, it lacks a
- rostral basin (c.66[0]; Fig. 15). At the base of the rostrum, there are at least three anterior dorsal
- infraorbital foramina ranging in diameter between 2-5 mm, with a fourth, more posterior
- foramen, dorsomedial to the antorbital notch (c.65[3]; Figs. 16, 17). The maxillae are eroded at
- the level of the antorbital notch, so it is uncertain if these formed part of the posterior wall of the
- 828 notch as in *Olympicetus avitus*. The ascending process of the maxillae partially covers the
- 829 supraorbital processes of the frontal, extending posteriorly beyond the anterior half of the
- processes, and posteromedially, coming into contact with the frontals and forming a gently
- sloping surface towards the edge of the orbits, but not reaching its borders (c.49[0], 77[1], 78[2],
- 832 79[0], 80[0], 130[0], 308[1]; Fig. 15).
- 833 **Vomer**—The vomer is mostly missing anterior to the antorbital notches and eroded
- anteroventrally, nevertheless, it is evident that it formed the lateral and ventral surfaces of the
- 835 mesorostral fossa. Ventrally, the vomer likely was exposed through a diamond-shaped window
- towards the posterior end of the palate as in other simocetids (Fig. 16). Dorsal and posterodorsal

PeerJ

837 to this point the vomer forms the nasal septum, forming the medial walls of the choanae. From the posterior palatal exposure, the vomer gently slopes posterodorsally, to form a triangular. 838 horizontal plate extending over the still open, basisphenoid-presphenoid contact, but not reaching 839 as far posterior as the fused basisphenoid/basioccipital contact (c.191[0]; Fig. 16). The horizontal 840 841 plate of the vomer has a triangular outline, contacting the dorsal laminae of the pterygoids along its anterolateral end (Figs. 16-17). 842 **Palatine**—Only some very small fragments of the right palatine are preserved. The contact 843 between the palatines and maxilla seems to have been bowed anteriorly (c.20[?0], 21[1]; Figs. 844 16-17). Posterodorsally, a fragment of the orbital lamina of the palatine reaches the frontal, 845 forming part of the infundibulum for the sphenopalatine and infraorbital foramen, as well as the 846 posterior border of a round (~5 mm diameter) sphenopalatine foramen (Fig. 17). The 847 infundibulum has an oval outline, being broader than high (20 mm x 10 mm), and is bounded 848 dorsally by the frontal and lacrimal, and the maxilla ventrally and ventrolaterally (Fig. 17). 849 850 Nasal—Although incompletely preserved, the nasals seem to have been the highest point of the vertex, were longer than wide and dorsoventrally thin, as in other simocetids (c.114[0], 116[0], 851 118[?0], 124[0], 125[0], 312[0]; Fig. 15). Along their posterior border, they are separated by the 852 narrow, narial process of the frontal (Fig. 15). The anterior edge of then nasals is incompletely 853 854 preserved, but extended far forward of the anterior edge of the supraorbital processes, while posteriorly they reach a level in line with midpoint of the supraorbital processes (c.81[3], 123[1]; 855 Fig. 15). 856 Frontal—As in other *Olympicetus*, there is a wedge-shaped exposure of the frontal along the 857 midline, surrounded by the maxilla laterally and nasals anteriorly, although poor preservation of 858 859 the surrounding bones does not allow precise determination of size relative to the nasals (Fig. 15). Along the midline, the bone is poorly preserved, although it does seem like the frontal are 860 lower than the nasals, preserving the saddle-like profile (in lateral view) seen in other species of 861 Olympicetus. Posteriorly, the frontal-parietal suture seems to have been broadly V-shaped 862 dorsally, and sinusoidal in the temporal region, with no interve no of the parietals into the 863 supraorbital processes. Laterally, the supraorbital processes slope very gently ventrolaterally 864 (c.47[?0]). Dorsally, the maxillae only cover the supraorbital processes to a point beyond their 865 mid-point, but do not extend laterally over the orbit (c.78[2]), leaving the preorbital and 866 867 postorbital processes broadly exposed dorsally (Fig. 15). Anteroventrally, the preorbital processes contact the lacrimal. The postorbital processes are incompletely preserved, but seem to 868 have been relatively short, robust, and oriented posteroventrolaterally (Fig. 15). In lateral view 869 the dorsal edge of the orbit is highly arched, but positioned at a lower position (c.48[1]), relative 870 to the lateral edge of the rostrum, than is observed in *Olympicetus avitus* or *O. thalassodon*. A 871 low, sharp temporal crest extends anterolaterally from near the frontal/parietal suture and into the 872 posterodorsal and dorsal surface of the supraorbital process (c.132[2]; Fig. 15), differing from 873 the condition in other *Olympicetus*. 874 875 Ventrally, the frontal contact the lacrimal anteroventrally, and the maxilla and/or palatine more

medially, resulting in the frontal forming part of the posterodorsal edge of the infundibulum for

876



- 877 the ventral infraorbital and sphenopalatine foramina (Figs. 16-17). The optic foramen is partially
- 878 covered by sediment, its general orientation seems to be anterolateral, with its posterior border
- being defined by a low, but sharp infratemporal crest (c.63[0]). Similar to other simocetids, a
- small (~3 mm diameter) ethmoid foramen is anterolateral to the optic foramen, and is
- accompanied by four to five smaller (1-2 mm) foramina located along the dorsolateral roof of the
- 882 orbit (Figs. 16-17).
- 883 Lacrimal + Jugal—Only a small portion of the jugal is preserved, but it is evident that it was
- not fused with the lacrimal (c.54[0], 55[0]; Fig. 17). The portion of the jugal that is preserved is
- stout and cylindrical, tapering medially, and wedged between the lacrimal and maxilla, which
- excludes it from forming part of the ventral infraorbital foramen (Fig. 17). The lacrimals are
- large, and rod-like, but with a relatively small ventral exposure (c.51[1], 56[0]). It contacts the
- preorbital process of the frontal anteroventrally, tapering medially, and seems to have been
- exposed anteriorly, forming part of the posterior wall of the antorbital notch, but not extending
- dorsally onto the supraorbital process (c.52[0]; Fig. 15, 17).
- Parietal— parietals are exposed dorsally, but badly eroded (c.135[0], 136[?]; Fig. 15). The
- parietals contact the frontal along a broad, V-shaped suture, but differ from other species of
- 893 *Olympicetus* in that they do not extend into the base of the supraorbital processes. In cross
- section through the intertemporal region, the parietals seem to have an ovoid outline (c.137[?1]).
- 895 resembling the condition in other *Olympicetus*. Along the temporal surface the parietal has a
- 896 sinuous suture with the frontals anteriorly, and the temporal surface becomes more inflated
- posteriorly towards its contact with the squamosal and alisphenoid (Fig. 17). Ventrally, the
- 898 parietal has an internal projection that contacts the squamosal medial to the periotic fossa,
- constricting the cranial hiatus as in other simocetids (c.184[2]; Fig. 16).
- 900 **Supraoccipital**—The supraoccipital is only partially preserved, with the exception of its
- 901 dorsolateral borders. The lambdoidal crests are sharp, directed dorsolaterally and only slightly
- 902 overhanging the temporal fossa (c.154[1]; Fig. 15), curving posteroventrally to join the
- 903 supramastoid crest of the squamosal.
- 904 Exoccipital—Gen ly poorly preserved. Dorsal to the remaining parts of the right occipital
- 905 condyle, there is what seems to be a shallow dorsal condyloid fossa (c.157[?1]). The surface
- 906 lateral to the condyles is flat to shallowly convex.
- 907 **Basioccipital**—As preserved, the basioccipital crests seem to have been relatively thick
- 908 transversely (c.192[?1]) and oriented posterolaterally, at about an angle of 45 degrees (c.195[3];
- 909 Fig. 16). The rest of the ventral surface is incompletely preserved.
- 910 **Squamosal**—The zygomatic processes are incompletely preserved. Posteromedially, the
- 911 sternomastoid fossa forms a distinct emargination that is overhung dorsally by the supramastoid
- 912 crest much more than in *Olympicetus avitus* (c.145[1]; Fig. 15). The supramastoid crest seems to
- 913 have been continuous with the lamboidal crest (c.150[0]). The squamous portion contacts the
- parietal along an anteroventrally sloping interdigitated suture, meeting the alisphenoid to form
- part of the subtemporal crest. Ventrally, the squamosal is heavily eroded, and only a small



- 916 portion of the periotic fossa is preserved, where it contacts the medial extension of the parietal
- (Fig. 16). 917
- **Pterygoid**—Most of the pterygoid is missing on both sides of the skull. A portion of the dorsal 918
- lamina extends posterodorsally towards the parietal and contributes to the posteroventral edge of 919
- 920 the optic infundibulum as in *Olympicetus avitus* (Fig. 17). As preserved, the pterygoid sinus
- fossa is anteroposteriorly longer than wide, and is located entirely anterior to the foramen ovale 921
- (c.164[2], 169[0]; Figs. 16-17). 922
- Alisphenoid—As in *Olympicetus avitus*, the alisphenoid forms the posterodorsal surface of the 923
- pterygoid sinus fossa (Figs. 16-17). The medial and posterior ends of the bone are incompletely 924
- preserved or eroded on both sides, making it difficult to determine the position of the alisphenoid 925
- squamosal suture or the path of the mandibular nerve (V3). On the temporal wall, the exposure 926
- of the alisphenoid is limited to a small sliver, as it is mostly overlapped by the parietal and the 927
- squamosal (c.142[1]; Fig. 17). 928
- 929 **Basisphenoid**—Posteriorly the basisphenoid is fused with the basioccipital, while anteriorly its
- contact to the presphenoid (sphenoidal synchondrosis) is still open, resembling the growth stage 930
- of the type of Olympicetus avitus (Velez-Juarbe, 2017). The ventral surface is flat, and covered 931
- by the horizontal plate of the vomer (Fig. 16). 932
- 933 Optic Infundibulum—The optic infundibulum is a slightly sinusoidal opening bounded by the
- frontal anteriorly and dorsally, parietal posteriorly, pterygoid ventrally and anteroventrally (Fig. 934
- 17). The optic foramen, orbital fissure and foramen rotundum are still partly covered by 935
- sediment. The frontal forms most of the borders of the optic foramen anterodorsally, while 936
- posteroventrally the foramen rotundum was bounded laterally by the parietals and floored by the 937
- 938 pterygoid. The anteroventral edge of the parietals that forms part of the infundibulum, has a
- narrow groove that trends anterodorsally, and would have carried the ophthalmic artery, 939
- resembling the condition in Simocetus rayi and Olympicetus avitus (Fig. 17; Fordyce, 2002; 940
- Velez-Juarbe, 2017). While along the ventral edge of the infundibulum, the pterygoid has a 941
- 942 distinct, but shallow groove, that would have presumably carried the maxillary nerve (V2),
- extending along its dorsolateral surface and diverging slightly over its lateral surface anteriorly 943
- 944 (Fig. 17).
- 945 Malleus—The left malleus is still articulated with the corresponding tympanic (Fig. 18). The
- 946 head has a semicircular outline, with paired facets for articulation with the incus, that are
- oriented at about 90 degrees to each other; the more anterior facet is about as twice as large as 947
- 948 the posterior one as in *Olympicetus avitus* (Fig. 18; Velez-Juarbe, 2017). The tubercle is
- relatively large, nearly as long as the head (c.199[0]; Fig. 18). The manubrium is prominent and 949
- slightly recurved posteroventrally (Fig. 18). The anterior process is fused laterally to the 950
- tympanic, dorsally forming a continuous surface with the mallear ridge, while its ventral edge is 951
- shelf-like, together forming a deep, narrow sulcus for the chorda tympani (Fig. 18A, C, E). 952
- **Tympanic Bulla**—Only the left tympanic bulla is preserved (Fig. 18), but missing its posterior 953
- process, overall it closely resembles in size and morphology that of Olympicetus avitus (Velez-954
- 955 Juarbe, 2017). In dorsal or ventral view, the bulla has a heart-shaped outline, being relatively



short and wide (c.252[1]), unlike the larger and transversely narrower bulla of Olympicetus 956 thalassodon (Figs. 10, 18). The ateral surface is broadly convex, while medially it is straight; the 957 posterior prominences gives the bulla a bilobed outline posteriorly while anteriorly, the lateral 958 surface converges medially more steeply than the medial surface along a smooth curve, there is 959 960 no indication of the presence of an anterior spine (c.251[0]). Posteriorly, a broad interprominential notch extends from the level below the elliptical foramen, continuing along the 961 ventral surface of the bulla for only about a third of its length (c.267[0]). The interprominential 962 notch is divided by a transverse ridge (c.268[0]; Fig. 18D), resembling the condition observed in 963 Olympicetus thalassodon, differing from that of O. avitus, which does not have an 964 interprominential ridge. The inner and outer prominences extend posteriorly to nearly the same 965 level (c.270[0]). The ventromedial keel is poorly defined, forming a smooth curve around the 966 posterior part of the involucrum, its posteromedial surface just slightly bulging farther medially 967 than the rest of the involucrum (c.253[0], 274[2], 275[0], 276[0]). The elliptical foramen seems 968 969 to have been narrow, and nearly vertical (c.262[0]). In lateral view, the ventral edge of the bulla is nearly flat (c.269[0]), differing from the more 970 broadly concave ventral margin observed in some xenorophids, like *Albertocetus meffordorum* 971 (Uhen, 2008). The ventrolateral keel forms a blunt ridge that descends ventrolaterally from the 972 conical pyramidal process. The lateral furrow is nearly vertical, forming a relatively broad sulcus 973 (c.257[0], 258[0]; Fig. 18B). Dorsally, the sigmoid process is vertical and perpendicular to the 974 long axis of the bulla (c.259[0]), with its posterior edge curving anteriorly along a smooth curve 975 (c.260[0]). The mallear ridge extends obliquely from the anteromedial base of the sigmoid 976 process towards the dorsalmost extension of the lateral furrow. A narrow, dorsally open sulcus 977 978 for the chorda tympani extends anteriorly for a length of 17 mm along the dorsomedial edge of the outer lip, originating at the junction between the anterior process of the malleus and the 979 mallear ridge (Fig. 18A, C, E). The anterodorsal crest descends steeply towards the anterior edge 980 of the bulla. 981 982 In medial view the dorsal and ventral edges of the involucrum gradually converge towards the anterior end of the bulla (c.271[0]; Fig. 18A). The involucrum has numerous, faint vertical ridges 983 (c.272[1]), differing from the deeper grooves observed in xenorophids, like *Albertocetus* 984 meffordorum (Uhen, 2008). 985 986 **Periotic**—Only the right periotic is preserved (Fig. 19A-H) and is overall very similar to that of CCNHM 1000 described by Racicot et al. (2019). The anterior process is oriented anteriorly and 987 short relative to the length of the cochlea, with its anteroventral and anterodorsal ends being 988 bluntly pointed, that together gives it a nearly squared-off outline (c.201[0], 202[0], 204[2]; Fig. 989 19C-D). In medial view, the apex of the anterior process is slightly deflected ventrally, forming a 990 991 slightly convex to flat surface (c.203[1], 205[0]; Fig. 19C-D). In lateral view, at the base of the anterior process there is a shallow, C-shaped sulcus that begins near the anterodorsal edge. 992 curves posteroventrally towards the lateral tuberosity, then curving anterodorsally, that is 993 interpreted as a combined anteroexternal+parabullary sulcus (sensu Tanaka and Fordyce, 2014; 994 995 Fig. 19G-H). This condition resembles that of other early odontocetes such as Waipatia



996 maerewhenua Fordyce, 1994, Papahu taitapu Aguirre-Fernández and Fordyce, 2014, and Notocetus vanbenedeni Moreno, 1892, but differs from others like Otekaikea marplesi (Dickson, 997 1964) where these sulci are separate, and from the much deeper sulcus in *P. taitapu* (Tanaka and 998 Fordyce, 2014; Viglino et al., 2022). In cross-section, the anterior process is ovoid, being taller 999 1000 $(\sim 14 \text{ mm})$ than wide $(\sim 9 \text{ mm})$ (c.209[1]). The anteroventral surface of the anterior process has as well-defined anterior bullar facet (c.210[3]; Fig. 19E-F). Posterior to the anterior bullar facet, the 1001 fovea epitubaria forms a smooth curve that is interrupted by a prominent lateral (ventrolateral) 1002 1003 tuberosity (c.212[1]). The lateral process has a triangular outline in ventral view, but does not 1004 extend as far laterally as in other stem odontocetes such as Cotylocara macei (Geisler et al., 1005 2014), being instead barely visible in dorsal view. A similarly, broadly arched epitympanic hiatus lies posterior to the lateral tuberosity and anterior to the base of the posterior process 1006 1007 (c.213[1]). Posteromedial to the epitympanic hiatus, is a small (diameter: ~2 mm) rounded fossa 1008 incudis, while anterior to it and medial to the lateral tuberosity is a broad (diameter: ~6 mm), 1009 circular mallear fossa (c.214[1], 215[0]; Fig. 19E-F). The lateral surface of the periotic is generally smooth with the exception of the posterior process, whose lateral surface is rugose 1010 (c.217[2]; Fig. 19G-H). Medially, the anterior process is separated from the cochlea by a well-1011 defined groove (anterior incisure, sensu Mead and Fordyce, 2009) that extends anterodorsally, 1012 and marks the origin for the tensor tympani muscle (c.218[1]). 1013 1014 In dorsal view, a low crest delimits the dorsolateral surface of the periotic, it extends from the 1015 low pyramidal process towards the anterodorsal spine of the anterior process (Fig. 19A-B). Medial to this crest is an elongated depression, the suprameatal fossa, which is about 13.5 mm 1016 1017 long by 7 mm wide, and around 1.5 mm deep (Fig. 19A-B). The fundus of the internal acoustic 1018 meatus is funnel-shaped, with an oval outline, delimited by a low ridge (c.235[0]; 236[0]). The area cribosa media and the spiral cribiform tract are separated by a very low ridge, these two are 1019 1020 in turn separated from the superior vestibular area (previously called the foramen singulare; Ichishima et al., 2021) by a low transverse crest that lies about 3 mm below the upraised rim of 1021 1022 the internal acoustic meatus, while its separation from the dorsal opening of the facial canal by a 1023 ridge that is slightly lower (~4 mm from the edge of the rim) (c.237[2]; Fig. 19A-B). The proximal opening of the facial canal has an oval outline and located anterolateral to the spiral 1024 cribriform tract (c.238[0], 239[1]); anterodorsally it is bridged, forming a "second" foramen, 1025 1026 which is smaller and rounded (Fig. 19A-D), resembling the condition observed in other early odontocetes, such as Waipatia maerewhenua, and similarly, it is interpreted as the foramen for 1027 the greater petrosal nerve (Fordyce, 1994). The endolymphatic duct (vestibular aqueduct) is slit-1028 like (~4 mm long by 1 mm wide), and located posterolateral to the internal acoustic meatus, just 1029 below the more vertical posterior surface of the pyramidal process, and separated from the 1030 1031 fenestra rotunda by a very wide distance (c.230[3]; Fig. 19A-D). In contrast, the perilymphatic duct (cochlear aqueduct) is rounded (diameter = 3mm) and located posteromedial to the internal 1032 acoustic meatus and medial to the endolymphatic duct, and broadly separated from the fenestra 1033 1034 rotunda (c.228[1], 229[2]). A small, curved depression posteroventral to the endolymphatic duct is interpreted as a shallow stylomastoid fossa (c.225[1]). The dorsomedial surface of the cochlear 1035



1036 portion has a shallow depression that accentuates the raised medial rim of the internal acoustic 1037 meatus. In medial view, the cochlea is relatively flat (maximum height ~11 mm), its ventromedial surface is anteroposteriorly convex and a low, faint ridge extends along its 1038 1039 ventrolateral end (c.221[0]; Fig. 19C-F). In ventral view, the cochlear portion has a subrectangular outline (c.219[1], 220[1], 222[1]). Posteriorly, the fenestra rotunda is located 1040 1041 towards the lower half of the posterior surface, and it is wider than high (4 x 2 mm), with a 1042 kidney-shaped outline (c.223[0]). Posterolateral to the fenestra rotunda, the caudal tympanic process projects farther posteriorly than the rest of the posterior surface of the cochlea, although 1043 1044 it is not as prominent as that of other simocetids (i.e. CCNHM 1000; Racicot et al., 2019), and its 1045 ventral and posterior borders intersect along a curved edge (c.226[1]; Fig. 19C-F). Ventrally, the 1046 foramen ovale is longer than wide (4 x 3 mm), and located towards the posterior half of the 1047 cochlea. The ventral opening of the facial canal (~2 mm in diameter) is lateral to the foramen 1048 ovale, and are separated by a sharp crest. The facial canal opens posteroventrally, and continues 1049 as a groove that merges with the stapedial muscle fossa at the base of the posterior process; the fossa is deep and rounded, with its posterodorsal edge nearly in line with the fenestra rotunda 1050 1051 (c.224[0]).1052 The posterior process is short and robust, with its long axis is oriented posterolaterally (c.246[1], 247[1], 249[0]; Fig. 19A-B, E-F). Proximally, the lateral surface of the posterior process is 1053 1054 rough, with an irregular, near vertical ridge interpreted here as a poorly-developed articular rim (c.240[1]), resembling the condition in other simocetids (i.e. CCNHM 1000) and early 1055 odontocetes like *Notocetus vanbenedeni*, and differing from the more prominent articular rim 1056 1057 observed in platanistids (Muizon, 1987; Racicot et al., 2019; Viglino et al., 2022; Fig. 19A-B). the dorsal edge of the posterior process forms a straight line (c.248[0]). The posterior bullar facet 1058 1059 has a kite-shaped outline, its surface is smooth and shallowly concave transversely (c.242[0], 1060 243[0]); the edges of the facet are sharp, with the exception of the posteromedial edge which is rounder (c.244[0]). 1061 1062 **Dentition**—Only two, incompletely preserved teeth are associated with LACM 124105 (Fig. 1063 19I-L). Both are postcanine teeth, with striated enamel and ecto- and entocingula and denticles (c.27[1], 32[1] 33[0], 35[?1]). As in other simocetids, the buccal surface of the crowns are more 1064 concave. The roots are long and conical, becoming fused proximally. Tooth PCa (Fig. 19I, K) 1065 1066 measures 12 mm long by 6 mm wide, while tooth PCb (Fig. 19J, L) measures 9 mm high and 6 1067 mm wide. 1068 Remarks—LACM 124105 shows multiple diagnostic features with the other named species of Olympicetus, such as having a broadly open temporal fossa, unfused lacrimal/jugal (c.54[0]), 1069 lacking a maxillary foramen (c.76[0]), and maxilla covering only about the anterior half of the 1070 1071 supraorbital process (c.77[1]). However, it does differ by having a more sharply defined infratemporal crest, orbit at a lower position relative to the edge of the rostrum (c.48[1]). 1072 1073 dorsolateral edge of ventral infraorbital foramen formed by the maxilla (c.58[0]), and more 1074 notably, the lateral end of the temporal crest extends along the posterodorsal surface of the 1075 supraorbital process of the frontal (c.132[2); Fig. 15). These differences are considered to be



species-related, and not the result of ontogenetic change as this specimen shows a similar growth stage as the type of *Olympicetus avitus* (LACM 149156; Vélez-Juarbe, 2017). Nevertheless, because of its incomplete preservation, it is preferably left in open nomenclature until better material belonging to this taxon is identified.

1080 1081

Discussion

- 1082 While particular attention has been paid to Oligocene mysticetes from the North Pacific over the
- 1083 last few decades (e.g. Barnes et al., 1995; Okazaki, 2012; Marx et al., 2015; Peredo et al., 2018;
- 1084 Solis-Añorve et al., 2019; Hernández-Cisneros, 2022; Hernández-Cisneros and Nava-Sánchez,
- 1085 2022), the same cannot be said with regards to the odontocetes. Oligocene odontocetes from
- around the North Pacific are not entirely missing from the scientific literature and have been
- mentioned multiple times, often identified informally as "non-squalodontid odontocetes",
- "agorophiid" or "Agorophius-like" (see Whitmore and Sanders, 1977; Goedert et al., 1995;
- Barnes, 1998; Barnes et al., 2001; Fordyce, 2002; Hernández Cisneros et al., 2017). However,
- 1090 given their importance, most of these have yet to be properly described and our understanding of
- species richness and relationships between Oligocene odontocetes from the North Pacific is not
- 1092 fully understood.
- 1093 The first of these taxa to be described was *Simocetus rayi* from the early Oligocene Alsea Fm. of
- 1094 Oregon which was placed in its own family, Simocetidae (Fordyce, 2002). Since then, only two
- other North Pacific Oligocene odontocetes had been named, specifically, the platanistoid
- 1096 Arktocara yakataga from the Oligocene Poul Creek Fm. in Alaska, which is likely one of the
- 1097 earliest crown odontocetes, and the stem odontocete *Olympicetus avitus* from the Pysht Fm. in
- Washington (Boersma and Pyenson, 2016; Vélez-Juarbe, 2017). More recently, Racicot et al.
- 1099 (2019) described a neonatal skull (CCNHM 1000) from the Pysht Fm. in Washington, that
- 1100 closely resembles *Olympicetus avitus*, but did not group with *Simocetus ravi* nor with *O. avitus*,
- and instead all three taxa occupied different positions outside of crown odontocetes (Racicot et
- 1102 al., 2019).
- 1103 Herein, the description of three additional specimens from the mid-Oligocene Pysht Formation in
- 1104 Washington have potentially clarified the relationship between stem odontocetes from the North
- 1105 Pacific. The phylogenetic analysis including these new specimens, resulted in 36 most
- parsimonious trees 3649 steps long, with retention index (RI) = 0.520 and consistency index (CI)
- 1107 = 0.182. Other statistical values are shown in the strict consensus tree (Fig. 20). Based on these
- 1108 results, Simocetidae now seem to form a monophyletic group that includes S. rayi, CCNHM
- 1109 1000, *Olympicetus* spp. and a large unnamed simocetid (Fig. 20). Furthermore, the phylogenetic
- analysis recovered CCNHM 1000 as part of the Simocetidae, differing from the analysis of
- 1111 Racicot et al. (2019) where it was recovered at the base of a clade including all odontocetes, with
- the exception of Xenorophidae. As discussed by Racicot et al. (2019) CCNHM 1000 does
- 1113 resemble *Olympicetus avitus*, more specifically, based on the new specimens described here, it
- shares with *Olympicetus* spp. having-closely-spaced posterior buccal teeth (c.26[0]), buccal teeth
- with ecto- and entocingula (c.32[1], 33[0]), presence of a small maxillary infraorbital plate



1116 (c.60[1]), and the presence of a transverse cleft on the apex of the zygomatic process (c.335[1]). 1117 amongst others. However, CCNHM 1000, does show some dental characteristics that sets it apart 1118 from O. avitus as discussed by Racicot et al. (2019), and others that differentiates it from other 1119 specimens of *Olympicetus*, such as having a relatively lower position of the orbit (c.48[1]; shared 1120 with S. rayi and Olympicetus sp.), 63[1], presence of an interparietal (c.136[0]), a more anterior position of the apex of the supraoccipital (c.140[1]), and a very low lambdoidal crest (c.154[2]). 1121 1122 Some of these characters, such as the position of the apex of the supraoccipital and the morphology of the lambdoidal crest are also observed in the neonate skull referred to O. avitus, 1123 1124 suggesting that these characters change ontogenetically, with neonatal individuals displaying 1125 more plesiomorphic conditions. Along these same lines, the presence of a distinct interparietal in 1126 CCNHM 1000 is considered as another plesiomorphic character, that when combined with the other characters mentioned previously, it is suggestive that this may account for the more basal 1127 1128 position of CCNHM 1000 in the phylogenetic analysis (Fig. 20). Besides this, it seems clear that 1129 CCNHM 1000 should be regarded as a neonate of *Olympicetus* sp. The inclusion of CCNHM 1000 has some interesting implications for Simocetidae. Racicot et al. 1130 (2019) described the inner ear morphology of CCNHM 1000 showing that it does not have the 1131 capability of ultrasonic hearing, which is suggestive that other taxa within this clade are also 1132 non-echolocating odontocetes and may be a characteristic unique to this family. Future studies 1133 1134 on the inner ear morphology of the periotics of other simocetids, such as Simocetus ravia 1135 Olympicetus sp. 1 (LACM 124105), will likely provide more information to this regard.

11361137

Stem Odontocetes from the North Pacific

1138 The early odontocete clade Simocetidae now includes six OTUs: Simocetus rayi, Olympicetus avitus, Olympicetus sp. (LACM 124105), O. thalassodon (LACM 158720), an unnamed large 1139 1140 simocetid (LACM 124104) and CCNHM 1000 (Fig. 20). All specimens, with the exception of S. rayi, are from the Pysht Fm., with four of them: LACM 124104, LACM 124105, LACM 158720 1141 1142 and CCNHM 1000, coming from the same general area (LACM Loc. 5123). The results of the 1143 phylogenetic analysis resemble those of an earlier, preliminary study that also recovered a monophyletic Simicetidae composed of most of the OTU's used here as well as a few others 1144 undescribed specimens from the eastern North Pacific, but that also recovered Ashleycetus 1145 1146 planicapitis, from the early Oligocene of South Carolina, as part of that clade (Velez-Juarbe, 2015). In contrast, the results of the present work suggest that Simocetidae represents an endemic 1147 radiation of North Pacific stem odontocetes, that parallels that of the Aetiocetidae in the same 1148 region (Hernández Cisneros and Velez-Juarbe, 2021), and the Xenorophidae (here considered to 1149 include Ashlevcetidae and Mirocetidae; Fig. 20) in the North Atlantic and Para-Tethys (Marx et 1150 al., 2016a). The occurrence of crown (i.e. *Arktoca akataga*) as well as stem (Simocetidae) 1151 odontocetes in the Oligocene of the North Pacific suggest that the initial diversification of crown 1152 1153 odontocetes must have occurred during the latest Eocene to earliest Oligocene (Boersma and 1154 Pyenson, 2016). This highlights the importance of the fossil record of the North Pacific towards 1155 further understanding the early history and radiation of odontocetes.



1156 At present, there are no published accounts of simocetids from the western North Pacific. although these are expected to be present based on the occurrence of closely-related marine 1157 tetrapods in Oligocene deposits on both sides of the basin (e.g., plotopterids, desmostylians, 1158 aetiocetids; Olson, 1980; Domning et al., 1986; Ray et al., 1994; Olson and Hasegawa, 1996; 1159 Inuzuka, 2000; Barnes and Goedert, 2001; Sakurai et al., 2008; Ohashi and Hasegawa, 2020; 1160 Mayr and Goedert, 2016, 2022; Mori and Miyata, 2021; Hernández-Cisneros and Vélez-Juarbe, 1161 2021), which makes this apparent absence an interesting question. However, some records from 1162 Japan bear close resemblance to simocetids and should be analyzed further. These include a 1163 mandible with two cheek teeth (KMNH VP 000011) and an isolated tooth (KMNH VP 000012) 1164 1165 referred by Okazaki (1988) to Squalodon sp. from the Oligocene Waita Formation of the Ashiya Group. The general morphology of the mandible (KMNH VP 000011) resembles *Olympicetus* 1166 thalassodon and other basal odontocetes with multi-cusped cheek teeth, such as Prosqualodon 1167 1168 davidis Flynn, 1947, and Waipatia maerewhenua, where the dorsal surface of the condyle is at 1169 about the same level as the horizontal ramus and the ventral border is relatively straight (Flynn, 1947; Fordyce, 1994). Furthermore, the two cheek teeth preserved with KMNH VP 000011 are 1170 much more like those of *Olympicetus* with the more anterior tooth (B3 in Okazaki, 1988) having 1171 only a small accessory denticle along the base of the mesial edge, while three larger ones 1172 distally, that increase in size apically, greatly resembling the premolars of O. thalassodon (Figs. 1173 11A, C, 12G). Meanwhile, the second tooth (B7 in Okazaki, 1988) resembles the m3 of 1174 1175 Olympicetus thalassodon, by being smaller than the more anterior teeth, and having three 1176 accessory denticles along the distal edge that diminish in size towards the base of the crown, 1177 lacking accessory denticles along the mesial carina, and little to no ornamentation on the buccal 1178 side. The isolated tooth (KMNH VP 000012) resembles cheek tooth 'pp4' of Olympicetus avitus, as they are relatively low and long, with multiple accessory denticles along the mesial and distal 1179 1180 edges, as well as having lingual and buccal cingula (Okazaki, 1988; Vélez-Juarbe, 2017). One distinguishing character is that the accessory denticles of *Olympicetus* spp. and the Waita Fm. 1181 1182 odontocetes are closer in size to the main cusp than those of other basal odontocetes with multi-1183 cusped cheek teeth. For example, lower cheek teeth of Squalodon calvertensis, Prosqualodon davidis, P. australis Lydekker, 1894, Phoberodon arctirostris Cabrera, 1926, and Waipatia spp. 1184 do have accessory denticles along their distal edges, but are obviously much smaller than the 1185 1186 main cusp (Kellogg, 1923; Flynn, 1947; Fordyce, 1994; Tanaka and Fordyce, 2015; Gaetan et al., 2019; Viglino et al., 2019). The combination of these morphological features suggest that the 1187 specimens described by Okazaki (1988), could be considered as aff. Olympicetus sp., although 1188 this needs to be confirmed by direct observation of the specimens. Other cetaceans from the 1189 Ashiva Group include a toothed mysticete from the Waita Fm., originally assigned to 1190 1191 Metasqualodon synthetricus, but now considered to represent an aetiocetid, and the eomysticetid Yamatocetus caniliculatus from the Jinnobaru Fm. (Okazaki, 1987, 2012; Fitzgerald, 2010). 1192 1193 Similarly, other potential records of simocetids are found in the late Oligocene El Cien 1194 Formation of Baja California Sur. Hernández-Cisneros et al. (2017) briefly discussed two skulls 1195 from the El Cien Fm., comparing one with Simocetus rayi and the other with an undescribed



- 1196 skull (USNM 205491) from the Alsea Fm., and may represent other undescribed simocetids. These odontocetes from El Cien Fm. are currently under study (A. E. Hernández-Cisneros, pers. 1197 comm.), and other described taxa from this formation include kekenodontids, aetiocetids, 1198 eomysticetids and other stem mysticetes (Hernández-Cisneros and Tsai, 2016; Hernández-1199 1200 Cisneros et al., 2017; Solis-Añorve et al., 2019; Hernández-Cisneros, 2022; Hernández-Cisneros 1201 and Nava-Sánchez, 2022). These records from the Jinnobaru Fm., and El Cien Fm., resemble the odontocete assemblage of the Pysht Fm. which includes simocetids, aetiocetids and other early 1202 mysticetes, and is therefore likely that simocetids are would be present in these units as well 1203 1204 (Barnes et al., 1995; Peredo and Uhen, 2016; Vélez-Juarbe, 2017; Shipps et al., 2019; Hernández
- 1205 Cisneros and Vélez-Juarbe, 2021; this work).

1206 1207

Dentition and Feeding in Simocetids

1208 As in most other groups of stem odontocetes (e.g. xenorophids, agorophiids), simocetids have 1209 heterodont dentition, but do seem to have a more conservative tooth count, closer to that of basilosaurids such as Cynthiacetus peruvianus (Martínez-Cáceres and Muizon, 2011), which 1210 1211 consists of three incisors, one canine, four premolars, two upper and three lower molars, a pattern that is also observed in early mysticetes like *Janjucetus hunderi* Fitzgerald, 2006, and 1212 1213 Mystacodon selenensis (Fitzgerald, 2010; Lambert et al., 2017). While the tooth count of some 1214 simocetids is hard to interpret (e.g. Olympicetus avitus; Vélez-Juarbe, 2017), others such as Simocetus ravi and Olympicetus thalassodon offer more definite clues with regards to their 1215 1216 dentition. In the case of Simocetus rayi, its tooth count seems to be secondarily reduced from the 1217 plesiomorphic condition through the loss of the upper incisors, while the lower ones are retained (Fordyce, 2002). Although mostly missing, the teeth of S. rayi were widely separated and 1218 comparatively small (when compared to those of Olympicetus). In contrast, the teeth of 1219 1220 Olympicetus thalassodon are closely spaced and based on the preserved teeth and alveoli, its 1221 dental formula is tentatively interpreted as ?I3, C, P4, M2/?i3, c, p4, m3. If these interpretations 1222 are correct, then the dentition of simocetids is the most plesiomorphic amongst odontocetes, 1223 paralleling that of basal mysticetes. This would contrast with xenorophids which seem to have polydont dentition, for example, *Xenorophus sloanii* and *Echovenator sandersi*, both have 1224 significantly higher count of postcanine teeth (Sanders and Geisler, 2015; Churchill et al., 2016). 1225 1226 Nevertheless, the dentition of many xenorophids is still unknown, including key taxa, such as Archaeodelphis patrius, which may offer additional insight into early odontocete dental 1227 1228 evolution.

229 Although simocetids seem to share similar conservative tooth counts and generalized features of their teeth, there are some interesting differences between some of the species. One conspicuous difference between the dentition of *Olympicetus avitus* and *O. thalassodon* is the presence of a "carnassial"-like tooth in the former (tooth 'mo3' in Velez-Juarbe, 2017:fig.7O,Bb). This tooth is distinguished from all other postcanine teeth by having a ridge with accessory denticles that descends lingually from the apex, while its root is expanded lingually, giving the impression of the presence of three roots (mesial, distal and lingual), rather than two (mesial and distal) as in



the other postcanine teeth. Meanwhile, a third, linguary oot seems to be present in the P4 of 1236 1237 Simocetus ravi (Fordyce, 2002), as well as in an unnamed Simocetus-like taxon from the Lincoln Creek Fm. (Barnes et al., 2001), and could be a character that is shared among some simocetids. 1238 1239 although better preserved specimens are needed to corroborate this. Interestingly, tooth B7 1240 (sensu Sanders and Geisler, 2015) of Xenorophus sloani seems to present a more inconspicuous version of the "carnassial" tooth of simocetids, this tooth occupies a similar position of that of P4 1241 of Simocetus rayi, and is likely a character that should be explore further as more specimens 1242 1243 become available. 1244 Some of the morphological characters observed in described simocetids, such as the arched 1245 palate, short and broad rostrum, smaller and widely-spaced teeth, as in *Simocetus ravi*, are interpreted as features of a bottom suction feeder (Fordyce, 2002; Werth, 2006; Johnston and 1246 Berta, 2011). Some of these features, such as the arched palate are also present in *Olympicetus*. 1247 1248 however, O. thalassodon, has closely spaced, larger teeth, as well as a relatively gracile, unfused 1249 hyoid apparatus (Figs. 11-13A-C; Johnston and Berta, 2011; Viglino et al., 2021), which suggest that this taxon was instead a raptorial or combined feeder. Taking this into account, it is likely 1250 1251 that simocetids employed different methods of prey acquisition, likely akin to the amount of variation observed in other contemporaneous groups, such as xenorophiids, which include taxa 1252 with long narrow rostra (e.g. Cotylocara macei; Geisler et al., 2014) that can be interpreted as 1253 1254 raptorial feeders, as well as brevirostrine suction feeding taxa (i.e. *Inermorostrum xenops*; 1255 Boessenecker et al., 2017). Thus it seems that multiple methods of prey acquisition evolved 1256 iteratively across different groups of odontocetes soon after their initial radiation. 1257

Conclusions

1258

1259 Three new specimens of odontocetes from the middle Oligocene Pysht Formation were described 1260 herein further increasing our understanding of richness and diversity of early odontocetes, specially for the North Pacific region. Inclusion of this new material in a phylogenetic analysis 1261 1262 showed that Simocetidae is a much more inclusive clade, that, besides Simocetus rayi, it-now 1263 includes Olympicetus avitus, O. thalassodon sp. nov., Olympicetus sp. 1, and a large unnamed taxon. Of these, *Olympicetus thalassodon* is the one of the most completely known simocetids, 1264 offering new information on the morphology of early odontocetes, while the inclusion of 1265 CCNHM 1000 within this clade suggest that simocetids may represent a clade of non-1266 echolocating odontocetes. This shows that some morphological features that have been 1267 1268 correlated with the capacity to echolocate, such as an enlarged attachment area for the maxillonasolabialis muscle, and presence of a premaxillary sac fossae (Fordyce, 2002; Geisler et 1269 1270 al., 2014), appeared before the acquisition of ultrasonic hearing. Furthermore, the dentition of 1271 simocetids, as interpreted here, seems to be the most plesiomorphic amongst odontocetes, while 1272 other craniodental features within members of this clade suggests various forms of prey 1273 acquisition, including raptorial or combined in *Olympicetus* spp., and suction feeding in 1274 Simocetus (as suggested by Fordyce, 2002). Meanwhile, body size estimates for simocetids show 1275 that small to moderately large taxa are present in the group, with the largest taxon represented by



- 1276 LACM 124104 with an estimated body length of 3 meters, which places it as the largest known
- simocetid, and amongst the largest Oligocene odontocetes, only surpassed in bizygomatic width
- 1278 (and therefore estimated body length) by the xenorophids *Mirocetus riabinini* and *Ankylorhiza*
- 1279 tiedemani (Boessenecker et al., 2020; Sander et al., 2021). Finally, the new specimens described
- here add to a growing list of Oligocene marine tetrapods from the North Pacific, further
- 1281 facilitating faunistic comparisons across other contemporaneous and younger assemblages, thus
- 1282 improving our understanding of the evolution of marine faunas in the region.

Acknowledgements

- 1285 I wish to extend my gratitude to E. M. G. Fitzgerald (MV), N. D. Pyenson (USNM), R. E.
- 1286 Fordyce (UO) and M. Viglino (CONICET-CENPAT) for discussions about early odontocete
- morphology. To E. M. G. Fitzgerald (MV), N. D. Pyenson (USNM) and D. J. Bohaska (USNM)
- 1288 for access to collections under their care. Also, to James L. Goedert and the late Gail H. Goedert,
- 1289 for collecting and donating the specimens described in this work to the Natural History Museum
- 1290 of Los Angeles County.

1291 1292

References

- 1293 Aguirre-Fernández, G., and R. E.Fordyce. 2014. *Papahu taitapu*, gen. et sp. Nov., an early
- 1294 Miocene stem odontocete (Cetacea) from New Zealand. Journal of Vertebrate Paleontology
- 1295 34:195–210.

1296

- 1297 Albright III, L. B., A. E. Sanders, and J. H. Geisler. 2018. An unexpectedly derived odontocete
- 1298 from the Ashley Formatio (upper Rupelian) of South Carolina, U.S.A. Journal of Vertebrate
- 1299 Paleontology 38(4):e1482555.

1300

- Allen, G. M. 1921. A new fossil cetacean. Bulletin of the Museum of Comparative Zoology at
- 1302 Harvard College 65:1–14.

1303

- Allen, J. A. 1887. Note on squalodont remains from Charleston, S.C. Bulletin of the American
- 1305 Museum of Natural History 12:35–39.

1306

- 1307 Andrews, C. W. 1906. A descriptive catalogue of the Tertiary Vertebrata of Fayum, Egypt.
- 1308 British Museum of Natural History, London 324 pp.

1309

- 1310 Barnes, L. G. 1984. Fossil odontocetes (Mammalia: Cetacea) from the Almejas Formation, Isla
- 1311 Cedros, Mexico. PaleoBios 42:1–46.

1312

- 1313 Barnes, L. G. 1998. The sequence of fossil marine mammal assemblages in Mexico. Avances en
- 1314 Investigación, Paleontología de Vertebrados, Publicación Especial 1:26–79.



- 1316 Barnes, L. G. 2008. Miocene and Pliocene Albireonidae (Cetacea, Odontoceti), rare and unusual
- 1317 fossil dolphins from the eastern North Pacific Ocean. Natural History Museum of Los Angeles
- 1318 County Science Series 41:99–152.

- 1320 Barnes, L. G., and J. L. Goedert. 2001. Stratigraphy and paleoecology of Oligocene and Miocene
- desmostylian occurrences in Western Washington State, U.S.A. Bulletin of Ashoro Museum of
- 1322 Paleontology 2:7–22.

1323

- Barnes, L. G., J. L. Goedert, H. Furusawa. 2001. The earliest known echolocating toothed whales
- 1325 (Mammalia; Odontoceti): preliminary observations of fossils from Washington State. Mesa
- 1326 Southwestern Museum Bulletin 8:92–100.

1327

- 1328 Barnes, L. G., M. Kimura, H. Furusawa, and H. Sawamura. 1995. Classification and distribution
- 1329 of Oligocene Aetiocetidae (Mammalia; Cetacea; Mysticeti) from western North America and
- 1330 Japan. Island Arc 3:392–431.

1331

- 1332 Beatty, B. L. 2006. Specimens of *Cornwallius sookensis* (Desmostylia, Mammalia) from
- 1333 Unalaska Island, Alaska. Journal of Vertebrate Paleontology 26:785–787.

1334

- 1335 Beatty, B. L., and T. Cockburn. 2015. New insights on the most primitive desmostylian from a
- 1336 partial skeleton of *Behemotops* (Desmostylia, Mammalia) from Vancouver Island, British
- 1337 Columbia. Journal of Vertebrate Paleontology e979939.

1338

- 1339 Berta, A. 1991. New *Enaliarctos** (Pinnipedimorpha) from the Oligocene and Miocene of
- Oregon and the role of "enaliarctids" in pinniped phylogeny. Smithsonian contributions to
- 1341 Paleobiology 69:1–33.

1342

- Blainville, H. de. 1838. Sur les cachalots. Annales Françaises et Étrangères D'anatomie et de
- 1344 Phsiologie. 2:335–337.

1345

- Boersma, A. T., and N. D. Pyenson. 2016. *Arktocara yakataga*, a new fossil odontocete
- 1347 (Mammalia, Cetacea) from the Oligocene of Alaska and the antiquity of Platanistoidea. PeerJ
- 1348 4:e2321. DOI 10.7717/peerj.2321

1349

- Boessenecker, R. W., D. Fraser, M. Churchill, and J. H. Geisler. 2017. A toothless dwarf dolphin
- 1351 (Odontoceti: Xenorophidae) points to explosive feeding diversification of modern whales
- 1352 (Neoceti). Proceedings of the Royal Society B 284:20170531.



- Boessenecker, R. W., M. Churchill, E. A. Buchholtz, B. L. Beatty, and J. H. Geisler. 2020.
- 1355 Convergent evolution of swimming adaptations in modern whales revealed by a large
- macrophagous dolphin from the Oligocene of South Carolina. Current Biology 30:3267–3273.

- 1358 Brisson, M. J. 1762. Regnum Animale in Classes IX Distributum, Sive Synopsis Methodica
- 1359 Sistens Generalem Animalium Distributionem in Classes IX, et Duarum Primarum Classium,
- 1360 Quadrupedum Scilicet & Cetaceorum, Particulare Divisionem in Ordines, Sectiones, Genera, et
- 1361 Species. T. Haak, Paris, 296 pp.

1362

- 1363 Cabrera, A. 1926. Cetáceos fósiles del Museo de La Plata. Revista Museo de La Plata 29:363-
- 1364 411.

1365

- 1366 Churchill, M., M. Martinez-Caceres, C. de Muizon, J. Mneckowski, and J. H. Geisler. 2016. The
- origin of high-frequency hearing in whales. Current Biology 26:1–6.

1368

- 1369 Cohen, K. M., S. C. Finney, P. L. Gibbard, and J. X. Fan. 2013 (updated). The ICS international
- 1370 chronostratographic chart. Episodes 36:199–204.

1371

- 1372 Domning, D. P., C. E. Ray, and M. C. McKenna. 1986. Two new Oligocene desmostylians and a
- discussion of tethytherian systematics. Smithsonian Contributions to Paleobiology 59:1–56.

1374

- Dickson, M. R. 1964. The skull and other remains of *Prosqualodon marplesi*, a new species of
- 1376 fossil whale. New Zealand Journal of Geology and Geophysics 7:626–635.

1377

- 1378 Dubrovo, I. A., and A. E. Sanders. 2000. A new species of *Patriocetus* (Mammalia, Cetacea)
- 1379 from the late Oligocene of Kazakhstan. Journal of Vertebrate Paleontology 20:577–590.

1380

- Dyke, G. J., X. Wang, and M. B. Habib. 2011. Fossil plotopterid seabirds from the Eo-Oligocene
- of the Olympic Peninsula (Washington State, USA): descriptions and functional morphology.
- 1383 PLoS ONE 6(10):e25672.

1384

- Emlong, D. R. 1966. A new archaic cetacean from the Oligocene of Northwest Oregon. Bulletin
- of the Oregon University Museum of Natural History 3:1–51.

1387

- 1388 Fitzgerald, E. M. G. 2006. A bizarre new toothed mysticete (Cetacea) from Australia and the
- early evolution of baleen whales. Proceedings of the Royal Society B 273:2955–2963.

- 1391 Fitzgerald, E. M. G. 2010. The morphology and systematics of *Mammalodon colliveri* (Cetacea:
- 1392 Mysticeti), a toothed mysticete from the Oligocene of Australia. Zoological Journal of the
- 1393 Linnean Society 158:367–476.



- 1394
 - 1395 Flower, W. H. 1867. Description of the skeleton of *Inia geoffensis* and the skull of *Pontoporia*
- 1396 *blainvilii*, with remarks on the systematic position on these animals in the order Cetacea.
- 1397 Transactions of the Zoological Society of London 6:87–116.

- 1399 Flynn, T. T. 1947. Description of *Prosqualodon davidi* Flynn, a fossil cetacean from Tasmania.
- 1400 Transactions of the Zoological Society of London 26:153–197.

1401

- 1402 Fordyce, R. E. 1994. Waipatia maerewhenua, a new genus and species (Waipatiidae, new
- 1403 family), an archaic late Oligocene dolphin (Cetacea: Odontoceti: Platanistoidea) from New
- 1404 Zealand. Proceedings of the San Diego Society of Natural History 29:147–176.

1405

- 1406 Fordyce, R. E. 2002. Simocetus rayi (Odontoceti: Simocetidae, New Family): a bizarre new
- 1407 archaic Oligocene dolphin from the Eastern Pacific. Smithsonian Contributions to Paleobiology
- 1408 93:185-222.

1409

- 1410 Gaetan, C. M., M. R. Buono, and L. C. Gaetano. 2019. Prosqualodon australis (Cetacea:
- 1411 Odontoceti) from the early Miocene of Patagonia, Argentina: redescription and phylogenetic
- 1412 analysis. Ameghiniana 56:1–27.

1413

- 1414 Geisler, J. H., M. W. Colbert, and J. L. Carew. 2014. A new fossil species supports an early
- origin for toothed whale echolocation. Nature 508:383–386.

1416

- 1417 Goedert, J. L., R. L. Squires, and L. G. Barnes. 1995. Paleoecology of whalefall habitats from
- 1418 deep-water Oligocene Rocks, Olympic Peninsula, Washington State. Paleogeography,
- 1419 Palaeoclimatology, Paleoecology 118: 151–158.

1420

- 1421 Hernández Cisneros, A. E. 2022. A new aetiocetid (Cetacea, Mysticeti, Aetiocetidae) from the
- 1422 late Oligocene of Mexico. Journal of Systematic Palaeontology 20:2100725.

1423

- 1424 Hernández Cisneros, A. E., and E. H. Nava-Sánchez. 2022. Oligocene dawn baleen whales in
- 1425 Mexico (Cetacea, Eomysticetidae) and paleobiogeographic notes. Paleontología Mexicana 11:1-
- 1426 12.

1427

- 1428 Hernández Cisneros, A. E., and C.-H. Tsai. 2016. A possible enigmatic kekenodontid (Cetacea,
- 1429 Kekenodontidae) from the Oligocene of Mexico. Paleontología Mexicana 5:147–155.

- 1431 Hernández Cisneros, A. E., and J. Vélez-Juarbe. 2021. Paleobiogeography of the North Pacific
- 1432 toothed mysticetes (Cetacea, Aetiocetidae): a key to Oligocene cetacean distributional patterns.
- 1433 Palaeontology 64:51–61.



1434	
1435	Hernández Cisneros, A. E., G. González Barba, and R. E. Fordyce. 2017. Oligocene cetaceans
1436	from Baja California Sur, Mexico. Boletín de la Sociedad Geológica Mexicana 69:149-173.
1437	
1438	Hirota, K., and L. G. Barnes. 1995. A new species of middle Miocene sperm whale of the genus
1439	Scaldicetus (Cetacea; Physeteridae) from Shiga-mura, Japan. Island Arc 3:453-472.
1440	
1441	Hunt, R. M., Jr., and L. G. Barnes. 1994. Basicranial evidence for ursid affinity of the oldest
1442	pinnipeds. Proceedings of the San Diego Society of Natural History 29:57-67.
1443	
1444	Ichishima, H., S. Kawabe, and H. Sawamura. 2021. The so-called foramen singulare in cetacean
1445	periotics is actually the superior vestibular area. Anatomical Record 304:1792–1799.
1446	
1447	Inuzuka, N. 2000. Primitive late Oligocene desmostylians from Japan and phylogeny of the
1448	Desmostylia. Bulletin of the Ashoro Museum of Paleontology 1:91–123.
1449	
1450	Johnston, C., and A. Berta. 2011. Comparative anatomy and evolutionary history of suction
1451	feeding in cetaceans. Marine Mammal Science 27:493–513.
1452	
1453	Kellogg, R. 1923. Description of an apparently new toothed cetacean from South Carolina.
1454	Smithsonian Contributions to Knowledge 76(7):1–7.
1455	
1456	Kiel, S., WA. Kahl, and J. L. Goedert. 2013. Traces of the bone-eating annelid Osedax in
1457	Oligocene whale teeth and fish bones. Paläontologische Zeitschrift 87:161–167.
1458	
1459	Kimura, T., and Y. Hasegawa. 2019. A new species of Kentriodon (Cetacea, Odontoceti,
1460	Kentriodontidae) from the Miocene of Japan. Journal of Vertebrate Paleontology 39:e1566739.
1461	
1462	Lambert, O., M. Martínez-Cáceres, G. Bianucci, C. Di Celma, R. Salas-Gismondi, E. Steurbaut,
1463	M. Urbina, and C. de Muizon. 2017. Earliest mysticete from the late Eocene of Peru sheds new
1464	light on the origin of baleen whales. Current Biology 27:1535–1541.
1465	
1466	Lydekker, R. 1894. Cetacean skull from Patagonia. Anales del Museo de La Plata 2:1–13.
1467	
1468	Martínez-Cáceres, M., and C. de Muizon. 2011. A new basilosaurid (Cetacea, Pelagiceti) from
1469	the late Eocene to early Oligocene Otuma Formation of Peru. Comptes Rendus Palevol 10:517-
1470	526.
1471	



- 1472 Martínez-Cáceres, M., O. Lambert, and C. de Muizon. 2017. The anatomy and phylogenetic
- 1473 affinities of *Cynthiacetus peruvianus*, a large durodontine basilosaurid (Cetacea, Mammalia)
- 1474 from the late Eocene of Peru. Geodiversitas 39:7–163.

- 1476 Marx, F. G., C.-H. Tsai, and R. E. Fordyce. 2015. A new early Oligocene toothed 'baleen' whale
- 1477 (Mysticeti: Aetiocetidae) from western North America: one of the oldest and the smallest. Royal
- 1478 Society Open Science 2:150476.

1479

- 1480 Marx, F. G., O. Lambert, and M. D. Uhen. 2016a. Cetacean Paleobiology. John Wiley & Sons,
- 1481 Hoboken, 319 pp.

1482

- 1483 Marx, F. G., D. P. Hocking, T. Park, T. Ziegler, A. R. Evans, and E. M. G. Fitzgerald. 2016b.
- 1484 Suction feeding preceded filtering in baleen whale evolution. Memoirs of Museum Victoria
- 1485 75:71–82.

1486

- Mayr, G., and J. L. Goedert. 2016. New late Eocene and Oligocene remains of the flightless,
- 1488 penguin-like plotopterids (Aves, Plotopteridae) from western Washington State, U.S.A. Journal
- 1489 of Vertebrate Paleontology 36:e1163573.

1490

- 1491 Mayr, G., and J. L. Goedert. 2022. New late Eocene and Oligocene plotopterid fossils from
- 1492 Washington State (USA), with a revision of "Tonsala" buchanani (Aves, Plotopteridae). Journal
- 1493 of Paleontology 96:224–236.

1494

- 1495 McGowen, M. R., G. Tsagkogeorga, A. Álvarez-Carretero, M. dos Reis, M. Struebig, R.
- 1496 Deaville, P. D. Jepson, S. Jarman, A. Polanowski, P. A. Morin, and S. J. Rossiter. 2020.
- 1497 Phylogenomic resolution of the cetacean tree of life using target sequence capture. Systematic
- 1498 Biology 69:479–501.

1499

- 1500 Mchedlidze, G. A. 1970. Nekotorye Obschchie Chery Istorii Kitoobraznykh, Chast' I. Akademia
- 1501 Nauk Gruzinskoi S.S.R., Institut Paleobiologii. Metsniereba, Tbilisi, 112 p.

1502

- 1503 Mead, J. G., and R. E. Fordyce. 2009. The therian skull: a lexicon with emphasis on the
- odontocetes. Smithsonian Contributions to Zoology 627:1–248.

1505

- 1506 Montagu, G. 1821. Description of a species of *Delphinus*, which appears to be new. Memoirs of
- the Wernerian Natural History Society 3:75–82.

1508

- Moreno, F. 1892. Ligeros apuntes sobre dos géneros de cetáceos fósiles de la República
- 1510 Argentina. Museo La Plata, Revista 3:393–400.



- 1512 Mori, H., and K. Miyata. 2021. Early Plotopteridae specimens (Aves) from the Itanoura and
- 1513 Kakinoura Formations (latest Eocene to early Oligocene), Saikai, Nagasaki Prefecture, western
- 1514 Japan. Paleontological Research 25:145–159.

- 1516 Muizon, C. de. 1987. The affinities of *Notocetus vanbenedeni*, an early Miocene platanistoid
- 1517 (Cetacea, Mammalia) from Patagonia, southern Argentina. American Museum Novitates
- 1518 2904:1–27.

1519

- 1520 Muizon, C. de, G. Bianucci, M. Martínez-Cáceres, and O. Lambert. 2019. *Mystacodon*
- 1521 selenenesis, the earliest known toothed mysticete (Cetacea, Mammalia) from the late Eocene of
- 1522 Peru: anatomy, phylogeny, and feeding adaptations. Geodiversitas 41:401–499.

1523

- 1524 Müller, J. 1849. Über die fossilen Reste der Zeuglodonten von Nordamerika mit Rücksicht auf
- die europäischen Reste aus dieser Familie. G. Reimer, Berlin, 38 pp.

1526

- 1527 Ohaski, T., and Y. Hasegawa. 2020. New species of Plotopteridae (Aves) from the Oligocene
- 1528 Ashiya Group of Northern Kyushu, Japan. Paleontological Research 24:285–297.

1529

- 1530 Okazaki, Y. 1987. Additional material of *Metasqualodon symmetricus* (Cetacea: Mammalia)
- 1531 from the Oligocene Ashiya Group, Japan. Bulletin of the Kitakyushu Museum of Natural History
- **1532** 7:133–138.

1533

- Okazaki, Y. 1988. Oligocene squalodont (Cetacea: Mammalia) from the Ashiya Group, Japan.
- 1535 Bulletin of the Kitakyushu Museum of Natural History 8:75–80.

1536

- 1537 Okazaki, Y. 2012. A new mysticete from the upper Oligocene Ashiya Group, Kyushu, Japan and
- 1538 its significance to mysticete evolution. Bulletin of the Kitakyushu Museum of Natural History
- 1539 and Human History, Series A 10:129–152.

1540

- Olson, S. L. 1980. A new genus of penguin-like pelecaniform bird from the Oligocene of
- Washington (Pelecaniformes: Plotopteridae). Contributions in Science 330:51–57.

1543

- Olson, S. L., and Y. Hasegawa. 1996. A new genus and two new species of gigantic
- 1545 Plotopteridae from Japan (Aves: Plotopteridae). Journal of Vertebrate Paleontology 16:742–751.

1546

- 1547 Peredo, C. M., and M. D. Uhen, 2016. A new basal Chaeomysticete (Mammalia: Cetacea) from
- the late Oligocene Pysht Formation of Washington, USA. Papers in Palaeontology 2:533–554.



- 1550 Peredo, C. M., and N. D. Pyenson. 2018. *Salishicetus meadi*, a new aetiocetid from the late
- 1551 Oligocene of Washington State and implications for feeding transitions in early mysticete
- evolution. Royal Society Open Science 5:172336.

- Peredo, C. M., N. D. Pyenson, C. D. Marshall, and M. D. Uhen. 2018. Tooth loss precedes the
- origin of baleen in whales. Current Biology 28:3992–4000.

1556

- Poust, A. W., and R. W. Boessenecker. 2018. Expanding the geographic and geochronologic
- range of early pinnipeds: new specimens of *Enaliarctos* from Northern California and Oregon.
- 1559 Acta Palaeontologica Polonica 63:25–40.

1560

- 1561 Pritchard, G. B. 1939. On the discovery of a fossil whale in the older Tertiaries of Torquay,
- 1562 Victoria. Victorian Naturalist 55:151–159.

1563

- Prothero, D. R., A. Streig, and C. Burns. 2001. Magnetic stratigraphy and tectonic rotation of the
- 1565 upper Oligocene Pysht Formation, Clallam County, Washington. Pacific Section, SEPM, Special
- 1566 Publication 91:224–233.

1567

- 1568 Pyenson, N. D., and S. N. Sponberg. 2011. Reconstructing body size in extinct crown Cetacea
- 1569 (Neoceti) using allometry, phylogenetic methods and tests from the fossil record. Journal of
- 1570 Mammalian Evolution 18:269–288.

1571

- 1572 Racicot, R. A., R. W. Boessenecker, S. A. F. Darroch, and J. H. Geisler. 2019. Evidence for
- 1573 convergent evolution of ultrasonic hearing in toothed whales (Cetacea: Odontoceti). Biology
- 1574 Letters 15:20190083.

1575

- 1576 Ray, C. E., D. P. Domning, and M. C. McKenna. 1994. A new specimen of *Behemotops proteus*
- 1577 (Order Desmostylia) from the marine Oligocene of Washington. Proceedings of the San Diego
- 1578 Society of Natural History 29:205–222.

1579

- Russel, L. S. 1968. A new cetacean from the Oligocene Sooke Formation of Vancouver Island,
- 1581 British Columbia. Canadian Journal of Earth Sciences 5:929–933.

1582

- Reidenberg, J. S., and J. T. Laitman. 1994. Anatomy of the hyoid apparatus in Odontoceti
- 1584 (toothed whales): specializations of their skeleton and musculature compared with those of
- 1585 terrestrial mammals. Anatomical Record 240:598–624.

- 1587 Sakurai, K., M. Kimura, and T. Katoh. 2008. A new penguin-like bird (Pelecaniformes:
- 1588 Plotopteridae) from the late Oligocene Tokoro Formation, northeastern Hokkaido, Japan.
- 1589 Oryctos 7:83–94.



1590 1591 Sander, P. M., E. M. Griebeler, N. Klein, J. Vélez-Juarbe, T. Wintrich, L. J. Revell, and L. 1592 Schmitz. 2021. Early giant reveals faster evolution of large body size in ichthyosaurs than in cetaceans. Science 374:eabf5787. 1593 1594 1595 Sanders, A. E., and J. H. Geisler. 2015. A new basal odontocete from the upper Rupelian of 1596 South Carolina, U.S.A., with contributions to the systematics of *Xenorophus* and Mirocetus (Mammalia, Cetacea). Journal of Vertebrate Paleontology 35:e890107. 1597 1598 1599 Shipps, B. K., C. M. Peredo, and N. D. Pyenson. 2019. *Borealodon osedax*, a new stem mysticete (Mammalia, Cetacea) from the Oligocene of Washington State and its implications for 1600 fossil whale-fall communities. Royal Society Open Science 6:182168. 1601 1602 1603 Solis-Añorve, A., G. Gozález-Barba, and R. Hernández-Rivera. 2019. Description of a new 1604 toothed mysticete from the late Oligocene of San Juan de La Costa, B.C.S., México. Journal of 1605 South American Earth Sciences 89:337–346. 1606 1607 Swofford, D. L. 2003. PAUP*. Phylogenetic Analysis Using Parsimony (*and Other Methods), 1608 Version 4.0 B10. Sunderland, MA, Sinauer Associates. 1609 1610 Tanaka, Y., and R. E. Fordyce. 2014. Fossil dolphin Otekaikea marplesi (latest Oligocene, New 1611 Zealand) expands the morphological and taxonomic diversity of Oligocene cetaceans. PLoS 1612 ONE 9(9):e107972. 1613 1614 Tanaka, Y., and R. E. Fordyce. 2015. A new Oligo-Miocene dolphin from New Zealand: Otekaikea huata expands diversity of the early Platanistoidea. Paleontologia Electronica 1615 1616 18.2.23A:1-71. 1617 1618 Uhen, M. D. 2004. Form, function, and anatomy of *Durodon atrox* (Mammalia, Cetacea): an archaeocete from the middle to late Eocene of Egypt. University of Michigan Papers on 1619 1620 Paleontology 34:1-222. 1621 1622 Uhen, M. D. 2008. A new *Xenorophus*-like odontocete cetacean from the Oligocene of North 1623 Carolina and a discussion of the basal odontocete radiation. Journal of Systematic Palaeontology 1624 6:433-452. 1625

1626 Vélez-Juarbe, J. 2015. Simocetid diversity in the Oligocene of the Eastern Pacific region. Journal 1627 of Vertebrate Paleontology, Program and Abstracts 2015:230.

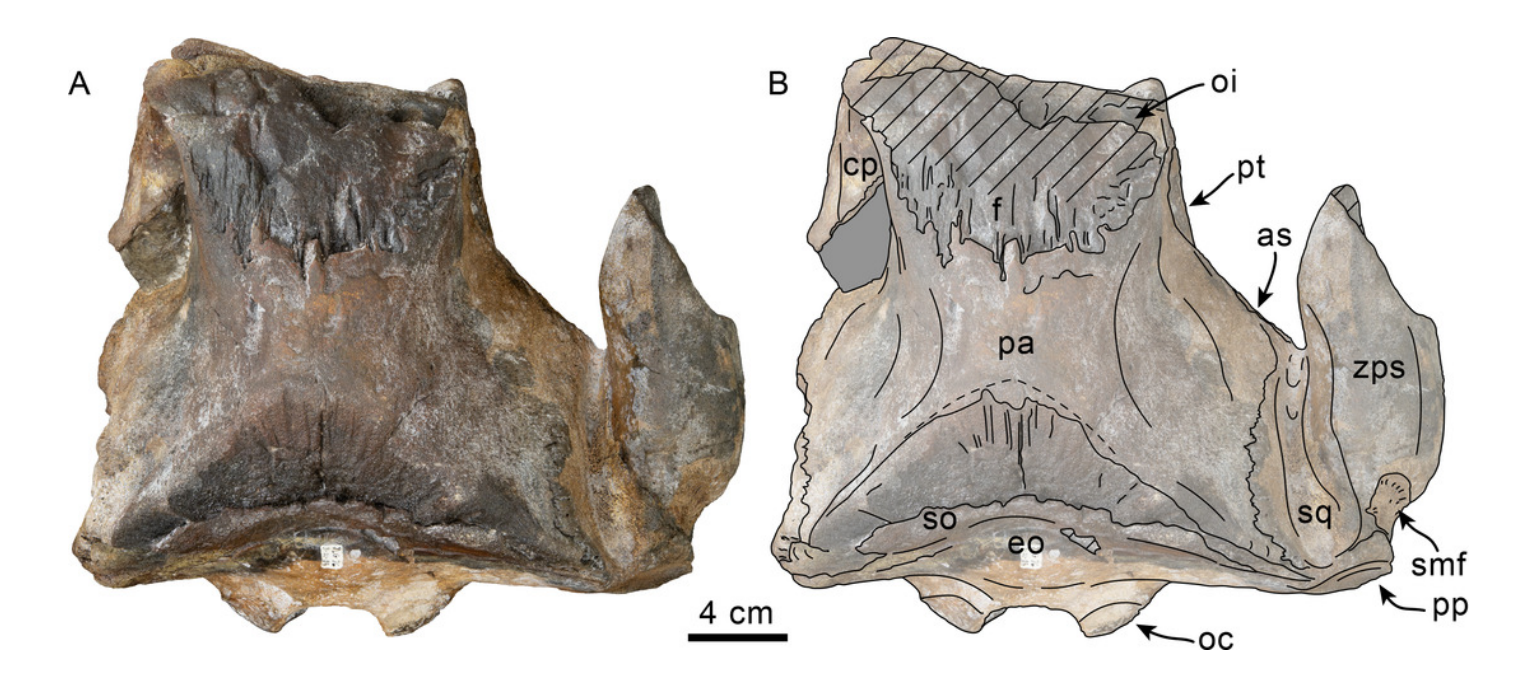


PeerJ

1629 1630 1631	Vélez-Juarbe, J. 2017. A new stem odontocete from the late Oligocene Pysht Formation in Washington State, U.S.A. Journal of Vertebrate Paleontology 37(5):e1366916.
1632 1633 1634 1635	Viglino, M., C. M. Gaetán, J. I. Cuitiño, and M. R. Buono. 2021. First toothless platanistoid from the early Miocene of Patagonia: the golden age of diversification of the Odontoceti. Journal of Mammalian Evolution 28:337–358.
1636 1637 1638 1639 1640	Viglino, M., M. R. Buono, R. E. Fordyce, J. I. Cuitiño, and E. M. G. Fitzgerald. 2019. Anatomy and phylogeny of the large shark-toothed dolphin <i>Phoberodon arctirostris</i> Cabrera, 1926 (Cetacea: Odontoceti) from the early Miocene of Patagonia (Argentina). Zoological Journal of the Linnean Society 185:511–542.
1641 1642 1643 1644	Viglino, M., M. R. Buono, Y. Tanaka, J. I. Cuitiño, and R. E. Fordyce. 2022. Unravelling the identity of the platanistoid <i>Notocetus vanbenedeni</i> Moreno, 1892 (Cetacea, Odontoceti) from the early Miocene of Patagonia (Argentina). Journal of Systematic Palaeontology 20:2082890.
1645 1646 1647	Werth, A. J. 2006. Mandibular and dental variation and the evolution of suction feeding in odontoceti. Journal of Mammalogy 87:579–588.
1648 1649	Whitmore, F. C., Jr., and A. E. Sanders. 1977. Review of the Oligocene Cetacea. Systematic Zoology 25:304–320.

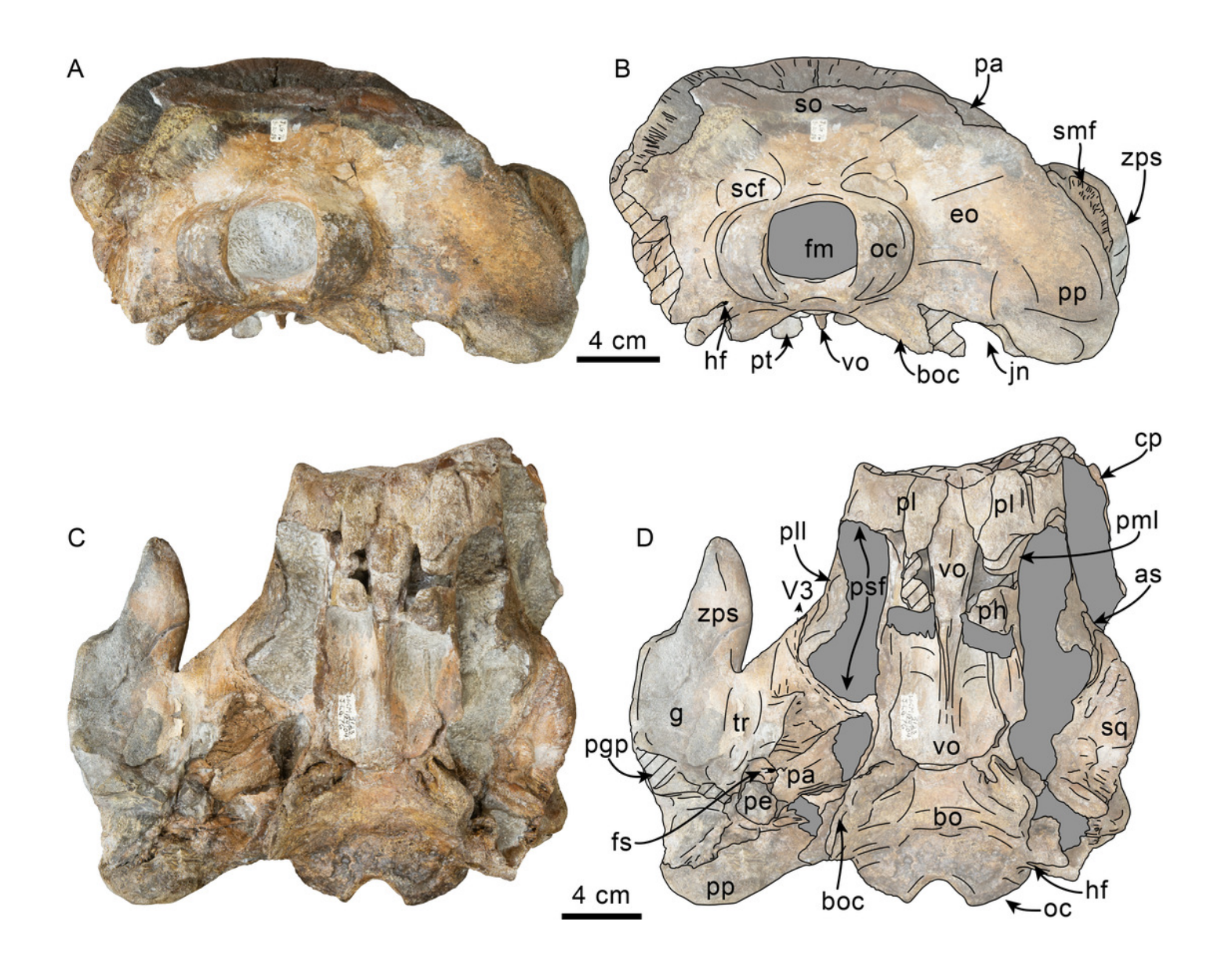
Dorsal view of skull of Simocetidae gen. et sp. A (LACM 124104).

Unlabeled (A) and labeled (B) skull in dorsal view. Diagonal lines denote broken surfaces, gray shaded areas are obscured by sediment. Abbreviations: as, alisphenoid; cp, coronoid process; eo, exoccipital; f, frontal; oc, occipital condyle; oi, optic infundibulum; pa, parietal; pp, paroccipital process; pt, pterygoid; smf, sternomastoid fossa; so, supraoccipital; sq, squamosal; zps, zygomatic process of squamosal.



Posterior and ventral views of skull of Simocetidae gen. et sp. A (LACM 124104).

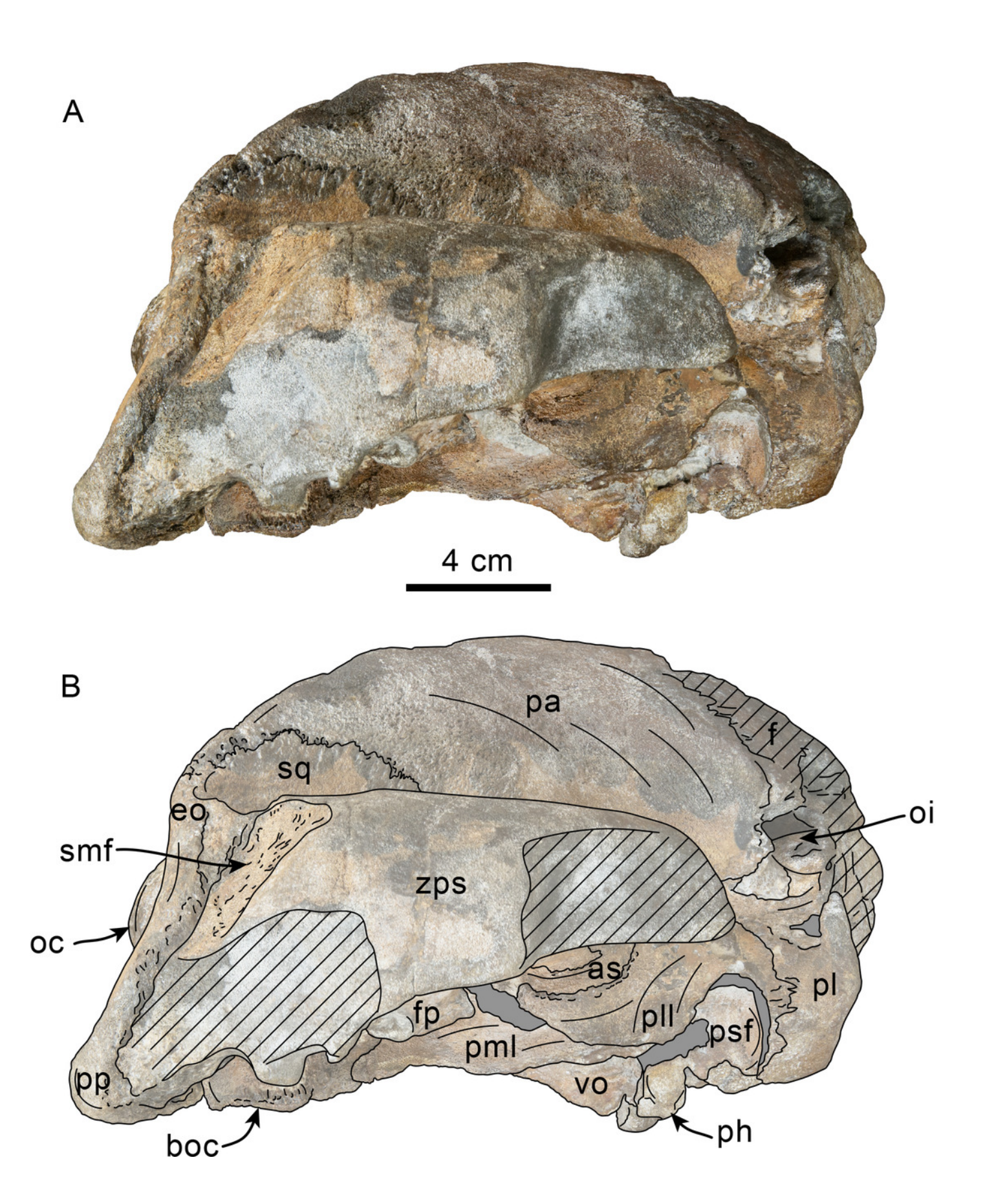
Unlabeled (A) and labeled (B) skull in posterior view; unlabeled (C) and labeled (D) skull in ventral view. Diagonal lines denote broken surfaces, gray shaded areas are obscured by sediment. Abbreviations: as, alisphenoid; bo, basioccipital; bo, basioccipital crest; cp, coronoid process; eo, exoccipital; fm, foramen magnum; fs, foramen spinosum; g, glenoid; hf, hypoglossal foramen; jn, jugular notch; oc, occipital condyle; pa, parietal; pe, periotic; pgp, postglenoid process; ph, pterygoid hamulus; pl, palatine; pll, pterygoid lateral lamina; pml, pterygoid medial lamina; pp, paroccipital process; psf, pterygoid sinus fossa; pt, pterygoid; scf, supracondylar fossa; smf, sternomastoid fossa; so, supraoccipital; sq, squamosal; tr, tympanosquamosal recess; V3, groove and path of mandibular branch of trigeminal nerve; vo, vomer; zps, zygomatic process of squamosal.





Lateral view of skull of Simocetidae gen. et sp. A (LACM 124104).

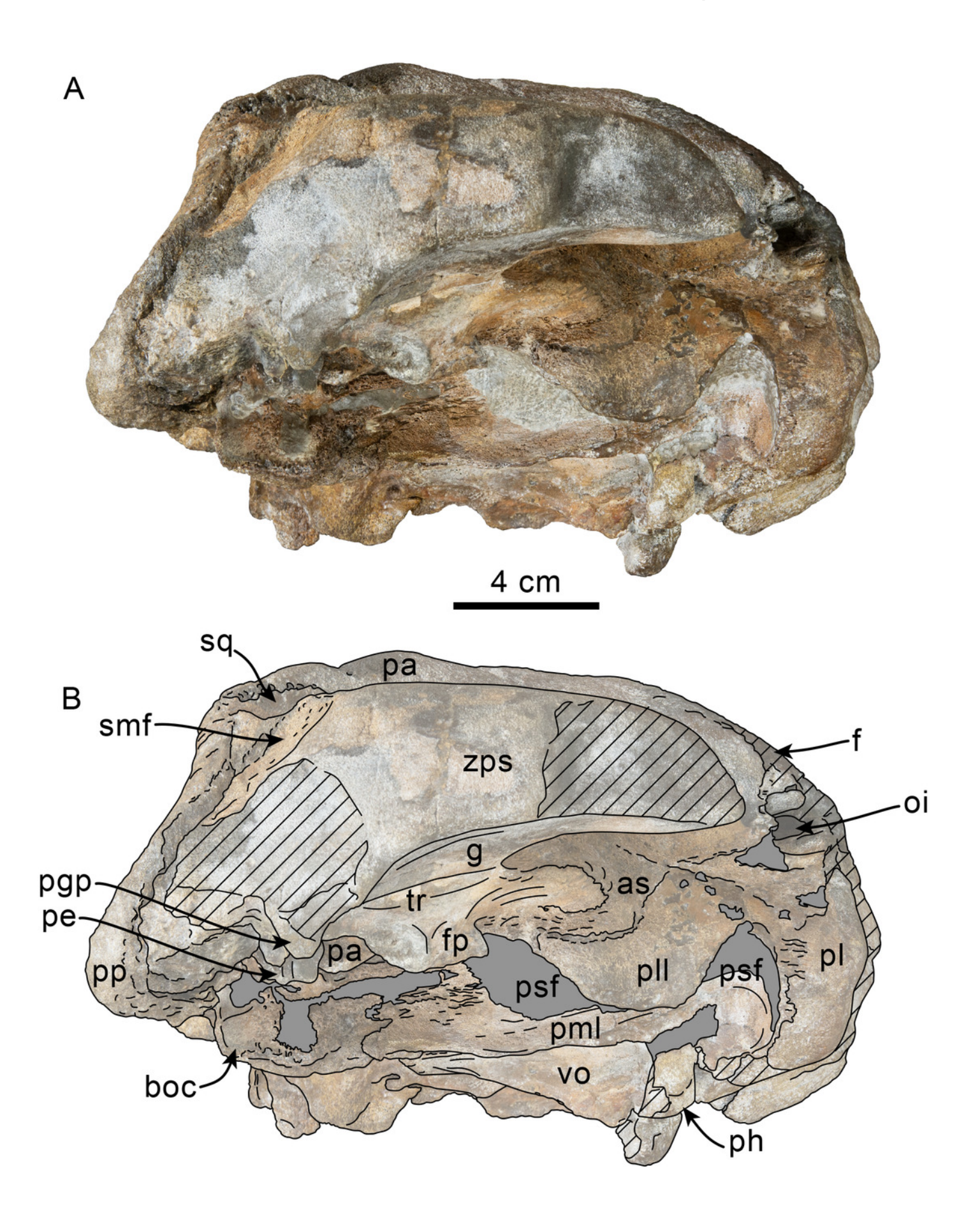
Unlabeled (A) and labeled (B) skull in right lateral view. Diagonal lines denote broken surfaces, gray shaded areas are obscured by sediment. Abbreviations: as, alisphenoid; boc, basioccipital crest; eo, exoccipital; f, frontal; fp, falciform process; oc, occipital condyle; oi, optic infundibulum; pa, parietal; ph, pterygoid hamulus; pl, palatine; pll, pterygoid lateral lamina; pml, pterygoid medial lamina; pp, paroccipital process; psf, pterygoid sinus fossa; smf, sternomastoid fossa; sq, squamosal; vo, vomer; zps, zygomatic process of squamosal.





Ventrolateral view of skull of Simocetidae gen. et sp. A (LACM 124104).

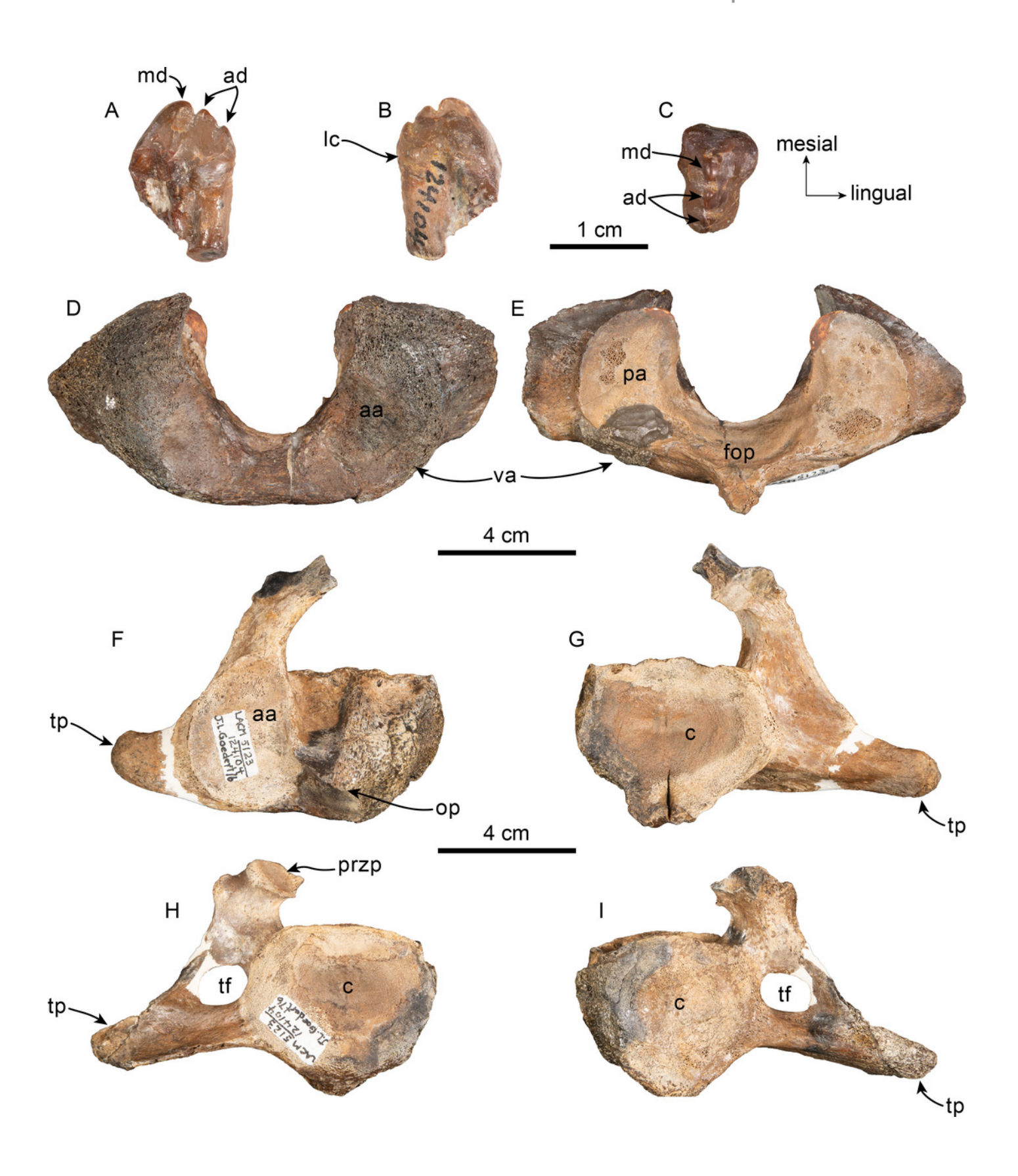
Unlabeled (A) and labeled (B) skull in right ventrolateral view. Diagonal lines denote broken surfaces, gray shaded areas are obscured by sediment. Abbreviations: as, alisphenoid; boc, basioccipital crest; f, frontal; fp, falciform process; g, glenoid; oi, optic infundibulum; pa, parietal; pe, periotic; pgp, postglenoid process; ph, pterygoid hamulus; pl, palatine; pll, pterygoid lateral lamina; pml, pterygoid medial lamina; pp, paroccipital process; psf, pterygoid sinus fossa; smf, sternomastoid fossa; sq, squamosal; tr, tympanosquamosal recess; vo, vomer; zps, zygomatic process of squamosal.





Tooth and vertebrae of Simocetidae gen. et sp. A (LACM 124104).

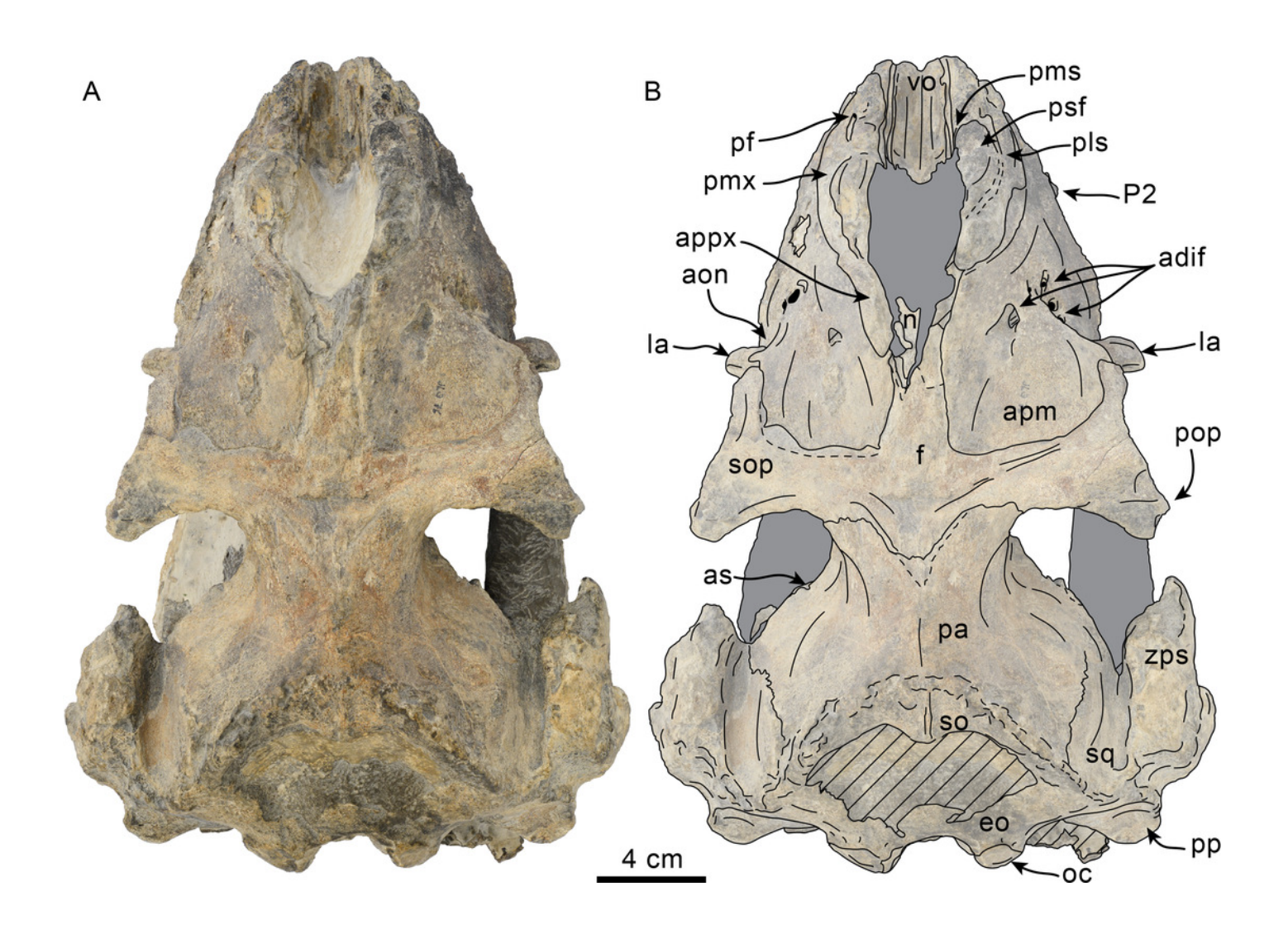
Upper postcanine tooth in buccal (A), lingual (B) and occlusal (C) views. Atlas (D, E), axis (F, G) and third cervical (H, I) vertebrae in anterior (D, F, H) and posterior (E, G, I) views. Abbreviations: aa, anterior articular facet; ad, accessory denticles; c, centrum; lc, lingual cingulum; fop, facet for odontoid process; md, main denticle; op, odontoid process; przp, prezygapophysis; tf, transverse foramen; tp, transverse process; va, ventral arch.





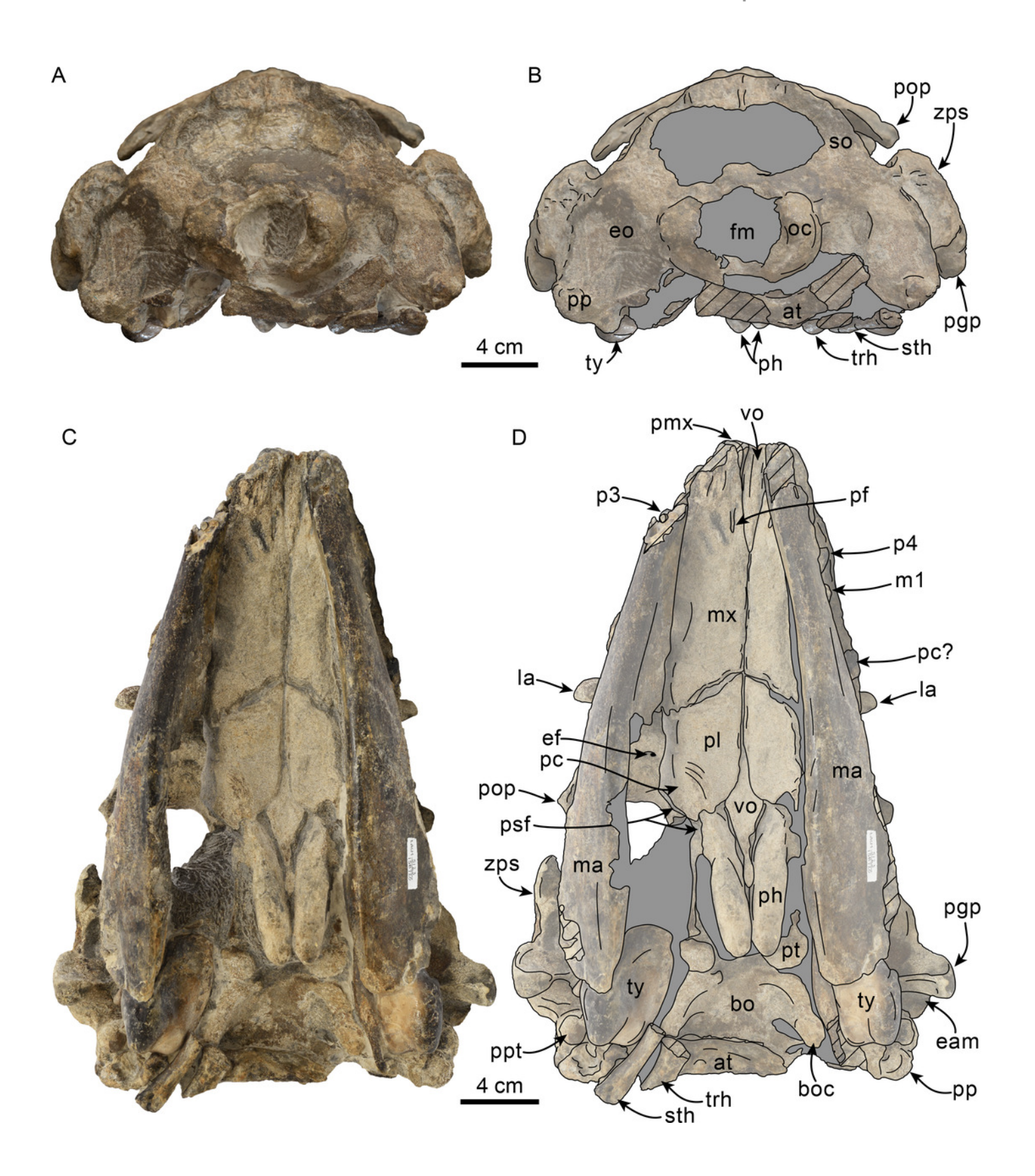
Dorsal view of skull of Olympicetus thalassodon sp. nov. (LACM 158720).

Unlabeled (A) and labeled (B) skull in dorsal view. Diagonal lines denote broken surfaces, gray shaded areas are obscured by sediment. Abbreviations: anterior dorsal infraorbital foramina; aon, antorbital notch; ascending process of maxilla; appx, ascending process of premaxilla; as, alisphenoid; eo, exoccipital; f, frontal; la, lacrimal; n, nasal; oc, occipital condyle; P2, second upper premolar; pa, parietal; pf, premaxillary foramen; pls, posterolateral sulcus; pms, posteromedial sulcus; pmx, premaxilla; pop, postorbital process; pp, paroccipital process; psf, premaxillary sac fossa; so, supraoccipital; sop, supraorbital process; sq, squamosal; vo, vomer; zps, zygomatic process of squamosal.



Posterior and ventral views of skull of Olympicetus thalassodon sp. nov. (LACM 158720).

Unlabeled (A) and labeled (B) skull in ventral view; (C) unlabeled and labeled skull in right lateral view. Diagonal lines denote broken surfaces, gray shaded areas are obscured by sediment. Abbreviations: at, atlas; bo, basioccipital; boc, basioccipital crest; eam, external auditory meatus; ef, ethmoid foramen; la, lacrimal; m1, first lower molar; ma, mandible; mx, maxilla; p3-4, third and fourth lower premolars; pc, palatal crest; pc?, postcanine teeth of unknown placement; pf, palatine foramen; pgp, postglenoid process; ph, pterygoid hamulus; pl, palatine; pmx, premaxilla; pop, postorbital process; pp, paroccipital process; ppt, posterior process of tympanic; psf, pterygoid sinus fossa; pt, pterygoid; sth, stylohyal; trh, thyrohyal; ty, tympanic; vo, vomer; zps, zygomatic process of squamosal.





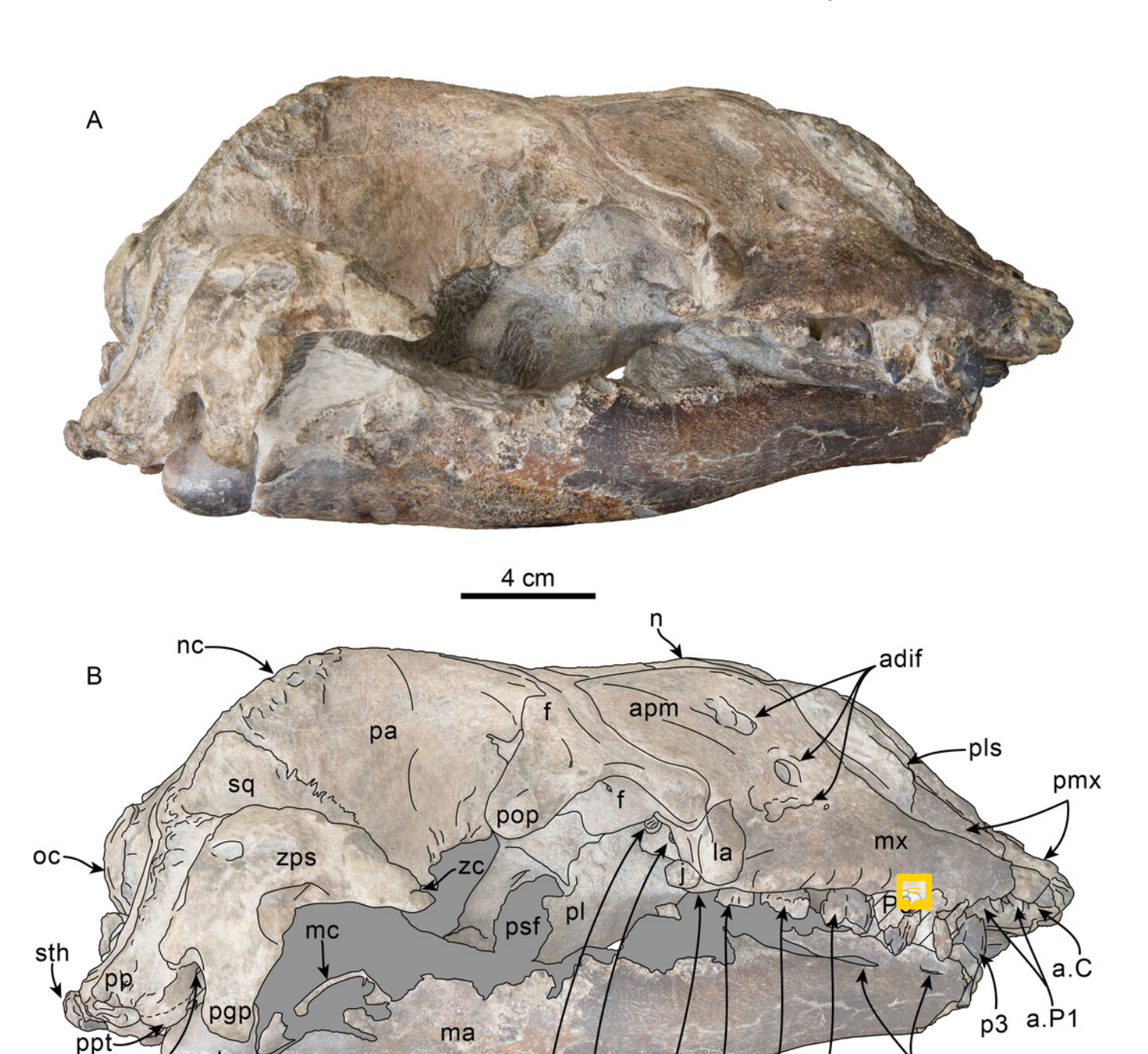
Lateral view of skull of Olympicetus thalassodon sp. nov. (LACM 158720).

Unlabeled (A) and labeled (B) skull in right lateral view. Diagonal lines denote broken surfaces, gray shaded areas are obscured by sediment. Abbreviations: a.C, alveolus for upper canine; a.P1, alveoli for upper premolar one; adif, anterior dorsal infraorbital foramina; apm, ascending process of maxilla; eam, external auditory meatus; f, frontal; j, jugal; la, lacrimal; m1–3, lower molars one, two and three; ma, mandible; mc, mandibular condyle; mip, maxillary infraorbital process; mf, mental foramina; mx, maxilla; n, nasal; nc, nuchal crest; oc, occipital condyle; p3, lower third premolar; P4, upper fourth premolar; pa, parietal; pgp, postglenoid process; pl, palatine; pls, posterolateral sulcus; pop, postorbital process; pp, paroccipital process; psf, pterygoid sinus fossa; ptp, posttympanic process; spf, sphenopalatine foramen; sq, squamosal; sth, stylohyoid; tym tympanic; viof, ventral infraorbital foramen; zc, zygomatic cleft; zps, zygomatic process of squamosal.

eam

mf

mip m3 m2 m1

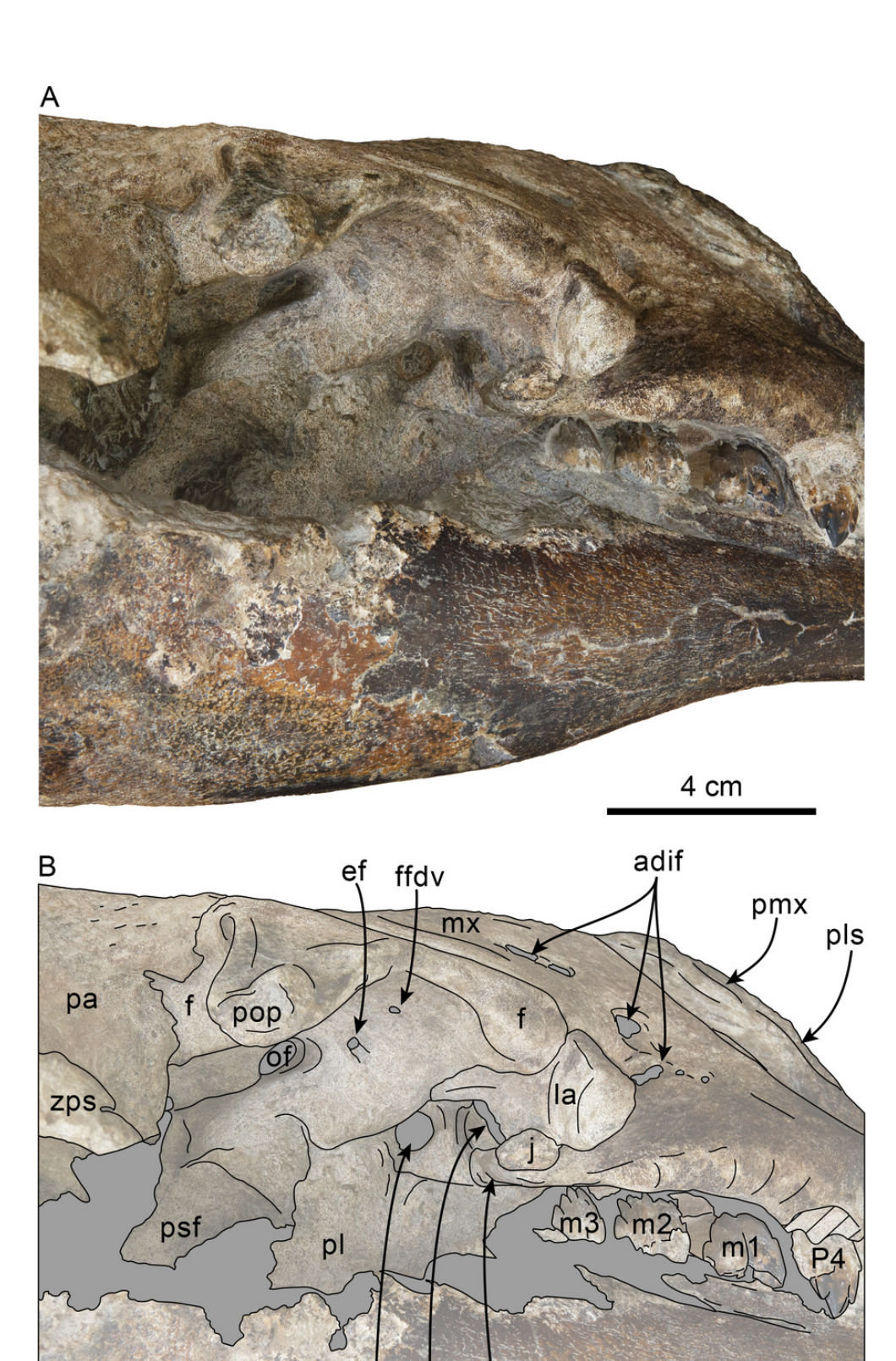


spf viof



Orbital region of skull of Olympicetus thalassodon sp. nov. (LACM 158720).

Unlabeled (A) and labeled (B) orbital region in right lateral view. Diagonal lines denote broken surfaces, gray shaded areas are obscured by sediment. Abbreviations: adif, anterior dorsal infraorbital foramina; ef, ethmoid foramen; f, frontal; ffdv, foramina for frontal diploic vein; j, jugal; la, lacrimal; m1-3, first through third lower molars; ma, mandible; mip, maxillary infraorbital plate; mx, maxilla; of, optic foramen; P4, fourth upper premolar; pa, parietal; pl, palatine; pls, posterolateral sulcus; pmx, premaxilla; pop, postorbital process; psf, pterygoid sinus fossa; spf, sphenopalatine foramen; viof, ventral infraorbital foramen; zps, zygomatic process of squamosal.



PeerJ reviewing PDF | (2022:12:80454:0:1:NEW 9 Jan 2023)

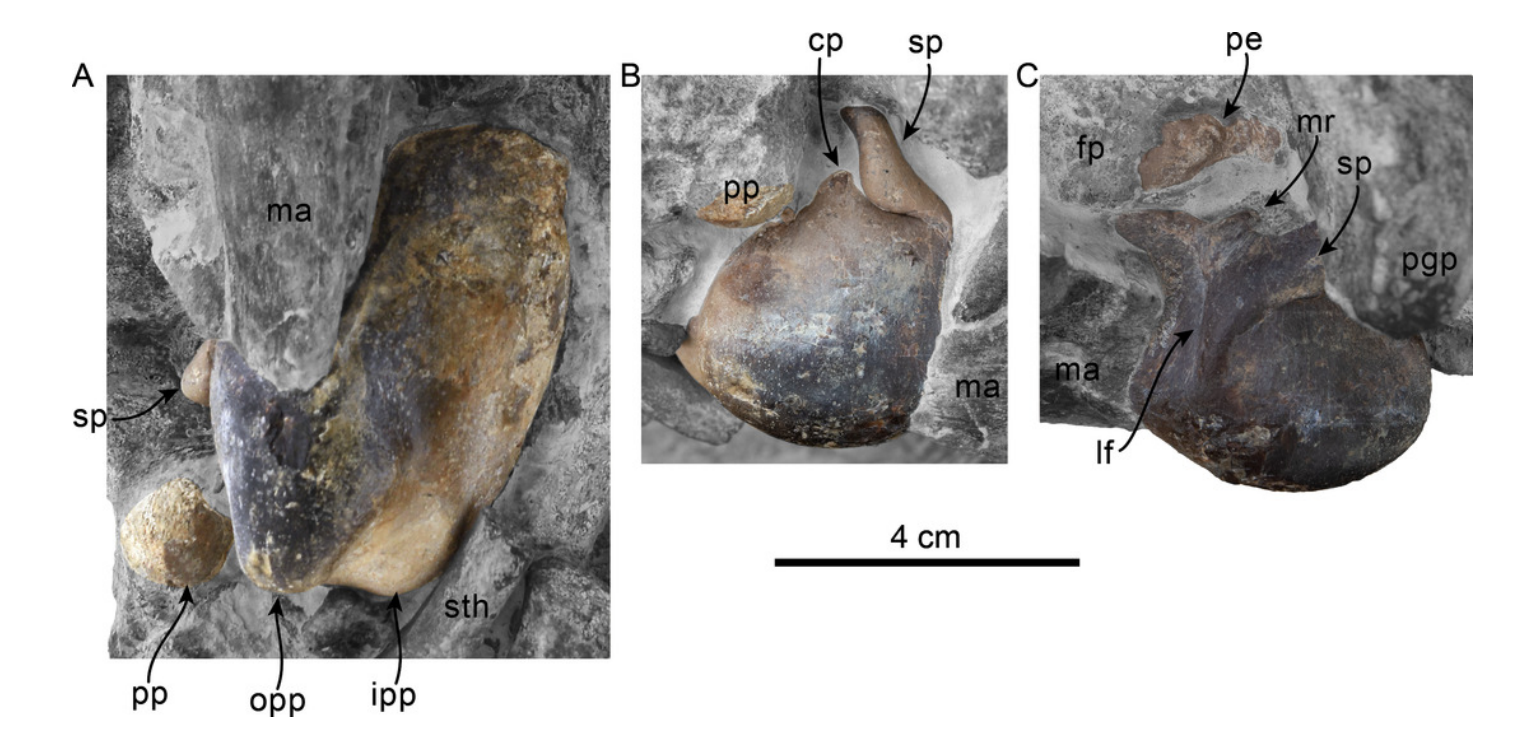
spf viof

mip

ma

Tympanic bullae of Olympicetus thalassodon sp. nov. (LACM 158720).

Articulated left tympanic bulla in ventral (A) and lateral (B) views; articulated right tympanic bulla in anterolateral (C) view. The bullae have been highlighted to differentiate them from the surrounding bones which obscure some parts. Abbreviations: cp, conical process; fp, falciform process; ipp, inner posterior prominence; lf, lateral furrow; ma, mandible; mr, mallear ridge; opp, outer posterior prominence; pe, periotic; pgp, postglenoid process; pp, posterior process; sp, sigmoid process; sth, stylohyal.

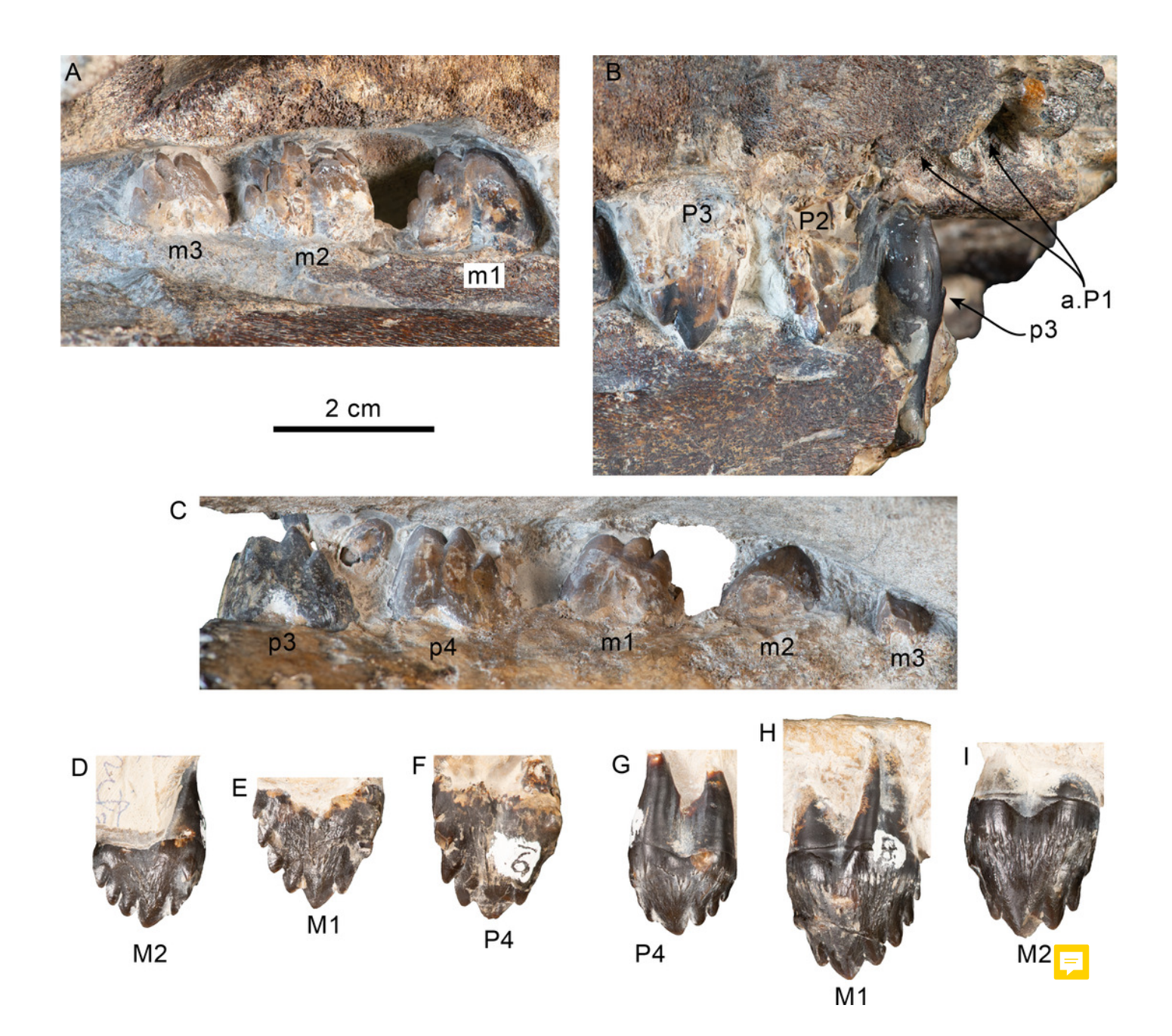




Upper and lower right dentition of Olympicetus thalassodon sp. nov. (LACM 158720).

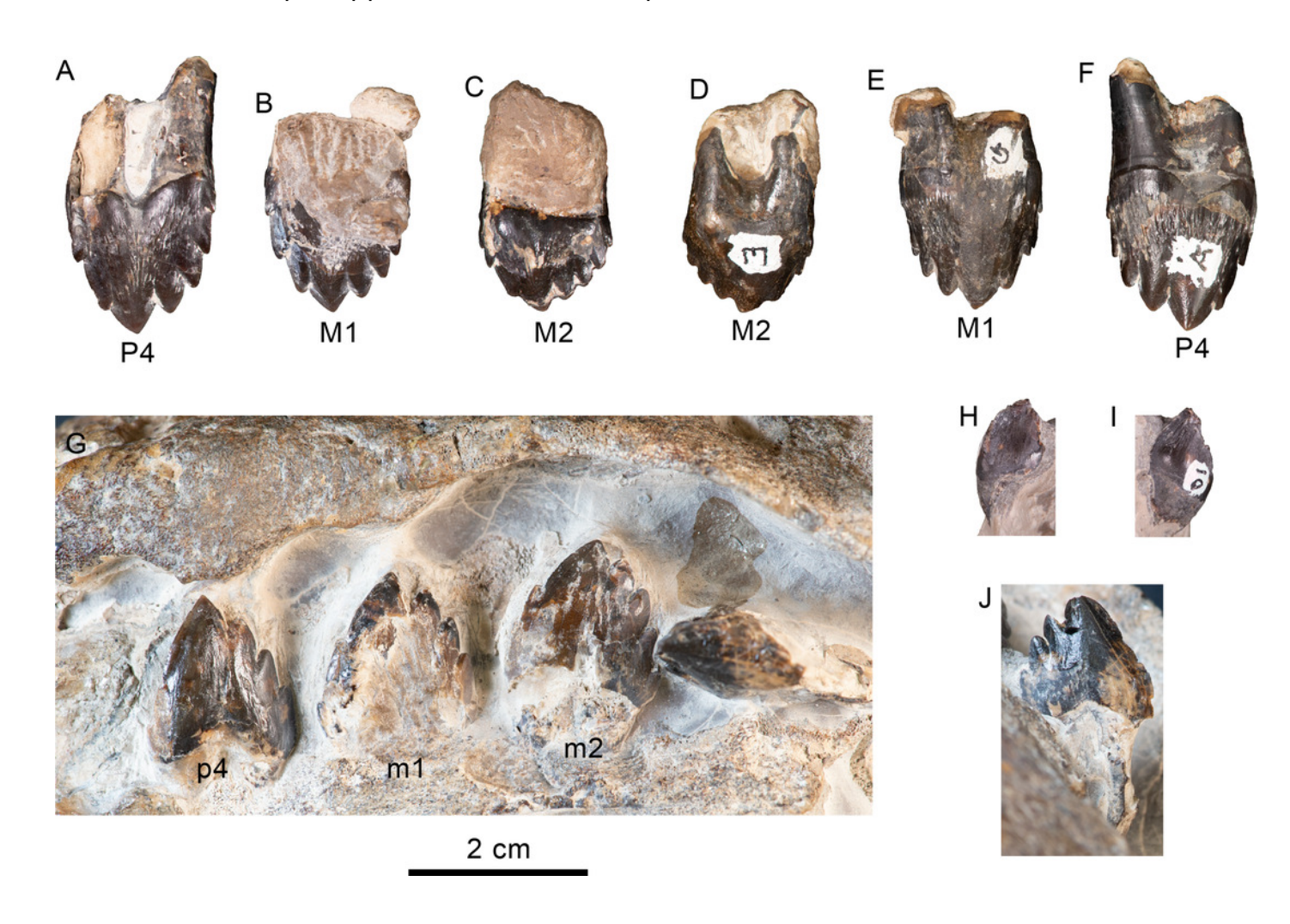
Upper and lower right postcanine teeth in buccal (A-B) views; lower right postcanine teeth (p3-m3) in lingual (C) view; upper right P4-M2 in buccal (D-F) and lingual (G-I) views.

Abbreviations: a.P1, alveoli for first upper premolar; M1-2, first and second upper molars; m1-3, first through third lower molars; P2-4, second through fourth upper premolars; p3-4, third and fourth lower premolars.



Upper and lower left dentition of Olympicetus thalassodon sp. nov. (LACM 158720).

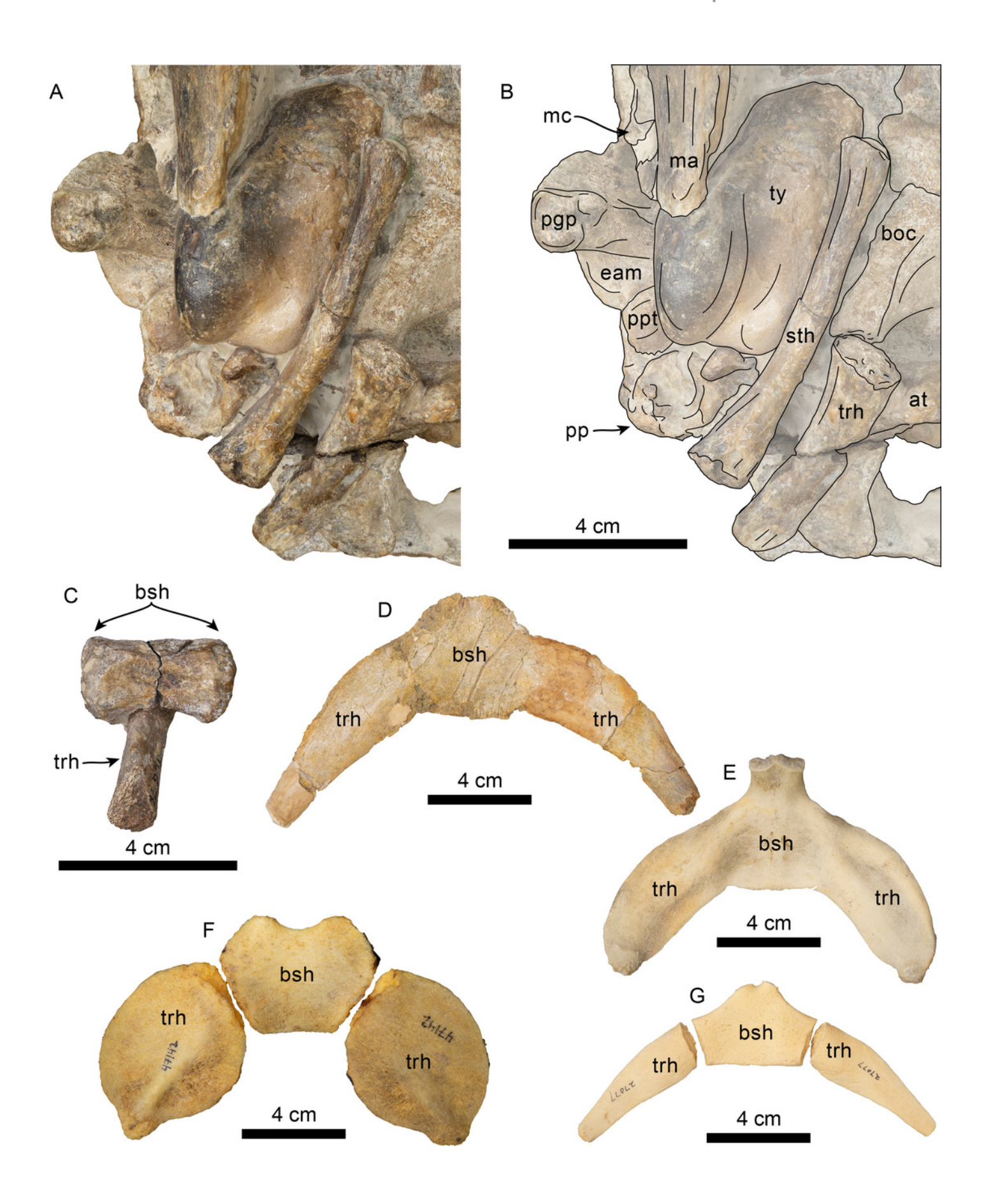
Upper left P4-M2 in buccal (A-C) and lingual (D-F) views; lower left postcanine teeth (p4-m2) in buccal (G) view; canine or incisor in buccal (H) and mesial (I) views; postcanine tooth in lingual (J) view. Abbreviations: M1-2, first and second upper molars; m1-2, first and second lower molars; P4/p4, upper and lower fourth premolars.





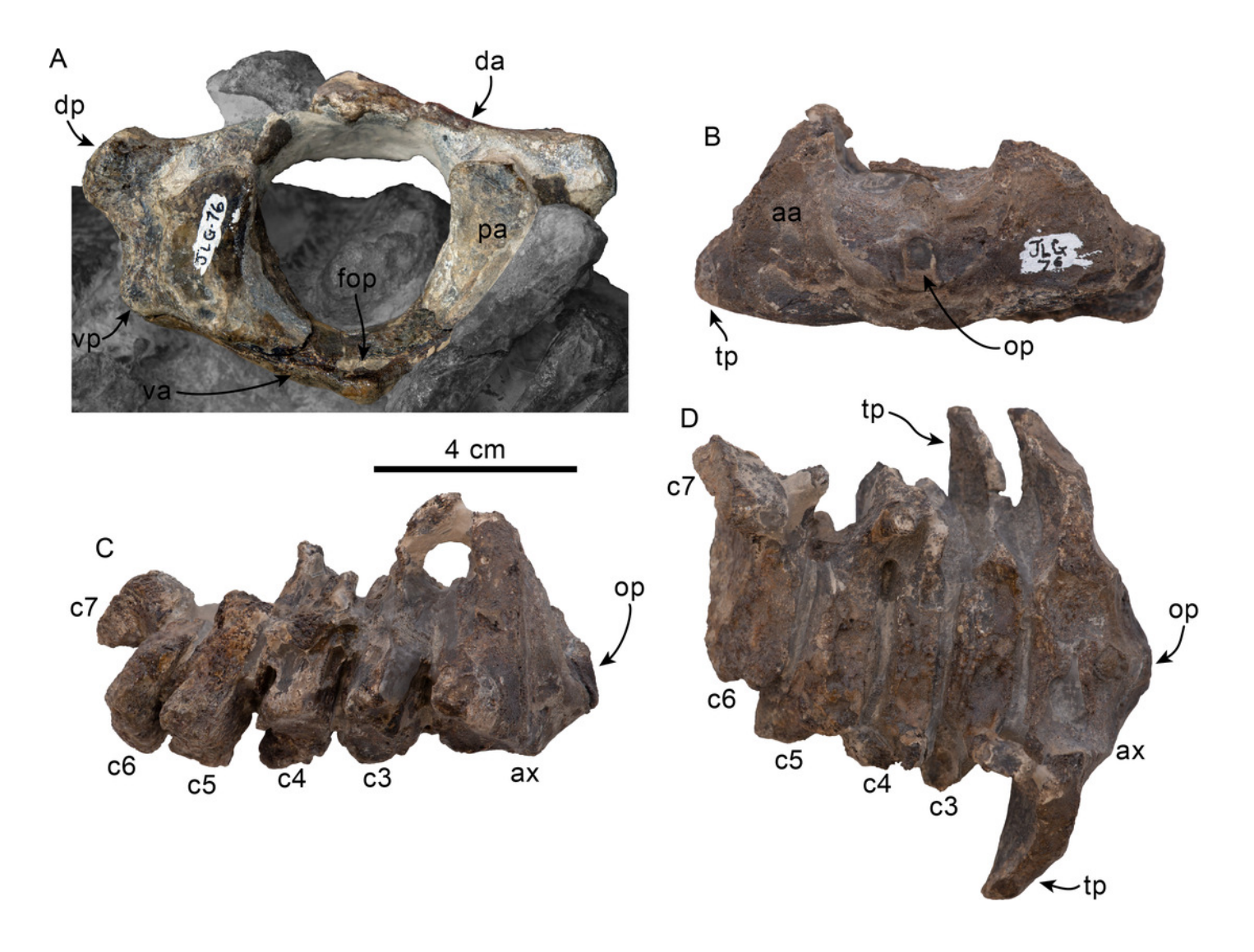
Hyoid elements of *Olympicetus thalassodon* sp. nov. (LACM 158720) and other odontocetes.

(A) Unlabeled and (B) labeled closeup of the right side of the basicranium of *Olympicetus* thalassodon in ventral view. Dorsal views of basihyal and thyrohyals of: (C) *Olympicetus* thalassodon (LACM 158720); (D) *Albireo whistleri* (UCMP 314589); (E) *Phocoenoides dalli* (LACM 43473); (F) *Kogia sima* (LACM 47142); and, (G), *Sagmatias obliquidens* (LACM 27077). Abbreviations: at, atlas; boc, basioccipital crest; bsh, basihyal; eam, external auditory meatus; ma, mandible; mc, mandibular condyle; pgp, postglenoid process; pp, paroccipital process; ppt, posterior process of the tympanic; sth, stylohyal; trh, thyrohyal; ty, tympanic.



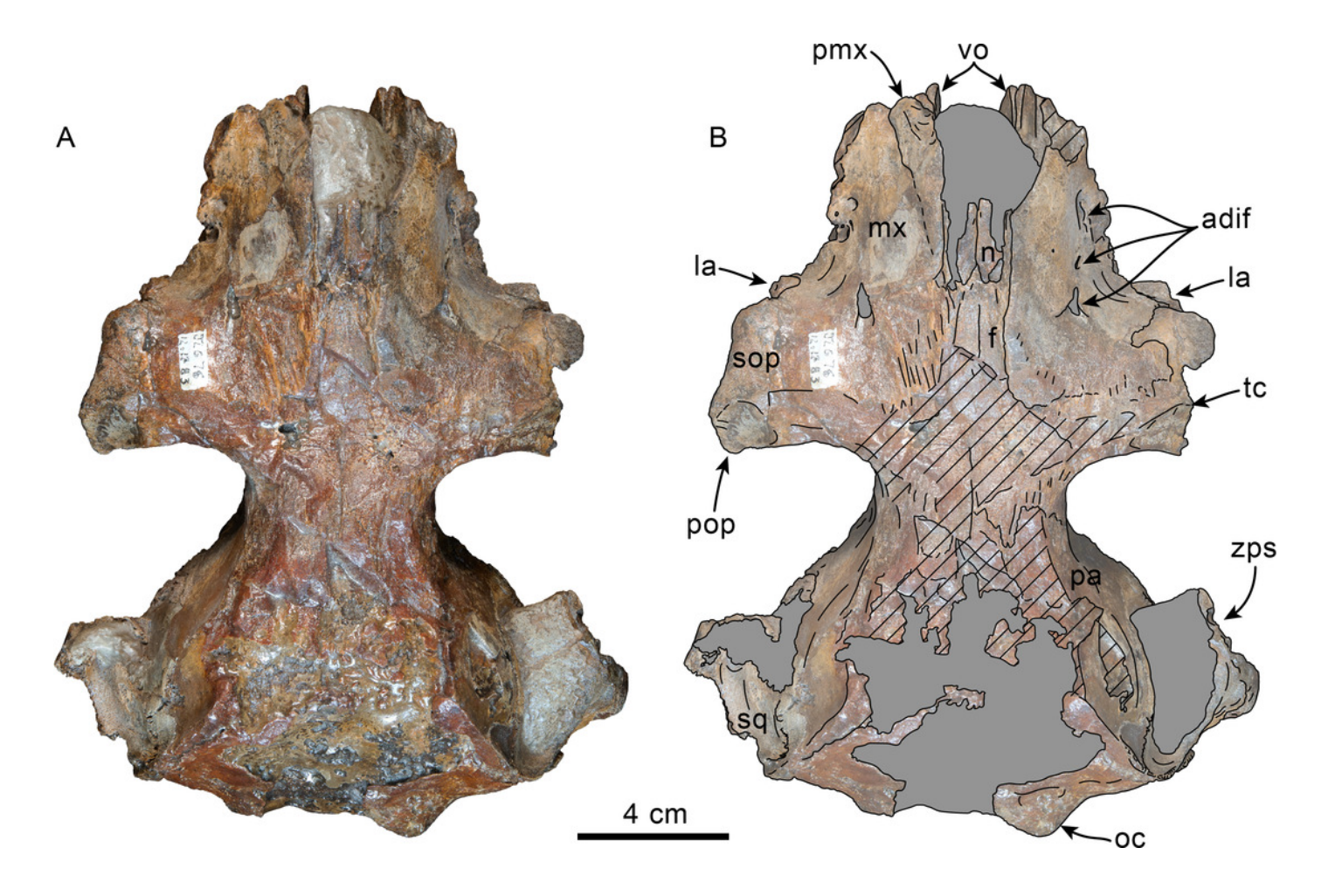
Cervical vertebrae of Olympicetus thalassodon sp. nov. (LACM 158720).

(A) atlas in posterior view; (B) axis in anterior view; (C) axis and third through seventh cervicals in right lateral view; (D) axis and third through seventh cervicals in dorsal view. Abbreviations: aa, anterior articular surface; ax, axis; c3-7, third through seventh cervical vertebrae; da, dorsal arch; dp, dorsal process; fop, facet for odontoid process; op, odontoid process; pa, posterior articular surface; tp, transverse process; vp, ventral process.



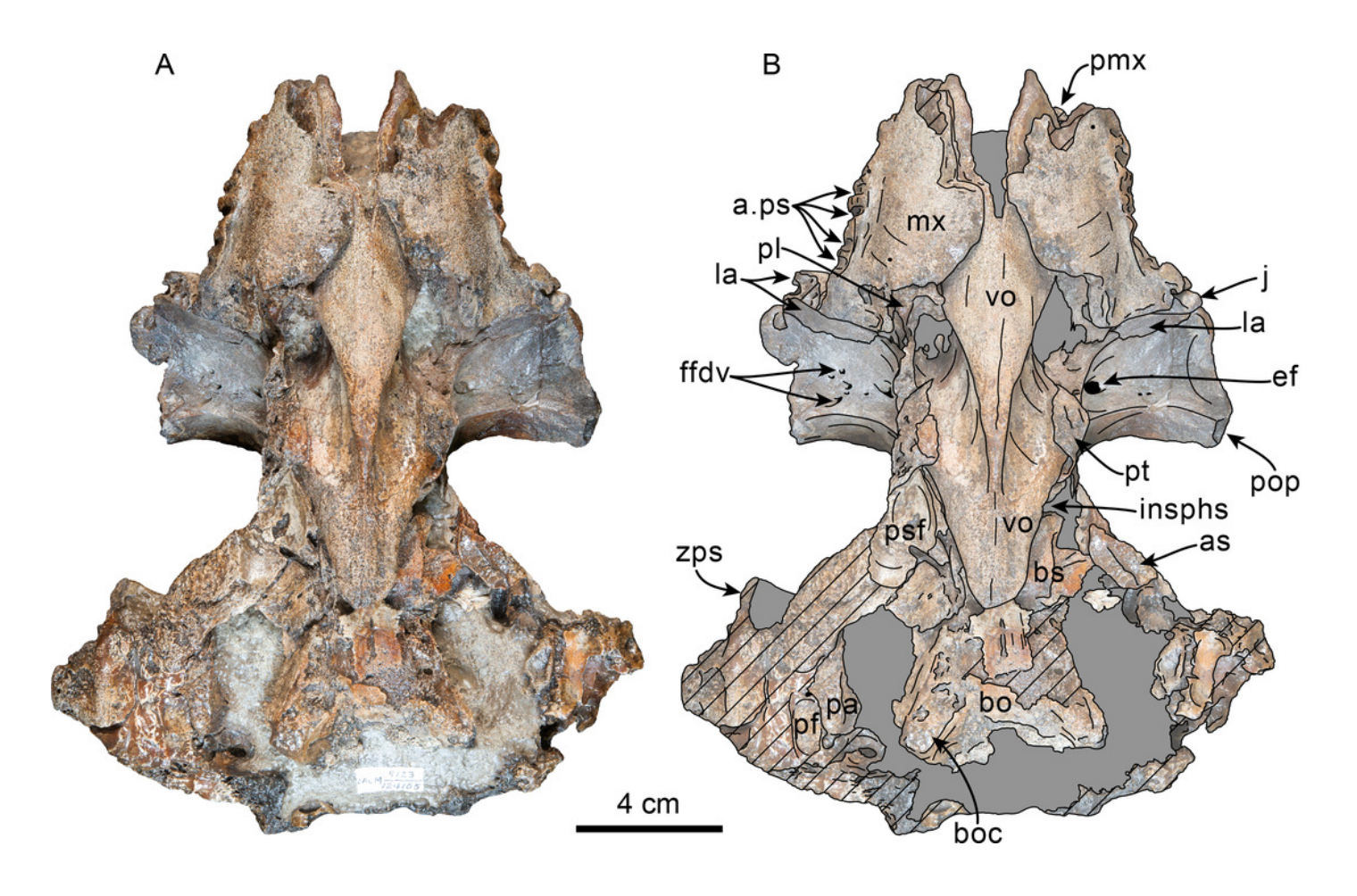
Dorsal view of skull of Olympicetus sp. 1 (LACM 124105).

Unlabeled (A) and labeled (B) skull in dorsal view. Diagonal lines denote broken surfaces, gray shaded areas are obscured by sediment. Abbreviations: adif, anterior dorsal infraorbital foramina; f, frontal; la, lacrimal; mx, maxilla; n, nasals; oc, occipital condyle; pa, parietal; pmx, premaxilla; pop, postorbital process; sop, supraorbital process of frontal; sq, squamosal; tc, temporal crest; vo, vomer; zps, zygomatic process of squamosal.



Ventral view of skull of *Olympicetus* sp. 1 (LACM 124105).

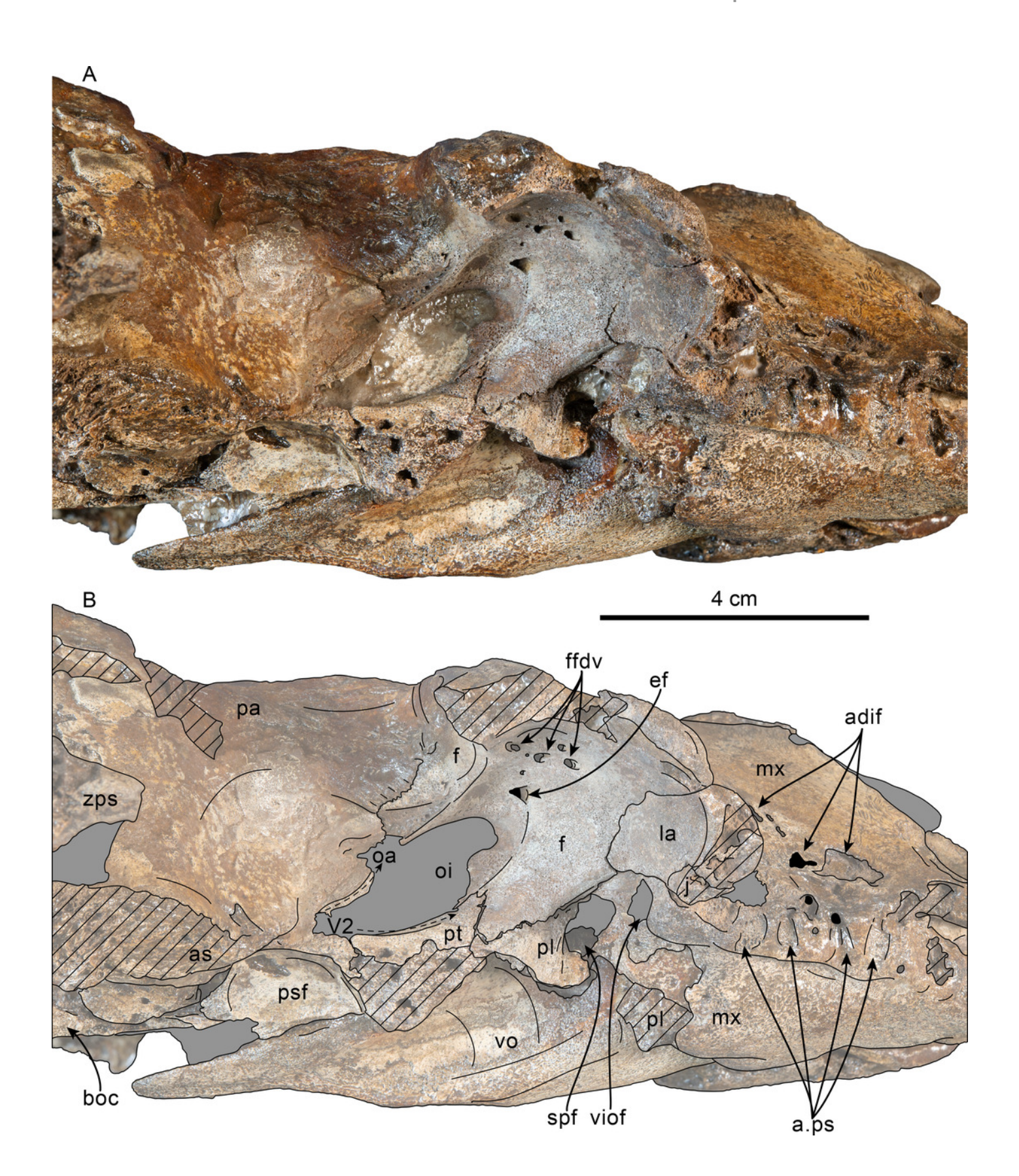
Unlabeled (A) and labeled (B) skull in ventral view. Diagonal lines denote broken surfaces, gray shaded areas are obscured by sediment. Abbreviations: a.ps, alveoli for postcanine teeth; as, alisphenoid; bo, basioccipital; boc, basioccipital crest; bs, basisphenoid; ef, ethmoid foramen; ffdv, foramina for frontal diploic veins; insphs, intersphenoidal synchondrosis; j, jugal; la, lacrimal; mx, maxilla; pa, parietal; pf, periotic fossa; pl, palatine; pmx, premaxilla, pop, postorbital process; psf, pterygoid sinus fossa; pt, pterygoid; vo, vomer; zps, zygomatic process of squamosal.





Ventrolateral view of skull of Olympicetus sp. 1 (LACM 124105).

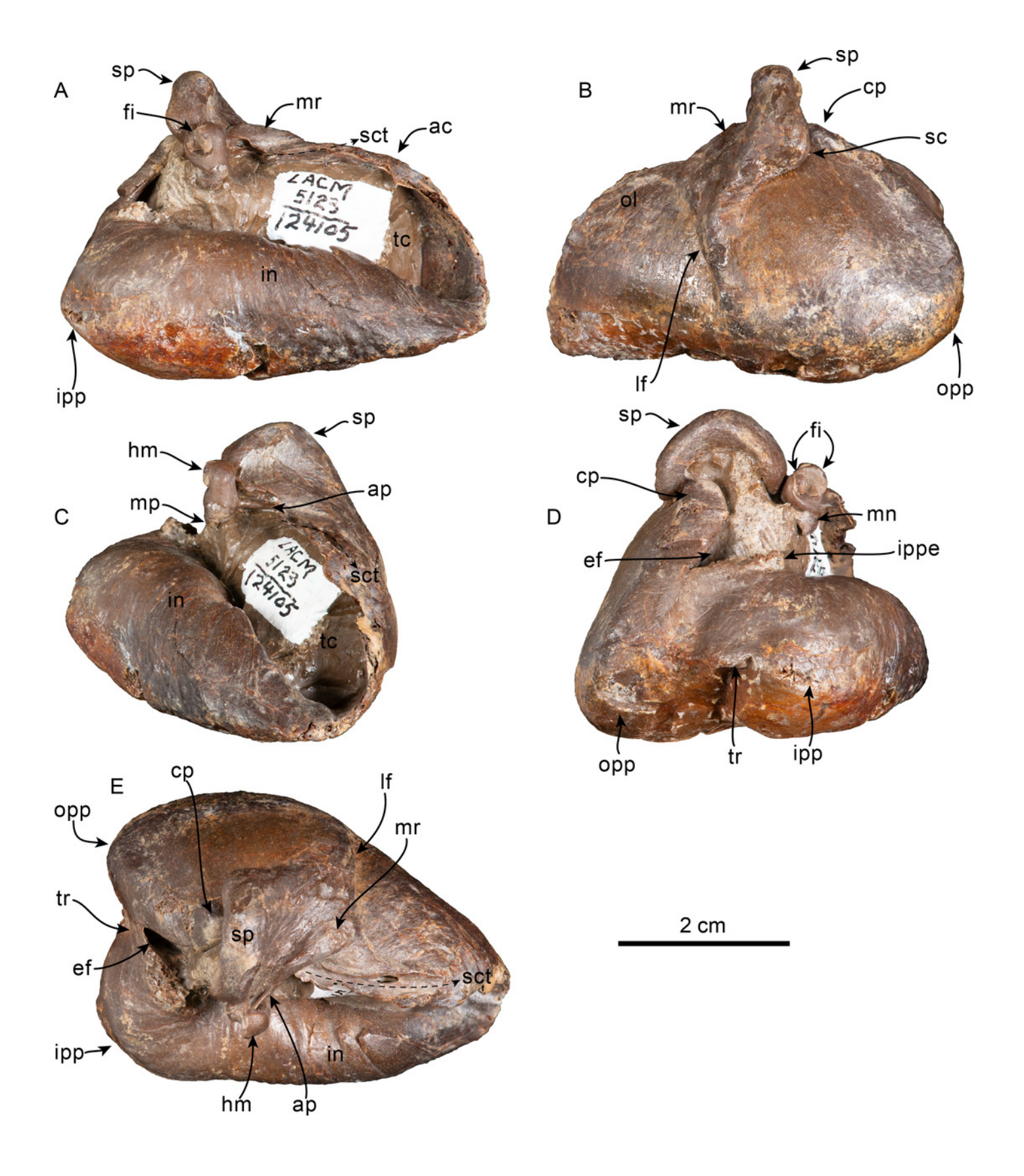
Unlabeled (A) and labeled (B) skull in right ventrolateral view focusing on the features of the orbital region. Diagonal lines denote broken surfaces, gray shaded areas are obscured by sediment. Abbreviations: a.ps, alveoli for postcanine teeth; adif, anterior dorsal infraorbital foramina; as, alisphenoid; boc, basioccipital crest; ef, ethmoid foramen; ffdv, foramina for frontal diploic veins; f, frontal; j, jugal; la, lacrimal; mx, maxilla; oa, path for ophthalmic artery; oi, optic infundibulum; pa, parietal; pl, palatine; psf, pterygoid sinus fossa; pt, pterygoid; spf, sphenopalatine foramen; viof, ventral infraorbital foramen; V2, path for maxillary nerve; vo, vomer; zps, zygomatic process of squamosal.





Malleus and tympanic bulla of Olympicetus sp. 1 (LACM 124105).

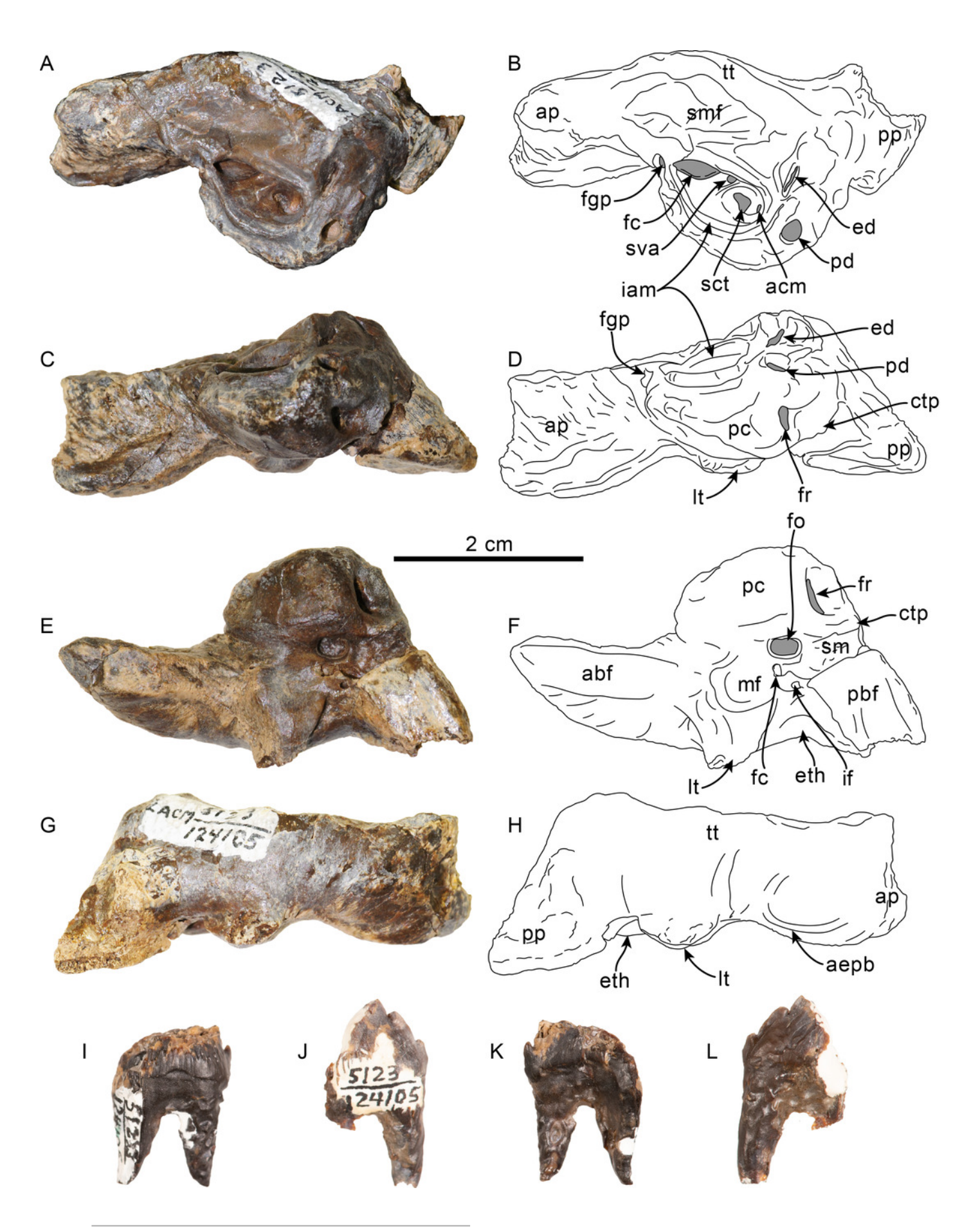
Left malleus and tympanic bullae in medial (A), lateral (B), anterior (C), posterior (D), and dorsal (E) views. Abbreviations: ac, anterodorsal crest; ap, anterior process; cp, conical process; ef, elliptical foramen; fi, facet for incus; hm, head of malleus; in, involucrum; ipp, inner posterior prominence; ippe, inner posterior pedicle; lf, lateral furrow; mn, manubrium; mp, muscular process; mr, mallear ridge; ol, outer lip; opp, outer posterior prominence; sc, sigmoid cleft; sct, sulcus for chorda tympani; sp, sigmoid process; tc, tympanic cavity; tr, transverse ridge.





Periotic and teeth of Olympicetus sp. 1 (LACM 124105).

Unlabeled and labeled right periotic in dorsal (A-B), medial (C-D), ventral (E-F), and lateral (G-H) views. Postcanine teeth in buccal (I-J) and lingual (K-L) views. Abbreviations: abf, anterior bullar facet; acm, area cribosa media; aepb, anteroexternal+parabullary sulcus; ap, anterior process; ctp, caudal tympanic process; ed, endolymphatic duct; eth, epitympanic hiatus; fc, facial canal; fgp, foramen for greater petrosal nerve; fo, foramen ovale; fr, foramen rotundum; iam, internal acoustic meatus; if, incudal fossa; pbf, posterior bullar facet; pc, pars cochlearis; pd, perilymphatic duct; lt, lateral tuberosity; mf, mallear fossa; pp, posterior process; sct, spiral cribiform tract; sm, stapedial muscle fossa; smf, supramastoid fossa; sva, superior vestibular area; tt, tegmen tympani.



Time calibrated phylogeny of Cetacea.

Phylogenetic tree showing relationship between Simocetidae with other odontocetes; mysticetes and crown odontocete clades are pruned. Strict consensus tree based on 32 most parsimonious trees of length = 2567, with retention index (RI) = 0.519, and consistency index (CI) = 0.231. Arcs denote stembased taxa, while closed circles denote node-based clades; the numbers at the nodes indicate decay indices/bootstrap values. Abbreviations: Aq., Aquitanian; Bar., Bartonian; Burd., Burdigalian; Chatt., Chattian; Holo., Holocene; La., Langhian; M., Messinian; P, Piacenzian; P., Pliocene; Ple., Pleistocene; Priab., Priabonian; Rupel., Rupelian; S., Serravalian; Tort., Tortonian; Z, Zanclean. Time scale based on Cohen et al. (2013); skull outline for *Simocetus rayi* modified from Fordyce (2002).

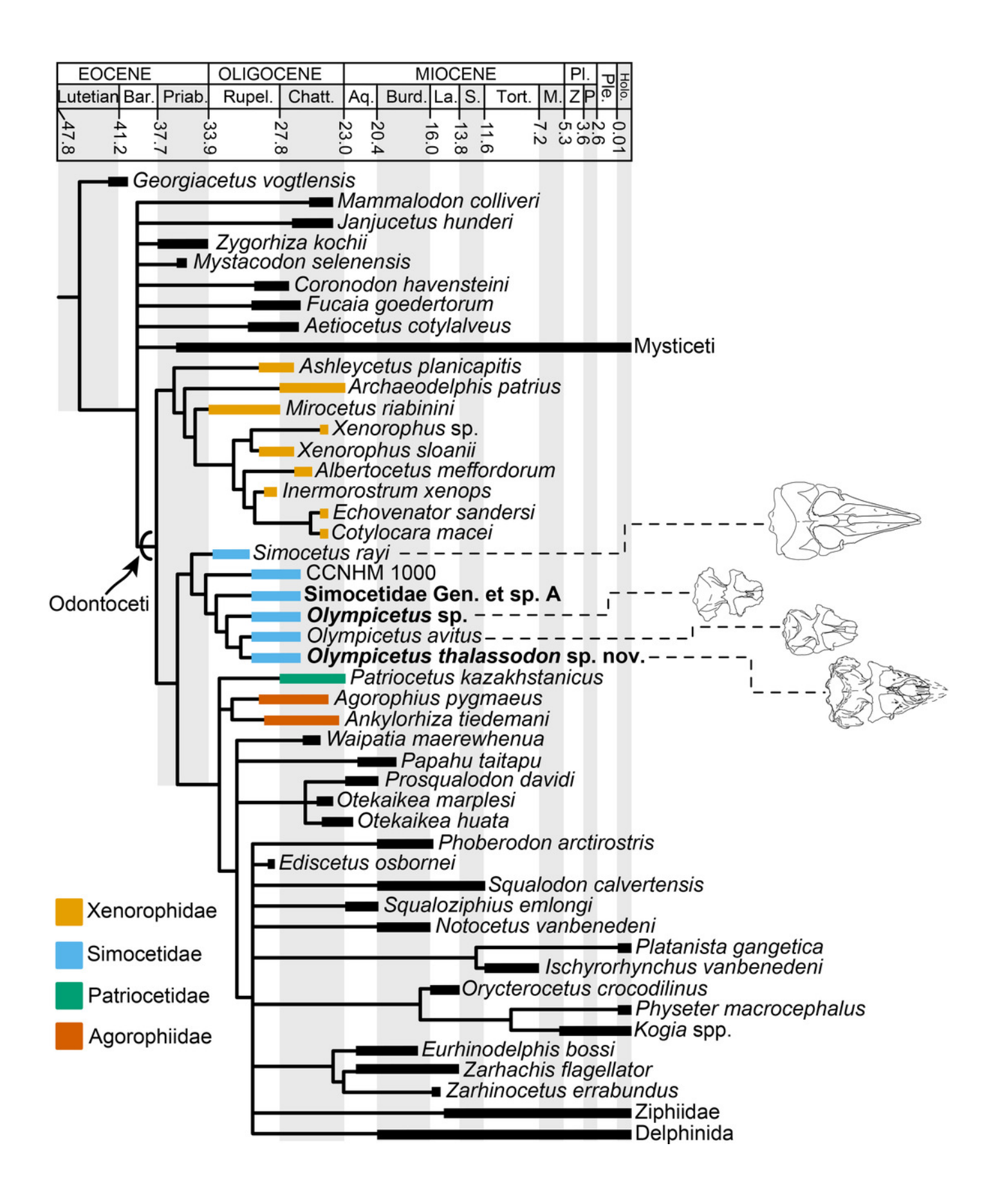




Table 1(on next page)

Measurements of simocetid skulls and mandibles.

Measurements (in mm) of simocetid skulls and mandible, Simocetidae gen. et sp. A (LACM 124104), *Olympicetus thalassodon* gen. et sp. nov. (LACM 158720) and *Olympicetus* sp. 1 (LACM 124105). Modified after Perrin (1975).



TABLE 1. Measurements (in mm) of simocetid skulls and mandible, Simocetidae gen. et sp. A (LACM 124104), *Olympicetus thalassodon* gen. et sp. nov. (LACM 158720) and *Olympicetus* sp. 1 (LACM 124105). Modified after Perrin (1975).

	LACM	LACM	LACM
	124104	158720	124105
Width of rostrum at base	-	135	93+
Width of rostrum at 60 mm anterior to line across hindmost limits	-	105	-
of antorbital notches			
Greatest preorbital width (width across preorbital processes)	-	153	136
Greatest postorbital width	-	187	150e
Mid-orbital width	-	151	140e
Maximum width of external nares	-	33	-
Greatest width across zygomatic processes of squamosal	322e	220	186e
Greatest width of premaxillaries	-	83	-
Greatest parietal width within temporal fossae	154	135	100
Vertical external height of braincase from midline of	135	112	-
basisphenoid to summit of supraoccipital, but not including			
external occipital crest			
Greatest length of left posttemporal fossa, measured to external	-	99	-
margin of raised suture			
Greatest width of left posttemporal fossa at right angles to	-	51	-
greatest length			
Major diameter of left temporal fossa proper	-	111	-



1

TABLE 1. Continued.

Minor diameter of left temporal fossa proper	59	45	-
Distance from foremost end of junction between nasals to	-	143e	-
hindmost point of margin of supraoccipital crest			
Length of orbit – from apex of preorbital process of frontal to	-	55	40+
apex of postorbital process			
Length of antorbital process of lacrimal	-	18	12
Greatest length of left pterygoid	132	79	-
Maximum width across occipital condyles	92	78	-
Height of foramen magnum	33	35	-
Width of foramen magnum	39	32	-
Cranial length – antorbital notch to condyles	-	211	165+
Greatest length of left mandibular ramus (as preserved)	-	251+	-
Greatest length of right mandibular ramus (as preserved)	-	244+	-
Maximum height at mandibular condyle	-	54	-

Abbreviations: **e**, estimate; + = measurement on incomplete element.

2



Table 2(on next page)

Measurements of simocetid cervical vertebrae.

Measurements (in mm) of cervical vertebrae of Simocetidae gen. et sp. A (LACM 124104) and *Olympicetus thalassodon* sp. nov. (LACM 158720).



TABLE 2. Measurements (in mm) of cervical vertebrae of Simocetidae gen. et sp. A (LACM 124104) and *Olympicetus thalassodon* sp. nov. (LACM 158720).

	LACM	LACM
	124105	158720
Atlas		
Maximum height	-	70
Maximum length	32	27
Width across anterior articular facets	80+	-
Width across posterior articular facets	94	74
Maximum width (across transverse processes)	-	108
Mid-dorsal length	-	24
Mid-ventral length (including odontoid process)	37	22
Neural canal height	-	44
Neural canal width	45	38
Axis		
Maximum height of centrum	46	33
Maximum width of centrum	47	-
Maximum length of centrum	44	30
Width across anterior articular facets	92e	77
Maximum width (across transverse processes)	144e	97
Width of neural canal	46	33
Cervical 3		
Height of centrum	49	34



Width of centrum	53	34
Length of centrum	20	12
Maximum width (across transverse processes)	164e	96e
Width of neural canal	38e	-
Cervical 4		
Height of centrum	-	34
Width of centrum	-	35
Length of centrum	-	12
Cervical 5		
Height of centrum	-	31
Width of centrum	-	32
Length of centrum	-	12
Cervical 6		
Height of centrum	-	27+
Length of centrum	-	10+

Abbreviations: **e** = estimate; + = measurement on incomplete element.



Table 3(on next page)

Measurements of simocetid tympanic bullae.

Measurements (in mm) of tympanic bullae of *Olympicetus thalassodon* sp. nov. (LACM 158720), *Olympicetus avitus* (LACM 126010), and *Olympicetus* sp. A (LACM 124105) (modified from Kasuya, 1973, and Geisler et al., 2014).



TABLE 3. Measurements (in mm) of tympanic bullae of *Olympicetus thalassodon* sp. nov. (LACM 158720), *Olympicetus avitus* (LACM 126010), and *Olympicetus* sp. A (LACM 124105) (modified from Kasuya, 1973, and Geisler et al., 2014).

	LACM	LACM	LACM
	158720	126010	124105
Maximum length (without posterior process)	65	50	49
Maximum length (including posterior process)	74	54	-
Distance from anterior tip to inner posterior	61	50	48
prominence			
Maximum width at level of the sigmoid process	40	35	34
Height at sigmoid process	46	37	36
Maximum width of sigmoid process	-	15	15
Maximum length of posterior process	16+	18	-

Abbreviations: +, measurement on incomplete or obscured element.



Table 4(on next page)

Measurements of simocetid teeth.

Measurements (in mm) of left (I) and right (r) teeth of *Olympicetus thalassodon* sp. nov. (LACM 158720).



TABLE 4. Measurements (in mm) of left (l) and right (r) teeth of *Olympicetus thalassodon* sp. nov. (LACM 158720).

Designation	Length	Width	Height
?Canine	7.4	7.2	7.7
P2 (r)	-	-	15.6
P3 (r)	15.7	-	17.5
P4 (r)	16.5	9.7	17.5
P4 (1)	17.9	9.3	18.3
M1 (r)	16.4	9.4	17.9
M1 (l)	16.5	9.4	16.7
M2 (r)	14.1	8.1	11.9
M2 (l)	14.6	8.4	11.7
p3 (r)	17.1	7.4	14.4+
p4 (r)	15.2	-	13.6+
p4 (l)	16.7	-	18.6
m1 (r)	17.8	6.4	13.9+
m1 (l)	17.6	-	18.3
m2 (r)	16.5	-	13.5+
m2 (l)	17.4	-	17.3
m3 (r)	13.4	-	11.6
Molariform indet.	15.4	9.0	13.5

Abbreviations: +, measurement on incomplete element.



Table 5(on next page)

Measurements of simocetid hyoid elements.

Measurements (in mm) of hyoid elements of *Olympicetus thalassodon* sp. nov. (LACM 158720) (modified after Johnston and Berta, 2011).



TABLE 5. Measurements (in mm) of hyoid elements of *Olympicetus thalassodon* sp. nov. (LACM 158720) (modified after Johnston and Berta, 2011).

Stylohyal (right)	
Maximum length	85
Maximum width of distal articular surface	11
Anteroposterior thickness at mid length	10
Transverse width at mid length	6
Maximum width of proximal articular surface	16
Anteroposterior thickness of proximal articular surface	8
Basihyal	
Maximum length along the midline	14
Maximum depth along the midline	10
Maximum transverse width	33
Length of articular surface	20
Height of articular surface	14
Thyrohyal (right)	
Maximum length	59
Maximum width of distal articular surface	11
Maximum height of distal articular surface	16
Dorsoventral thickness at mid length	7
Transverse width at mid length	11
Maximum width of proximal articular surface	18
Maximum height of proximal articular surface	13



Table 6(on next page)

Measurement of simocetid periotic.

Measurements (in mm) of periotic of *Olympicetus* sp. 1 (LACM 124105) (modified from Kasuya, 1973, and Racicot et al., 2019).



TABLE 6. Measurements (in mm) of periotic of *Olympicetus* sp. 1 (LACM 124105) (modified from Kasuya, 1973, and Racicot et al., 2019).

Maximum length	43		
Proximal dorsoventral thickness of anterior process	12		
Length of anterior process	16		
Transverse width of anterior process at mid-length	9		
Dorsoventral height of anterior process at mid-length	13		
Maximum width of periotic	22		
Least distance between fundus of internal auditory	2		
meatus and aperture for endolymphatic foramen			
Least distance between fundus of internal auditory	3		
meatus and aperture for perilymphatic foramen			
Least distance between fenestra rotunda and	7		
endolymphatic foramen			
Least distance between fenestra rotunda and	3		
perilymphatic foramen			
Length of articular surface of posterior process	11		
Width of articular surface of posterior process	8		
Transverse width of cochlear portion	10		
Anteroposterior length of cochlear portion	15		